THESIS FOR THE DEGREE OF DOCTOR OF PHILOSOPHY (PhD)

PREPARATION OF DYE-ANTIBODY CONJUGATES FOR STUDYING THE PLASMA MEMBRANE DISTRIBUTION OF CD1d PROTEINS IN B CELLS

BY: DILIP SHRESTHA

SUPERVISORS: Attila Jenei, PhD

János Szöllősi, PhD, DSc

UNIVERSITY OF DEBRECEN

DOCTORAL SCHOOL OF MOLECULAR MEDICINE

DEBRECEN, 2013

TABLE OF CONTENTS

1. ABBREVIATIONS

MHC	- Major Histocompatbility Complex
CD1	- Cluster of Differentiation 1
APC	- Antigen Presenting Cells
Mab	- Monoclonal Antibody
Igs	- Immunoglobulins
BCR	- B cell receptor
MW	- Molecular Weight
kDa	- Kilodalton
“L”	- Light Chain
“H”	- Heavy Chain
ABS	- Antigen Binding Site
“V”	- Variable Domain
“C”	- Constant Domain
$-NH_2$	-Amines
-SH	- Sulfhydryl or Thiol groups
-CHO	- Aldehyde
NHS ester	- N-hydroxysuccinimidyl ester
MEA	- Mercaptoethylamine
DTT	- Dithiothrietol
$NaIO_4$	- Sodium Periodate
LP	- Lymphoid Progenitors
“D”	- Diversity
“J”	- Joining
DC	- Dendritic Cell
HLA	- Human Leukocyte Antigen
TCR	- T cell receptor
NK cells	- Natural Killer cells
iNKT cell	- Invariant NKT cell
α-gal	- α-galactosylceramide
MIIC	- MHC II Containing Compartment
MHC I-HC	- MHC I Heavy Chain
β_2m	- β_2-Microglobulin
CD1d-HC	- CD1d Heavy Chain
GM-CSF	- Granulocyte Macrophage Colony Stimulating Factor
IL	- Interleukin
ER	- Endoplasmic Reticulum
AP	- Adaptor Protein
ARF6	- ADP-Ribosylation Factor
TGN	- Trans Golgi Network
LDL	- Low-Density Lipoprotein
PAMP	- Pathogen-Associated Molecular Patterns
iGb3	- Isoglobotrihexosylceramide
GSL	- Glycosphingolipids
PL	- Phospholipids

ILT4	- Ig-like transcript
MβCD	- Methyl-β-cyclodextrin
HMG-CoA	- 3-hydroxy-3-methylglutaryl coenzyme A
FRET	- Fluorescence Resonance Energy Transfer
ICAM1	- Intercellular Adhesion Molecule 1
TfR	- Transferrin Receptor
EDTA	- Ethylenediaminetetraacetic Acid
NEM	- N-ethylmaleimide
DMSO	- Dimethyl sulfoxide
MWCO	- Molecular Weight cutoff
CF	- Correction Factor
NCS	- Newborn Calf Serum
FCET	- Flow-cytometric FRET
Kd	- Dissociation Constant
SDS-PAGE	- Sodium Dodecyl Sulfate Polyacrylamide Gel Electrophoresis
'C'	- Cross-correlation Coefficient
CTxB	- Cholera Toxin subunit B
FCDR	- Flow Cytometric Detergent Resistance
TX100	- Triton X-100
PBMC	- Peripheral Blood Mononuclear Cells
PHA-M	- Phytohemagglutinin M
$NaBH_4$	- Sodium Borohydride
ADCC	- Antibody-dependent Cellular Cytotoxicity
NBS	- Nucleotide Binding Site
PET	- Photoinduced Electron Transfer
AFM	- Atomic Force Microscope

2. PREFACE

The immune system is a collective term for a broad range of defensive measures pursued by the human body to remain safe. Operationally, these vigilant immune responses could be categorized as innate and adaptive immune system. Innate immunity is a non-specific defense mechanism which is an “always ready service“ thus acts as the first line of defense in human beings while adaptive immunity is a specific response developed and evolved later after the exposure to a non-self threat, hence, also termed a second line of defense. Adaptive immunity is further classified into two subgroups: Humoral immunity -mediated by antibodies produced by B lymphocytes and cellular immunity -mainly mediated by T lymphocytes (1).

Primarily, the features of B lymphocytes will be discussed in this dissertation. B cells are not only pivotal in humoral immunity but are also involved in other aspects of immune responses, including antigen presentation and T cell functional regulation. Antibodies are used by the immune system to neutralize any toxins liberated by the pathogens extracellularly. In the first part of this thesis, I will elaborate on the important facet of antibody conjugation. Since organic fluorophores/dyes are easily found in the market with various functional modifications, and fluorescence has long been used to visualize cell biology at many levels, from molecules to complete organism, I would specifically describe various methods to conjugate fluorophores to antibodies. A comparison is also done between these strategies primarily with regards to the preservation of antigen binding function of antibody, involved financial cost and the ease in operation of these methods.

The second part of this dissertation deals with the application of dye-antibody conjugates. The adaptive immune system relies on its peptide-based arm mediated by Major Histocompatibility complex (MHC) proteins and lipid-based arm based on Cluster of Differentiation 1 (CD1) proteins. We have focused on lipid-based immunity in this part of the thesis. Specifically, a detailed analysis is presented on the topological features of CD1d proteins, a subtype of CD1 proteins, on the plasma membrane of B cells using dye-antibody conjugates. Eventually, the relationship of CD1d with MHC and lipid species on the plasma membrane has been critically analyzed.

3. INTRODUCTION

3.1. Dye-antibody conjugation

3.1.1. Magic bullets and monoclonals: A tale of confusion, pain and success

Antibodies essentially were the first elements to be identified in the immune system which gave birth to serum therapy. Delving into the history, Emil Adolf von Behring introduced the concept of serum therapy thus the curative powers of blood for which he was awarded the first-ever Nobel prize in medicine in 1901 (2). Behring also coined such molecules as "anti-body" because of its natural production within the body as an anti-dote. However, it was through Paul Ehrlich's contributions in the development of standardized antibody preparations that the breakthrough gained medical applicability. Being pragmatist and application oriented, he termed "magic bullets" for such molecules with specialized power envisioning that these molecules could precisely find and destroy specific toxins (3). Realization of the potentiality and applicability of such molecules thereafter led to the suggestion that by harnessing these magic bullets, researchers could develop cures for all kinds of disorders. However, it gained wider recognition only after the discovery of hybridoma technology in 1975, almost 70 years later, by the duo Cesar Milstein and Georges Kohler, which enabled the production of monoclonal antibodies (Mabs) that in theory opened up the flood gates of research areas and its therapeutic applications (3, 4). They have already become a centerpiece of the growing biotechnological and pharmaceutical industry now.

3.1.2. Immunoglobulins (Igs)

Antibodies, antigen-reactive globular glycoproteins present in the serum, are generated on the exposure of a host to a given antigen, called an immunogen. They are presumed to be soluble making up about 10 % to 20 % of plasma proteins; however, they are also found as membrane-bound receptors, often called as B cell receptors (BCRs), in B lymphocytes. The activity of antibody was found to be related to the γ-globulin fraction of the isolated serum proteins; therefore, immune globulins were otherwise designated as Igs (5). Antibodies are produced by plasma cells, which are terminally differentiated non-cycling B cells through a complex process of clonal expansion. Normally, these cells are not found in the circulation rather are observed residing in their organ of choice for life, for example, bone marrow. For the production of a specific antibody, stimulation of B cell by a particular antigen is a must. Once activated these B cells

differentiate and expand into an antibody-secreting plasmablast and ultimately into a plasma cell (6). Since most antigens are complex in structure, multiple epitopes of the same antigen can activate numerous lymphocytes. Each of these subsets of lymphocytes can differentiate into plasma cells resulting in the antibody response. Therefore, polyclonal antibodies are the mixture of antibodies produced against the same antigen but against multiple epitopes by different B cells. In contrast, Mabs are derived from a single clone of B cell producing an antibody against only one specific epitope (7).

3.1.3. Structural features of an antibody

The basic structural unit of most mammalian antibodies is a glycoprotein (molecular weight (MW) ~150 kilodaltons (kDa)) made up of four polypeptide chains -two identical heavy chains (H) and two identical light chains (L). The polypeptide chains are linked together by covalent and non-covalent forces providing stability and "Y" conformation to the antibody (7). A prototype of an Ig molecule is presented in the **Figure 1**. Both intra-chain disulfide bonds within each of the polypeptide chains and inter-chain disulfide bonds between 'H' and 'L' chains and 'H' and 'H' chains are important for maintaining the shape of an antibody. The pairing of 'H' and 'L' chains gives rise to two identical antigen binding sites (ABS). Both the class and sub-classes of Ig molecules are determined based on their 'H' chain identity. The larger 'H' chain is variable and structurally distinct for each class with a MW in the range of 50000-77000 Da, whereas, the smaller light chain is very similar for all classes and has a MW of ~25000 Da. Each 'H' and 'L' chain is made up of a series of homologous units of approximately 110 amino acids and is called Ig domains. Two such Ig domains are found in the 'L' chain, whereas, four Ig domains are seen in 'H' chain. The amino-terminal sequences of both the 'H' and 'L' chains demonstrate considerable variation in amino acid composition between different antibodies; therefore, it was referred to as a variable (V) region. This variation in sequence is limited to the first Ig domain and forms the ABS. Hence, 'H' chain consists of one variable domain (V_H) and three or four constant domains (C_H1, C_H2, C_H3 and C_H4, depending upon the antibody class or isotype) while 'L' chain has one variable (V_L) and one constant domain (C_L). The region between the C_H1 and C_H2 domains is called the hinge region, and it administers flexibility to the two Fab arms of the Y-shaped antibody molecule, allowing them to open and close freely so that the two arms, separated by a fixed distance, could bind easily to the antigens. Fab fragments are prepared by digestion of an antibody

with the papain enzyme which cuts an Ig molecule in the hinge region before the H-H inter-chain disulfide bonds. An antibody produces two identical Fab fragments that contain the whole 'L' chain (V_L and C_L) and two Ig domains of 'H' chain (V_H and C_H1), thus, is still capable of binding antigen but is monovalent in nature. The remainder of the fragments after papain digestion of an antibody, excluding Fab, is called as a Fc region because it was easily crystallizable. A Fc segment usually contains two identical C_H2 and two identical C_H3 domains from the two 'H' chains of an antibody. It is responsible for all the effector functions in an Ig molecule and is specific for each isotype. Likewise, digestion with pepsin cleaves an Ig molecule after the H-H inter-chain disulfide bonds resulting in the fragment called $F(ab')_2$ which has intact two ABS. In humans, Igs are grouped into five major classes, also called isotypes, which are listed here in the order of decreasing plasma or serum concentration: IgG, γ 'H'chain (70-75) %, IgA, α 'H'chain (15-20) %, IgM, μ 'H'chain (10) %, IgD, δ 'H'chain (<1) % and IgE, ε 'H'chain (0-0.01) %. Each isotype differs in size, charge, amino acid composition and carbohydrate content. In serum, IgG, IgD, IgE and IgA exist as a monomer; however, IgM has a pentamer structure formed from their monomer units. Dimers of IgA have also been observed. Additionally, four sub-classes of IgG (IgG1, IgG2, IgG3 and IgG4) and two sub-classes of IgA (IgA1 and IgA2) are known, however, none have been described for IgM, IgD or IgE. Differences in the 'H' chain confer distinct properties to Ig isotypes, including localization in different compartments of the immune system and its half-life in vivo. IgG is the most frequently used isotype of all Ig molecules most probably due to its smaller size, abundance in serum and its specific ability to activate the complement system (5, 8). Igs can also be sub-grouped based on their 'L' chain. Two isotypes of 'L' chains are found based upon the differences in the amino acid sequence in the 'C' regions: κ and λ. The hybridoma cell lines that we have used for our study only produce Mabs which are of the IgG class; therefore, in the following sections, we would mostly discuss about IgG isotypes.

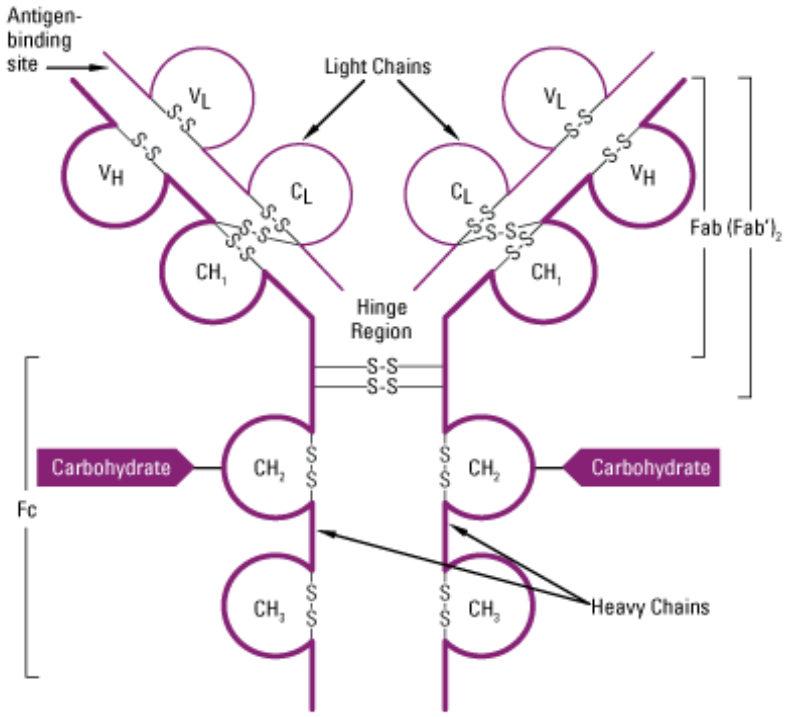

Figure 1.
General structure of an Immunoglobulin G.
(Adapted from Pierce's website, http://www.piercenet.com)

3.1.4. Amino acids and functional groups amenable to modifications in an antibody

The functionality and reactivity of a protein are mainly determined by its amino acid composition and tertiary structure. The side chain groups of amino acids do not participate in polypeptide formation and thus provide the functional groups available for modifications in proteins (9).
The various amino acids that form the side-chain functional groups and also offer the opportunity to modify the antibody can be classified as below:

3.1.4.1. Polar / hydrophilic amino acids

They contain side-chains with polar functional groups (e.g., -OH, -SH, -$CONH_2$, heterocyclic amines) and are usually found in the domains at or near the surface of proteins where they are exposed to the aqueous environment. Examples of this sub-group include asparagine, glutamine, threonine, serine, cysteine and tyrosine. Serine and threonine are uncharged where as asparagine and glutamine do not become charged at physiological pH values. Therefore, they are difficult to modify at aqueous conditions. Only cysteine and tyrosine, which have ionizable side chains, are

appropriate for modifications or conjugation purpose. Cysteine is a sulfur containing amino acids and is relatively less polar. Mostly, cysteine if present is in the form of disulfide bonds holding the polypeptide chains on a protein. For using -SH groups of a cysteine molecule, the disulfide bonds within a protein are required to be reduced. Unlike cysteine, tyrosine is usually present at the surface thus does not need prior treatment; however, most reactions proceed effectively only when tyrosine's ring is ionized to the phenolate anion form (9-12).

3.1.4.2. Acidic amino acids with negative charge

Aspartic acid and glutamic acid are the only standard amino acids with carboxylic acid groups on their side-chains and are ionized at pH values above their pKa, resulting in carboxylate ions. These carboxylate groups in proteins are an easy target of derivatization (9, 10, 12).

3.1.4.3. Basic amino acids with positive charge

Lysine, arginine, and histidine are basic amino acids containing ionizable amine side-chains. The side-chains of lysine and arginine are fully protonated, whereas, histidine is weakly protonated at neutral pH. The highest percentage of lysine (2-10 %) is present in proteins. It contains both α-amine and ε- amine, which differs in pKa values. The terminal amine residues can be selectively modified (9-12).

3.1.4.4. Nonpolar / hydrophobic amino acids

Glycine, alanine, valine, leucine, isoleucine, proline, methionine, phenylalanine and tryptophan are the examples from this category. Except tryptophan, these amino acids are unreactive towards common derivatizating agents (9, 10, 12).

3.1.4.5. Carbohydrate moieties in antibody

Igs are glycoproteins, and they display heterogeneous groups of terminal sugars. The carbohydrate content ranges from 2–3% for IgG, to 12–14% for IgM, IgD and IgE. IgG molecules have a highly conserved N-linked glycosylation site within the C_H2 domain at Asn297 of the Fc region; however, carbohydrates might also be present in other locations. The sugar constituents of glycoproteins contain vicinal hydroxyl groups that are prone to easy oxidation by treatment with periodic acids or

its salts. Once oxidized to dialdehyde, these sites can be specifically targeted with amine containing reagents (9-11, 13).

In summary, under most conditions, proteins may contain about nine amino acids that are modifiable at their side-chains: aspartic acid, glutamic acid, lysine, arginine, cysteine, histidine, tyrosine, methionine, and tryptophan. These nine amino acids contain eight side-chain groups for functional modifications: primary amines, carboxylates, sulfhydryls (or disulfides), thio ethers, imidazolyls, guanidinyl groups, and phenolic and indolyl rings. Besides amino acids, carbohydrates in proteins can also serve as an alternative target for conjugation purpose.

3.1.5. Dye-antibody conjugation methods

To understand the miniature world of cells and functioning of its biomolecular machinery, antibody conjugates are the first-hand choice reagents. Bioconjugation of proteins extends the advantages offered by a single molecule by combining the features of different proteins used in conjugation. Thus, they make them functionally more potent, stable or multimodal. Although, several molecules, practically everything with appropriate functional groups, can be conjugated to antibodies, we would consider fluorophores as an example in this chapter to explain the chemical reactions and the interplay of functional moieties that establish the covalent linkage between reactant fluorophores and an antibody. Furthermore, only direct covalent linkage between fluorophores and antibodies will be reviewed here, which means that cross-linkers, adaptor based conjugation or non-covalent reactions with the antibody will be excluded from discussion though it may follow similar reaction mechanisms.

Modification and conjugation approaches are dependent on two interrelated chemistries: the reactive functional groups on the fluorophores and the relevant side-chains on the target antibodies. Most importantly, the bioconjugation process should exclude any interference with the characteristic features of both proteins. Therefore, careful selection of the functional group is critical to circumvent any related interferences. In general, only three functional groups in any proteins, including antibodies, are the primary sites for modifications and covalent linkage: amines ($-NH_2$), thiol groups (-SH) and carbohydrate residues (hereon, it would be denoted as -CHO since aldehyde is formed after oxidation of sugars) (9, 11).

3.1.5.1. Amine (-NH_2) targeted fluorescent labels

Owing to the abundance of lysine residues in antibodies and existence of various methods to selectively modify primary amines, the favorite reactive group has always been amino groups. The principal coupling reactions for modification of amines proceed either by acylation or alkylation. Furthermore, high yield of conjugates form very easily with rapid reactions producing a stable amide bond or secondary amine bonds. The main classes of acylating fluorophores are isothiocyanates, isocyanates, N-hydroxysuccinimidyl (NHS) esters, acyl azides, carbodiimide, anhydrides and sulfonyl halides. Similarly, aldehydes and glyoxals, epioxides and oxiranes, and arylating agents form amine bonds with protein. The advantages of NHS ester fluorophore over other fluorophore derivatives are manifold since these fluorophores create stable bonds, achieve conjugation at pH 7.5-8.5 and offer selectivity towards aliphatic amines of protein. This is the primary reason why the most common amine-reactive cross linking or modification reagents commercially available today utilize NHS esters. In rest of the paragraph, the chemistry of NHS esters with amines in proteins is presented. Lysines are usually on the outside surface of a native protein at physiological pH due to its positive charge. Since the ionization potential is different for α-amine and ε-amine of lysine, their pKa value is also different thus allowing selective conjugation by controlling the pH of the conjugation buffer. At pH values lower than 9.3-9.5, ε-amine is usually protonated contributing a positive charge to the protein, while, at pH values greater than the pKa, the amines are unprotonated offering no net charge in the protein. NHS ester fluorophores react with primary amines in antibodies to form stable amide bonds in mild alkaline conditions. The reaction releases N-hydroxysuccinimide as a byproduct (**Figure 2**). Since, primary amine containing groups are distributed throughout the surface of the protein, -NH_2 based conjugation results in binding of fluorophores/cross-linkers at unknown locations (9).

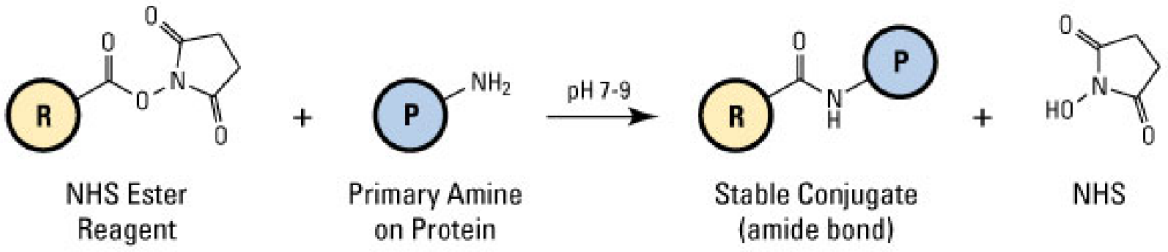

Figure 2. Schematic representation of a chemical reaction between NHS ester and primary amine. (R) represents an ester group in a fluorescent dye and (P) represents a primary amine group in an antibody (Adapted from Pierce's website, http://www.piercenet.com).

3.1.5.2. Sulfhydryl (-SH) targeted fluorescent labels

Thiolate ion is the most reactive functional group in proteins. Thus, they are the second most common targets for protein modification. However, cysteine is the only amino acid which possesses sulfhydryl groups; therefore, it is less prevalent in proteins. Often cysteine is present as a dimer, or cystine, as a result of disulfide bridge (-S-S-). Furthermore, cysteine is relatively hydrophobic and is the least exposed amino acid on the surface of proteins. Thus, they are typically buried within the polypeptide structure. Cystine residues hold and provide stability to the conformation of an antibody. Typically, only free or reduced -SH groups can react with thiol-reactive fluorophores. Therefore to access the -SH groups, an antibody must be cleaved with reducing agents. Compared to $-NH_2$ targeted conjugation; -SH method is more selective and ensures consistent labeling at a defined location in proteins. Also -SH targeted method provides greater certainty about the preservation of ABS and the uniformity in the density of labels in antibody after conjugation. Primarily, thiol based coupling reactions are achieved by either alkylation (usually the formation of thioether bond) or disulfide exchange (formation of a disulfide bond). Sulfhydryl-reactive chemical groups include maleimides, haloacetyls, aziridines, acryloyls, arylating agents, vinylsulfones, pyridyl disulfides, TNB-thiols and disulfide reducing agents. Since maleimides are specific for -SH groups within the pH range of 6.5-7.5, fluorophores or cross-linkers with maleimide groups are the preferred choice for sulfhydryl reaction. In addition, at pH 7.0, the reaction of maleimides to sulfhydryls is about 1000 times greater than its reaction with amines, allowing specificity in modifications by controlling the reaction with the pH of the conjugation buffer. A nucleophilic addition reaction occurs between maleimide and -SH groups resulting in a stable thioether bond (**Figure 3**). Reducing agents like mercaptoethylamine, MEA or dithiothrietol, DTT is generally used to cleave antibodies into two monovalent halves (9, 11).

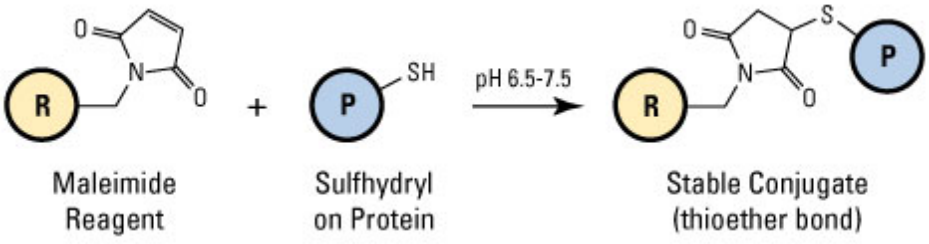

Figure 3. Schematic representation of a chemical reaction between maleimide dyes and reduced antibody containing sulfhydryl groups. (R) represents a maleimide group in a fluorescent dye and (P) represents a reduced antibody with the target sulfhydryl group,-SH (Adapted from Pierce's website, http://www.piercenet.com).

3.1.5.3. Carbohydrate (-CHO) targeted fluorescent labels

In most IgGs, a few carbohydrates are present within the Fc region. However, carbohydrates are not efficiently reactive towards any functional groups in normal condition. Therefore, modification of carbohydrates is required to generate reactive moieties. Aldehyde and ketone groups are reactive carbonyls (C=O) and can be easily produced from carbohydrates by gentle oxidation. Usually, a mild reagent like sodium periodate ($NaIO_4$) is used for oxidizing vicinal diols in carbohydrate sugars to yield aldehyde groups. The aldehydes can then be specifically targeted with a hydrazide or alkoxyamine containing fluorophores or cross-linkers. Since, carbohydrate moieties are located within the Fc region far from the ABS, such modification and subsequent conjugation are presumed to be site specific ensuring preservation of ABS. The reaction between electrophilic aldehyde and nucleophilic hydrazide proceeds efficiently at pH 5 to 7, resulting in the formation of hydrazone bonds (**Figure 4**) (9, 11, 13). The reaction rate can further be enhanced by using a catalyst like aniline (14). In most cases, reducing agent like sodium cyanoborohydride can also be used to stabilize the bond between aldehyde and hydrazide (9, 11, 13).

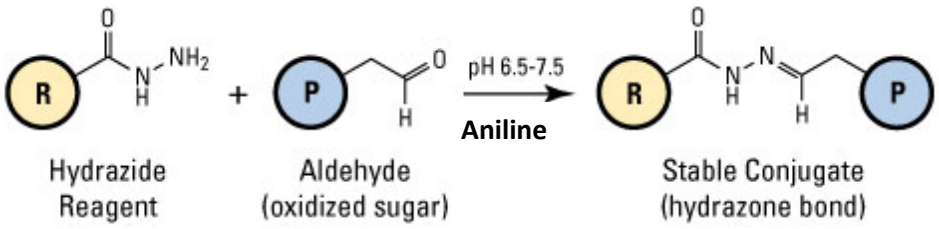

Figure 4. Schematic representation of a chemical reaction between hydrazide dyes and oxidized antibody containing aldehyde groups. (R) represents a fluorescent hydrazide dye and (P) represents an oxidized antibody with an aldehyde group (Adapted from Pierce's website, http://www.piercenet.com).

3.2. Application of dye-antibody conjugates

The natural propensity of the antibody molecules to metamorphosis makes them ideal probes for new applications and therapeutic challenges. The ubiquitous use of antibodies is primarily due to their high degree of affinity and specificity towards a particular region, an epitope, of an antigen making them hugely effective. As a reagent, no other material has contributed to this degree of success directly or indirectly to such a vast array of scientific discoveries. Accordingly, Mabs served as a panacea to most, if not all, biological problems. The areas of applications of antibodies are so wide that it is no way possible to elaborate each of them here.

Fluorescence methods are very versatile, can be applied to any system, and are easier to measure with incomparable efficiency. Particularly, the specificity of an antibody and the sensitivity of fluorescence allow the possibility of measuring small concentrations of molecules, observe the dynamics of molecular interactions, determine the cellular origin and location of molecules and follow the behavior of biological species in real time. Therefore, as an application of antibody conjugates, we have used dye conjugated fluorescent antibodies in determining the two-dimensional topological distribution of CD1d on the plasma membrane of a B lymphocyte. The main reasons for choosing this protein was the paucity of data regarding the distribution features of CD1d in the plasma membrane, our interest in MHC membrane biology, and the importance of CD1d expression in B lymphoid lineages. Though, the main focus of this section is CD1d protein, a comparison would be made throughout the paragraphs with other CD1 isoforms and MHC proteins.

3.2.1. Antigen presenting cells (APCs)

Cells with the capability to activate or prime naive T cells and initiate an adaptive immune response are termed APCs. These cells express dedicated special carrier proteins, for instance, MHC and CD1 proteins, efficient in displaying antigens on the cell surface as a carrier-antigen complex which could then be recognized by T cells (1).

3.2.1.1. B cells

B cells constitute 5–15% of human blood lymphocytes. Progeny of the lymphoid progenitors (LPs), which are derived from hematopoietic stem cells, gives rise to B lineage cells (15, 16). The most unambiguous marker of a B cell differentiation is the expression of Ig heavy (H) and light (L)

chains (16, 17). The Ig heavy chain variable region is generated by the joining of three gene segments, VH (variable), DH (diversity), and JH (joining), whereas the k and λ variable light chains are formed from VL and JL segments (16). They later evolve into BCRs.

3.2.1.2. B cells as antigen presenting cells

Though not as efficient as dendritic cells (DCs) in antigen presentation, B cells are definitely the most focused group of APCs. It is believed that the primary function of B cells is to initiate a humoral response rather than promulgating T cell responses unlike in the case of DCs. Resting B cells constitutively express high levels of cell surface MHC II but do not express co-stimulatory molecules; however, like macrophages once activated, B cells become a potent APC (18-21). Naive B cells migrate from bone marrow to secondary lymphoid tissues where they are able to encounter antigens. B cells are poorly phagocytic, nevertheless; they acquire exogenous proteins either by a receptor-independent mechanism, such as fluid phase pinocytosis, or specifically, through a receptor-mediated mechanism such as BCR-mediated endocytosis (21-23). Once inside the cells, these antigens are processed and are displayed together with MHC II on the plasma membrane that stimulates (and in turn receives help from) T cells, linking the specificity of the humoral and T cell responses. However, presentation of exogenous antigens on MHC I is poorly described in B cells and probably quite limited (18). Interestingly, two groups have recently confirmed phagocytic activity among B lineage cells in mice. Phagocytic features were found among B cells in the peritoneal cavity (24) and liver B1 and B2 subsets as well as splenic marginal zone B cells (25), accompanied by bactericidal and antigen-presenting capacities.

3.2.2. T cells

About 70% of human blood lymphocytes are T cells. Like B cells, T lymphocytes also originate from LPs. The main functions of T lymphocytes are to exert effects on other cells, either by regulating the activity of cells of the immune system or by killing cells that are infected or malignant (26). Like BCRs, the T cell receptors (TCRs) genes undergo V (D) J recombination of gene segments to produce a repertoire of receptors with immense sequence diversity. Based on functional behavior, T lymphocytes could be divided into two subsets: conventional adaptive T cells and innate like T cells. Classical T cells display αβ TCRs and respond to MHC antigens,

whereas, innate like T cells either have γδ TCRs or respond to non-peptides in an MHC independent fashion (1, 27). γδ T cells represent only a fraction (<5%), of the total T lymphocytes and are at their highest abundance in the gut mucosa. Recently a subtype of activated human γδ T cells, termed $V\delta2^{+}$T cells, was also reported to have potent antigen-presentation features similar to those seen in DCs (28). However, the exact nature and functional ability of these groups of cells still remain largely unexplored.

3.2.3. Natural Killer (NK) T cells

NK T cells are lymphoid lineage innate T cell subsets that combine several features of conventional T lymphocytes and NK cells. NK cell markers (DX5 and NK1.1 in mouse and CD56 in human) and T cell markers (CD3, CD5 and CD4) are found in NK T cells. They are activated early during infection and rapidly secrete cytokines upon activation, thus, are subjects of potential targets for therapeutic intervention. All these features portray NK T cells as an important link between innate and adaptive immunity (29, 30). Based on the diversity of TCRs and localization of NK T cells, it is divided into three subsets: type I or invariant NK (iNK) T, type II NK T and NK T-like cells. In this thesis, we have used CD1d restricted iNK T cells for co-culture assays, therefore, we will briefly describe about the immunological features of these cells here. iNK T cells express a conserved TCR α chain, Vα14-Jα18 in mice and Vα24-Jα18 in humans, associated with a limited set of TCR β chains (Vβ2, 7 or 8.3 in mice and Vβ11 in humans). iNK T cells have been found to be pivotal during immune responses against pathogenic infection, allergy, autoimmune diseases, inflammatory diseases and cancer. Furthermore, they also produce cytokines, chemokines and surface molecules which immunomodulate the phenotypic and functional features of other cells including NK cells, macrophages, neutrophils, B cells and DCs. The importance of iNK T cells is also underlined by the fact that these cells are either impaired in function or are decreased in number in various autoimmune diseases and obesity. However, the exact mechanisms how these cells are activated during a variety of disease still remain an unsolved problem. In addition, lipid antigens that activate iNK T cells have been shown to be excellent candidates as vaccine adjuvants. Clinical trials using α-galactosylceramide (α-Gal)-loaded autologous DCs to target iNK T cells and in vitro-expanded autologous NK T cells have also shown promise in treating cancer patients. Therefore, unraveling the features of iNK T cell activation would be crucial in understanding the iNK T cell biology and determining the success of iNKT cells based therapeutics (31-33).

3.2.4. Cytokines

Cytokines (Greek *cyto*-, cell; and *-kinos*, movement) are low molecular weight peptides or glycoproteins of diverse structure, which mediates intercellular communication. Cytokines are soluble in nature, and they exert their effects in a paracrine or autocrine fashion by binding to specific receptors on the cell surface. Leukocytes primarily produce cytokines; however, some non-hematopoietic cells can also synthesize these modulatory molecules (1).

3.2.5. Antigen presentation

APCs decorate their cell surface with antigen-bound carrier molecules, MHC or CD1d, which is recognized by TCRs in T cells. This process of antigen displaying features in APCs is known as antigen presentation. There are two major modes of antigen presentation: conventional antigen presentation and non-conventional antigen presentation.

3.2.6. Conventional antigen presentation

This mode of antigen presentation only considers peptide to be antigenic thus describes only peptide antigen presentation scheme. Peptides for antigen presentation are generated in the cellular system following two major routes. Endogenous proteins undergo cytosolic peptide processing pathway operated with the help of cytosolic proteases and proteosome complex. It is an MHC I dependent pathway and activates $CD8^{+}$T cells, specifically (18, 34, 35). In contrary, exogenous proteins follow a proteosome independent an exogenous peptide processing pathway. The peptide antigens are processed and generated in endocytic compartments where it is loaded onto MHC II proteins. It leads to the activation of helper $CD4^{+}$T cells and effective generation of antibodies against the antigen in display (1, 34-36).

3.2.7. Non-conventional antigen presentation

Although the conventional antigen presentation is stringently followed in the immune system, there are few exceptions to this scheme, which could be termed non-conventional antigen presentation. Here, we will only name the modes of antigen presentation, for a complete description, please visit the associated references:

3.2.7.1. Cross-presentation

Peptide antigens crossover from the exogenous pathway to endogenous pathway, and subsequently are presented by MHC I proteins (1, 35, 37).

3.2.7.2. Cross-dressing

It involves the transfer of antigen pre-loaded MHC I molecules from the surface of infected APCs to uninfected APCs (1, 38).

3.2.7.3. Peptide regurgitation

Exogenous proteins are processed by endocytic machineries; however, antigens are then released ("regurgitated") into the extracellular environment, and subsequently, they replace or occupy MHC binding groove (1, 39, 40).

3.2.7.4. Peptide interception

It involves loading of MHC I proteins in MHC II containing compartments (MIIC) (1).

3.2.7.5. Non-peptide antigen presentation

It covers the presentation of non-peptide antigens like vitamins (41), carbohydrates (42, 43), pyrophosphate (44, 45), and lipids (46). Though, the field of vitamin and carbohydrate antigen presentation is still emerging, next section will specifically focus on CD1 protein that performs lipid-based antigen presentation.

3.2.8. CD1 proteins

3.2.8.1. Evolution of CD1 proteins

CD1 functions as antigen presenting molecule like MHC proteins. Therefore, it is presumed that the evolution of CD1 is intimately connected to the larger story of the evolution of MHC. Accordingly, similarities in greater extent are found between CD1 and MHC I proteins in amino acid sequence alignments and crystal structure (47). However, CD1 homologs were not detected in teleosts and sharks but are present in birds and mammals; therefore, it is suggested that CD1 may not be as old

as MHC I (47-52). Nonetheless, the precise age of CD1 relative to MHC I has remained largely unknown; this would require comprehensive genome sequence data from additional extant amphibian, reptile, and fish species.

3.2.8.2. Genomic distribution and features of CD1 genes

The human CD1 locus spans ~175 kilobases as a tight cluster of genes on the long arm of chromosome 1 thus is located distantly to MHC genes present on chromosome 6 (53, 54). In mice, CD1 locus is located on chromosome 3 (55). The human CD1 gene family is comprised of five nonpolymorphic genes (CD1A, -B, -C, -D, and -E) (56). The intron/exon structure of CD1 genes is analogous to that of MHC I genes (57). The genomes of mice and rat possess only CD1D genes. In fact, duplication of CD1D genes (CD1D1 and CD1D2) seems to have occurred in mice while only single CD1D gene is found in rats. The homology between specific CD1 isoforms (orthologs) is typically higher between two mammalian species than among the multiple CD1 isoforms (paralogs) within a given species. Notably, the characteristic polymorphism of MHC genes is very limited in CD1 genes thus they are highly conserved (47, 58, 59). Only two alleles have been described for CD1 A, -B, -C, and -D genes in various ethnic groups (60, 61), whereas, CD1e seems to be the most polymorphic CD1 gene. Six alleles of CD1e have been reported so far. Most mutations were found in the exon 2 and exon 3 regions, which encode the α1 and α2 domains of the CD1 proteins (62-64). Apart from a few exceptions; these mutations within the CD1 genes were either silent or positioned on an irrelevant site away from the antigen binding pocket probably having none or minor effects on lipid antigen presentation (58, 60, 61). Few of the recent studies highlighted the biological relevance of CD1 gene polymorphism, especially in intracellular distribution and localization of the human CD1e variant affecting antigen presentation (64) and defective antigen presentation by mouse CD1d mutant (65). Gene conversion is the major force generating the HLA diversity, however, with the available information; the CD1 locus seems to evolve essentially through point mutations. In particular, no correlations have been found between CD1 gene polymorphism and most diseases, including various types of cancers (59) and infectious disease (66), except some conflicting reports on Guillain-Barre syndrome (67-69). However, some studies have lately identified the positive correlation features of CD1A and -E polymorphism in an autoimmune multiple sclerosis disease (70, 71).

3.2.8.3. Classification, morphology and structure of CD1 proteins

CD1 was the first human differentiation antigens to be identified by Mab (NA1/34; CD1a) on human thymocytes (72). Structural features of CD1 proteins are similar to that of MHC I heavy chain (MHC I-HC) proteins and consist of three extracellular domains (α1, α2 and α3), a transmembrane domain and a short cytoplasmic tail necessary for receptor-mediated endocytosis (except for CD1a, which lacks any internalization motif). All CD1 family members are highly homologous (70-88) % in the α3 domain. This homology is low for α3 domains of MHC I-HC and CD1 proteins (~21%) (56, 73, 74). Depending on the degree of amino acid and genomic sequence homology and immunological functions, CD1 proteins were divided into three subgroups: Group I (CD1a, CD1b and CD1c), Group 2 (CD1d) and Group 3 (CD1e) (56, 58, 75, 76). Like MHC I-HC, CD1 proteins are generally expressed as a β_2-microglobulin (β_2m) bound heterodimer on the cell surface except for CD1e, which is localized in various intracellular compartments and is absent from the plasma membrane. Primarily, β_2m is found to be very important for the surface expression of CD1 a, -b, -c, and -d proteins (77, 78). However, β_2m independent isoforms that is not bound to β_2m have also been reported for CD1d proteins (79, 80); though immunological functions of these β_2m free CD1d heavy chains (CD1d-HCs) are not well understood. All CD1 proteins have a peptide backbone of approximately 33 kDa molecular mass, nevertheless; variation in mass does occur among the CD1 proteins due to the linked glycans. CD1a, -b, and -c have masses of 49, 45, and 43 kDa (81, 82) whereas CD1d has a mass of 48 or 45 kDa in the presence or absence of β_2m proteins due to differences in the intracellular glycan processing (56, 80). The α1 and α2 regions of the extracellular domains form the antigen-binding groove in CD1 proteins exactly like in the case of MHC I-HC with similar characteristic of two antiparallel α-helical structures lying atop a floor of six β-pleated sheets. The α3 domain, binds with β_2m, and is proximal to the membrane. The 3D structure of domains in α3-β_2m association is largely conserved among CD1 proteins and with MHC I-HC. The inner surface of the antigen-binding grooves of all CD1 molecules consists of non-polar amino acids suited for binding lipids (83). All CD1 proteins except CD1e, which facilitates antigen processing (84, 85), are directly involved in the lipid antigen presentation to T cells (76). The structures of all CD1 proteins with / or without lipid ligands are presented in **Figure 5**.

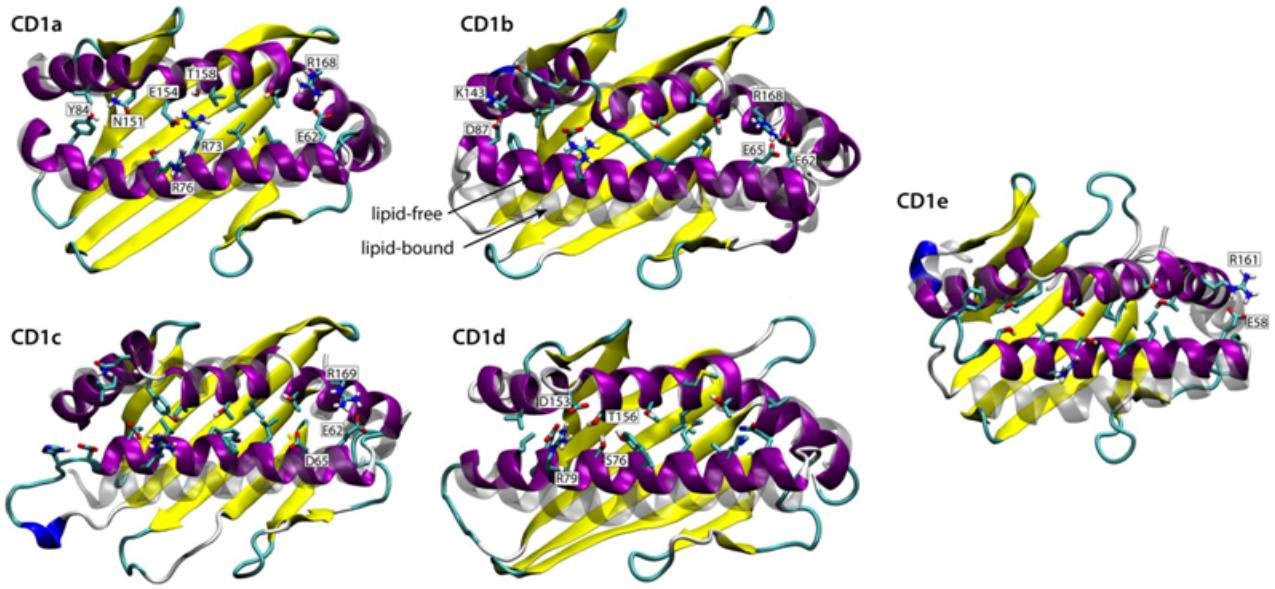

Figure 5. Simulation snapshot of each CD1 binding domain in the lipid-free state. Each domain is represented in the cartoon-format, colored according to the secondary structure; the configuration of helices α1 and α2 in the respective crystal structures are overlaid (fitted to the α2 helix backbone), and showed in transparent gray. Side-chains of key residues in α1 and α2 are labeled (86). (Adapted from Garzon, D. et al, J Biol Chem 2013)

3.2.8.4. CD1 expression and tissue distribution

The expression of CD1 proteins has been extensively studied in humans and rodents. Group 1 CD1 proteins are almost exclusively found on immature cortical thymocytes, mainly DP thymocytes (87), and various specialized APCs. Primarily, peripheral DCs express CD1a and CD1b while DCs and a subset of B cells can express CD1c (56, 88, 89). CD1a, -b, and -c are also used as markers of DC in humans. Langerhans cells express CD1a, a key phenotypic marker, and also express CD1c, but appear to lack expression of CD1b (90-92). In contrary, Group II CD1d proteins are heterogenous in distribution found in cells of both hematopoietic and non-hematopoietic origin in human and mice (92). CD1d is expressed on B cells (93), macrophages (94), freshly isolated monocytes (93, 94) and DCs (94). The expression of CD1d, but not of Group I CD1 molecules, is also acknowledged in epithelial cells from the intestine (95), skin (96) and liver (97, 98). Most Group II CD1d is undetectable in resting peripheral T cells, but it is inducible with certain chemicals. Interestingly, Group I CD1 proteins are downregulated by mature thymocytes and peripheral blood T cells. Upregulation of Group I CD1 proteins, but not CD1d, were also seen during differentiation of blood monocytes into immature DCs with granulocyte macrophage-colony

stimulating factor (GM-CSF) and Interleukin 4 (IL4) (93, 94). The components of serum are also found to promote or inhibit the expression of CD1 proteins. The prominent serum lipids, cholesterol and cholesteryl stearate had no effect on the expression of Group I CD1 proteins whereas lysophosphatidic acid and cardiolipin were found to be inhibitory on CD1a, -b, -c expression in DCs (99). In addition, the presence of Igs in serum inhibited the expression of Group I CD1 proteins while it favored the up regulation of CD1d proteins in the plasma membrane (100).

3.2.8.5. CD1 assembly, trafficking and antigen sampling

Not only, the structural features are similar between CD1 and MHC I-HC, but their assembly with β_2m and the requirement of chaperones, calnexin, calreticulin, ERp57, etc., have also been synonymously described. α1, α2 and α3 domains of CD1-HC are on the lumenal side of the endoplasmic reticulum (ER), whereas, the short tail is towards the cytoplasmic side. Glycosylation of the newly translocated CD1 α- chains occur at ER by resident glycosidases, which enable them to bind chaperones. Thus, maturation of CD1-HC is analogous to that of MHC I-HC (101). Studies suggested that CD1-HCs form a complex with chaperones, calnexin and calreticulin, while MHC I-HC associates only with calnexin. Disulfide bond formation in both proteins is mediated by the later recruitment of thiol oxidoreductase ERp57 (101-103). Inability to associate with these chaperones has been found to induce degradation of these proteins through proteosomes (103). In addition, association of β_2m to MHC I-HC and CD1-HC proteins are very important for proper glycosylation, degradation evasion and ER exit of HCs (80). Though the majority of heavy chains associate with β_2m to escape ER, a small but significant fraction of CD1d-HCs is also able to travel from ER to plasma membrane independently of β_2m (80, 102, 104). Peptide loading of MHC I and MHC II proteins in the ER is an essential step for their transport to other cellular sites. Though, diversity and generation of endogenous lipids still remains an open field, similar roles of endogenous lipids have been envisaged in stabilization of a CD1 containing protein assembly in ER (101, 105-107). After assembly and glycosylation dependent maturation, MHC I traffics to the plasma membrane for antigen presentation, whereas, MHC II travels to endosomal vesicles for exchanging invariant chain with foreign peptides. In the case of CD1 proteins, most CD1 traffic to the plasma membrane through the secretory pathway, although a small fraction may directly route to endosomes, before being reinternalized within different endosomal compartments to gather lipid antigens, and subsequently reemerges on the cell surface (**Figure 6**). Each of the CD1 isoforms has

evolved a different subcellular localization and trafficking behavior, thus, rendering them suitable for sampling a wide range of foreign and self-antigens. The steady-state distribution among endocytic compartments and intracellular trafficking of each type of CD1 proteins is mainly dependent on the cytoplasmic YXXZ motif (where Y =tyrosine, X =any amino acid, and Z =bulky hydrophobic residue) present in their CD1 tail conferring them the ability to bind cytosolic adaptor proteins (APs) that influence the cellular localization of these proteins. CD1a has a short cytoplasmic tail without any tyrosine based sorting motifs; therefore, it does not follow clathrin-mediated endocytosis. Instead, it undergoes AP-2, clathrin- and dynamin-independent endocytic pathways. Internalization of CD1a occurs in an ADP-ribosylation factor (ARF) 6-dependent manner preferentially to early recycling endosomes and is largely excluded from late endosomes. This is very much similar to the intracellular trafficking pathways followed by MHC I proteins. Unlike CD1a, other CD1 proteins CD1b, CD1c and CD1d contain cytoplasmic YXXZ motif, which helps them to bind AP-2 protein thus they get internalized through clathrin-coated pits. Mouse CD1d and human CD1b can also bind AP-3. CD1b and CD1d are almost exclusively found in the late endosomes and lysosomal vesicles while partial/sparse distribution of CD1c is found in these compartments. Interestingly, despite the presence of similar cytoplasmic tyrosine-based motif, human CD1c does not bind AP-3 in yeast two-hybrid assay (108) implying the existence of an AP-3 independent pathway for CD1 trafficking to lysosomes. In immature DCs, CD1e predominantly accumulates at the trans-Golgi network (TGN), whereas, in mature DCs, it is found in late endosomes and lysosomes where it is cleaved into a stable soluble form (109, 110). In addition, CD1d can alternatively route to lysosomes and MIIC based on its interaction with the invariant chain (111, 112). The capability of CD1 proteins to penetrate endosomal compartments in human and mouse can be ranked in the increasing order as huCD1a\huCD1c\huCD1d\huCD1b and muCD1d. Since, CD1 proteins undergo multiple rounds of recycling between the plasma membrane and intracellular compartments, these proteins may be capable of repeated sampling of various endosomal compartments.

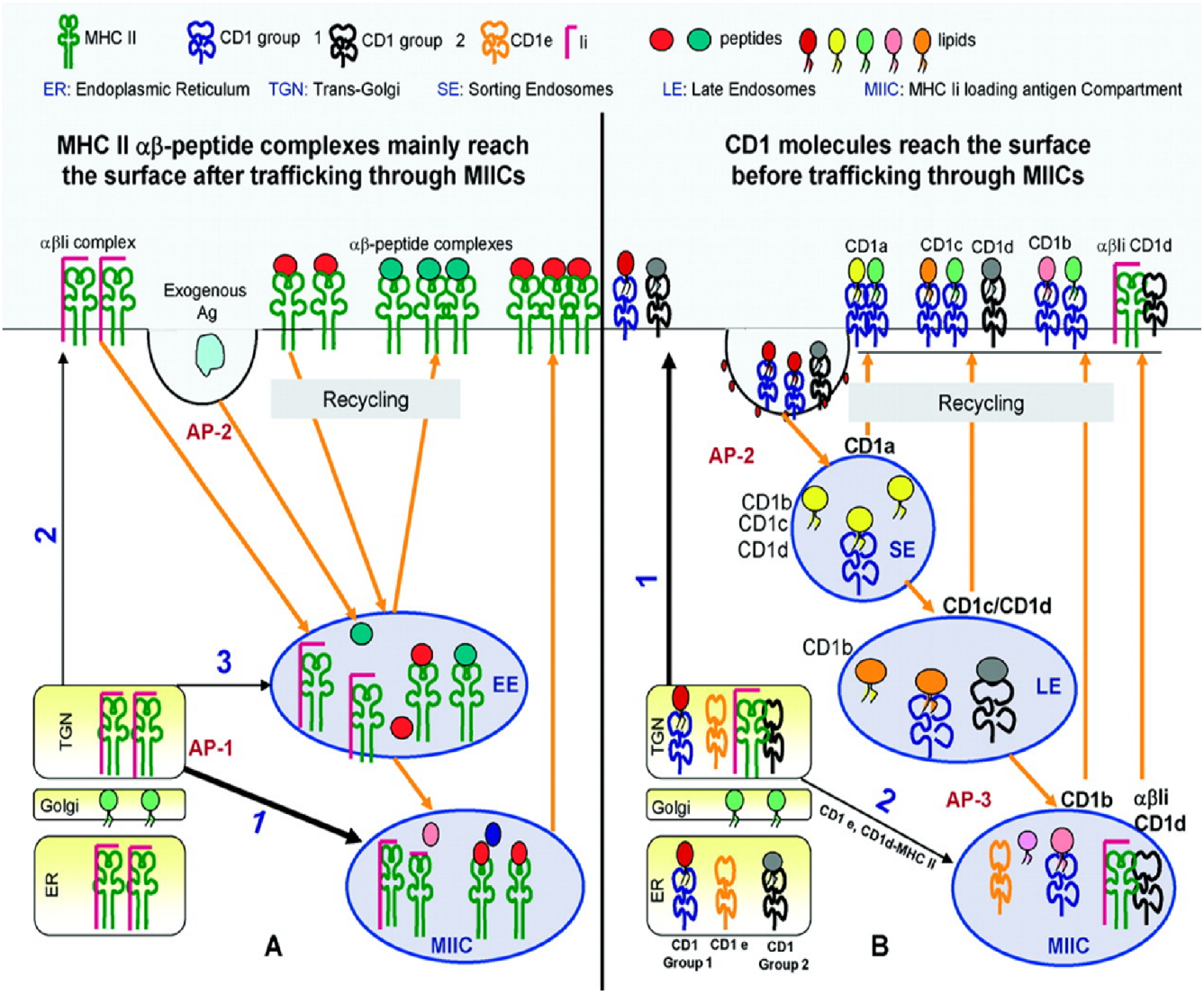

EE – Early Endosome; SE – Salvaging/Recycling Endosome; LE – Late Endosome; Ii- Invariant chain; αβ – subunits of MHC II
Numerical 1, 2 and 3 represent preferential routes by MHC II and CD1d.

Figure 6. Cellular trafficking modes of CD1 and MHC II proteins (113) (Adapted from Gelin, C. et al, J Leukoc Biol 2009)

(A) Journey of MHC II proteins from intracellular compartments to plasma membrane and vice versa.
(B) Journey of CD1 proteins from intracellular compartments to plasma membrane and vice versa.

3.2.8.6. Mechanism of lipid-antigen generation

The general molecular mechanisms governing lipid-based antigen presentation pathway reflect peptide antigen presentation pathway. It also acquires and generates antigen through cellular processes that facilitate uptake, processing and loading of compartmentally localized antigens in CD1 proteins. Although much remains to be understood, extraneous lipid particles are considered to be taken up by cells in surface receptor dependent and independent ways (114). Participation of scavenging receptors (115), low-density lipoprotein (LDL) receptors (114-116) and C-type lectin receptor (117, 118) in the CD1 antigen presentation pathway was also highlighted in recent studies. Thus, surface receptors mediated endocytosis is the dominant way of engulfing exogenous lipid antigens, although, indirect mechanisms of plasma membrane internalization through rafts, caveolae and other processes, including micropinocytosis can also contribute lipid antigens for presentation by CD1 molecules (101, 114). Depending on the place where they are generated, antigenic lipids are either self or non-self in origin. Non-self lipids are primarily products of microbes or environmental sources, though, our body can also contribute towards the production of aberrant lipids during abnormality. Because, many of the pathogen-associated molecular patterns (PAMPs) associated with microbes are lipids, CD1-restricted responses are very important in anti-microbial defenses. Endogenous self-glycolipids, such as isoglobotrihexosylceramide (iGb3) have β-linkages, while exogenous/pathogenic glycolipids (i.e., most bacterial glycolipids) typically have α-linkages. The first lipid antigen to be discovered was mycolic acid from *Mycobacterium tuberculosis* in 1994 (119).The most antigenic self-lipids are either glycosphingolipids (GSL) or phospholipids (PL). Some GSL, such as sulphatide, form stimulatory complexes with all CD1 molecules, thus behaving as promiscuous antigens (120). CD1a, CD1c and CD1d are flexible and can load short lipids at neutral pH, although, loading is enhanced at acidic pH. In contrast, CD1b favors endosomal acidification to bind lipids with very long aliphatic chains such as the mycolic acids and mycolate-containing glycolipids of mycobacteria. Typical examples of antigenic lipids presented by CD1 isoforms are presented in **Table 1** (114). Among all CD1 isoforms, CD1d is the best characterized glycoprotein and this is primarily due to the discovery of a GSL, α-gal, isolated from the marine sponge, *Agelas mauritianus*, which was serendipitously shown to activate the majority, if not all, mouse and human NKT cells (121). In addition, lack of group I CD1 tetramers and specific markers to identify group I CD1-restricted T cells, in conjunction with

the absence of expression of group 1 CD1 molecules in mice, have all hindered scientific advances in the study of group 1 CD1-restricted T cells.

Lipid class	Lipid name	Cellular compartment	CD1
Sphingolipids	Sphingomyelin	Golgi	sCD1d
			lyCD1d
			sCD1c
Acidic GSL	Sulfatide	Golgi	sCD1d
	LacCer	Golgi	sCD1d
	GM1	Golgi	sCD1d
	GM2	Golgi	sCD1d
	GM3	Golgi	sCD1d
	GD1a	Golgi	sCD1d
Neutral GSL	Di-hexosylcer	Golgi	sCD1d
	Tri-hexosylcer	Golgi	sCD1d
	Gb3	Golgi	sCD1d
	Tetra-hexosylcer	Golgi	sCD1d
	Asialo-GM1	Golgi	sCD1d
	Asialo-GM2	Golgi	sCD1d
Phospholipids	PA	ER	sCD1d
	PE	ER	sCD1d
	PC	ER	sCD1d
			lyCD1d
			sCD1b
			sCD1c
	PG	ER	sCD1d
	PS	ER	sCD1d
	PI	ER	sCD1d
			sCD1c
	CL	Mit	sCD1d
	Lyso-PE	Ly	sCD1d
			lyCD1d
	Lyso-PA	Ly	sCD1d
	Lyso-PG	Ly	sCD1d
	Lyso-PI	Ly	sCD1d
	Lyso-PC	Ly	sCD1d
			lyCD1d
	Lyso-PS	Ly	lyCD1d

CL, cardiolipin; Gb3, globoside 3; GM1-3, gangliosides GM1-3; GSL, glycosphingolipid; hexosylcer, hexosylceramide; LacCer, lactosylceramide; Ly, lysosomes; lyCD1d, lysosomal CD1d; Mit, mitochondria; PA: phosphatidic acid; PC: phosphatidylcholine; PE: phosphatidylethanolamine; PG:phosphatidylglycerol; PI: phosphatidylinositol; PS: phosphatidylserine; sCD1b, soluble CD1b; sCD1c, soluble CD1c; sCD1d, soluble CD1d. Cellular compartment indicates where the lipid is generated.

Table 1. Lipids found associated with CD1 molecules (114) (Adapted from De Libero, Trends in immunology (2012)

3.2.8.7. CD1d associated molecules and its biological implications

The plasma membrane is a highly dynamic structure and is composed of a multitude of various proteins and lipids. All biological functions performed by the membrane are presumed to be a result of compartmentalization and hierarchical organization of these molecules in compositionally and functionally variable "micro domains"" (122, 123). In this paragraph, the distribution and organization of CD1 proteins discovered on the membrane of various types of cells, mostly by biochemical methods are discussed. The possible biological implications of such molecular organizations are also elaborated. However, the chaperones and the APs which are covered in the earlier section and are mainly involved in the maturation and trafficking of CD1 proteins are not reviewed here. Almost all known CD1 protein binds to β_2m both at intracellular compartmental vesicles and, if expressed, on the plasma membrane as well. The CD1 association of β_2m has been shown essential in the maturation and function of these glycoproteins. Earlier studies, mainly with CD1a and CD1d, also suggested the possible existence of multimolecular complexes of CD1, tetraspanin proteins (CD82 and CD9), invariant chain and MHC family proteins in DCs and B lymphoid cells (112, 124). The association of invariant chain or MHC II-invariant chain complex with CD1d within the cell has been assumed to promote the entry of CD1d to lysosomes and MIIC directly from the TGN rather than by endocytosis from the plasma membrane (111, 112). The co-localization of the invariant chain with CD1d on the plasma membrane has not yet been demonstrated, however, studies with CD1a isoform indicated that invariant chain would help in the endocytosis of CD1 proteins. Cell surface stabilization and increase in the expression of CD1a occurred when the invariant chain was silenced using siRNA (124). Interestingly, intermolecular complexes of three CD1 isoforms (CD1a, CD1b and CD1c) have also been reported on the cell surface of normal thymus cells but not in leukemic T cell lines (82). Normal thymic cells also showed the presence of molecular complex of CD1a and MHC I-HC/CD8 proteins on the plasma membrane (125). Similarly, association of a glycoprotein, gp180, with CD1d in the plasma membrane of intestinal epithelial cells was found to be involved in the activation of $CD8^+$ T cells and probably in the development of mucosal tolerance (126). A membrane-associated protein, Ig-like transcript (ILT4) was also reported to inhibit CD1d-mediated NKT cell activation by virtue of physically binding the antigen binding groove, α1 and α2 domains, of CD1d thus blocking the loading/exchange of lipid antigens. This interaction was identified both on the cell surface and endolysosomal compartments (127). Additionally, CD1c was recently discovered to interact with

ILT4 with stronger affinity than with CD1d. In this fashion, CD1c acted as a molecular sink controlling the inhibitory effect of ILT4 on CD1d mediated antigen presentation (128). Thus, the expression of CD1c and CD1d simultaneously in the same cell, like in B cells, T cells and DCs, might influence the functional activity of each other. This suggests that the proteins forming the molecular complex could modulate the functions of each other either positively or negatively. Furthermore, studies mainly in murine cell lines indicated that CD1d is localized in lipid-based dynamic nano-/micro- assemblies termed rafts/lipid-rafts in the plasma membrane (129-132). Rafts are presumed to facilitate clustering of functional protein units implicated in various biological activities. In the case of CD1a and CD1d, raft restricted localization was found to be critical in efficient signal transduction to the target T cells, especially at low ligand densities (124, 130, 132). Interestingly, unlike the features of conventional rafts which are detergent resistant, CD1d rich regions in the plasma membrane were sensitive to low concentrations of detergent in murine DCs. It was suggested that either CD1d is associated with rafts, mainly in intracellular membranes or that its association with the rafts in the plasma membrane is very weak (131). Additionally, the extent of localization of CD1d in the raft was shown to be an important determinant of immunological responses, Th1 or Th2, due to iNKT stimulation (133). So far, most studies have been performed only in murine cells. Though, similar kinetics of lipid loading have been observed for human CD1d molecules, systematic investigation of its plasma membrane features is yet to be performed.

3.2.9. Statin and antigen presentation

Statins are a class of drugs that is widely used as hypocholesterolemic agents for the treatment of elevated levels of LDL cholesterol in the blood. The cholesterol-lowering effect of statin is due to its inhibition of 3-hydroxy-3-methylglutaryl coenzyme A (HMG-CoA) reductase, a key enzyme in the cholesterol biosynthesis pathway. However, inhibition of HMG-CoA also leads to depletion of mevalonate, which is the precursor of isoprenoids that regulate diverse cellular functions. Thus, statins have pleiotropic effects primarily mediated by inhibition of the isoprenoid pathway which is independent of their cholesterol-lowering features (134). In fact, statin is found to diminish both MHC II and CD1d antigen presentation by hindering isoprenylation in B cells (135-137). Additionally, disruption or modification of rafts is also observed upon treatment with statin (138-140).

3.2.10. Fluorescence Resonance Energy Transfer (FRET)

Förster Resonance Energy Transfer, an initial term used for FRET, is a photo physical process whereby energy is transferred by an excited donor molecule to a neighboring acceptor molecule in a non-radiative fashion. Such a process of radiation less transfer of energy occurs when the molecular states of donor and acceptor are in resonance and the distance separating these molecules are only a few nanometers, typically from 1 nm and up to 10 nm. When both the molecules are fluorescent species then the transfer of energy results in the decrease in the donor chromophore emission that corresponds to an increase in the emission by the acceptor molecule. Additionally, the FRET efficiency is inversely proportional to the sixth power of the distance separating the donor and acceptor molecules. The rate of energy transfer efficiency thus shows strong distance dependence between the donor and acceptor (FRET pair) and therefore, it is also termed "molecular yardstick" or "spectroscopic ruler". Interestingly, such distances are within the edge of the regular protein dimensions and similar to multimeric protein complexes observed in biological systems; therefore, it is widely used to understand a great variety of molecular interactions in biological systems. FRET is non-invasive thus can be applied to monitor in real time the spatio-temporal changes of molecular complex, conformation of protein, biochemical activities, and particularly transient molecular associations, which govern the signal transduction pathways. Therefore, FRET holds several advantages over biochemical methods, which is associated with the disruption of cells to examine changes in the cellular events. The absence of FRET also does not necessarily mean the lack of molecular proximity. Such situations can occur due to molecular steric hindrances. Therefore, the relatively short FRET working distance constitutes a limitation for studying multi-protein complexes or interactions between big proteins. From a practical perspective, 5% energy transfer value is considered a threshold, thus any energy transfer values above or close to this value is a strong evidence for molecular associations (141-143).

The energy transfer efficiency is illustrated by the following equation:

$$E_{FRET} = \frac{R_0^6}{R_0^6 + R^6}$$

Where R_0, Förster radius or critical distance, is the characteristic distance at which FRET efficiency is 50%. In practice, FRET is sensitive to distance within the range between 0.5 R_0 and $2R_0$, as FRET efficiency varies from 98.5 to 1.5% in this interval. FRET efficiency is closer to the maximum at distances less than R_0, and minimum for distances greater than R_0.

4. AIMS OF THE THESIS

We wanted to compare the most common dye-antibody conjugation strategies pursued by researchers today with an objective to provide an informative guidance for choosing and optimizing critical conditions necessary for dye-protein conjugation. It was motivated by the fact that protein conjugation is a common practice and an important facet of research in most laboratories. With the help of a batch of dye-antibody conjugates, we also describe that such conjugates could serve as valuable probes in exploring the dynamics and topological features of membrane proteins. As an example, we have demonstrated the features of organization and distribution of CD1d proteins in the plasma membrane of human B cells in the second part of this thesis.

To summarize, we had the following goals to achieve:

Dye-antibody conjugation strategies

1. To optimize dye conjugation strategies targeting amine, sulfhydryl and carbohydrate functional groups in antibodies.
2. To lay out guidelines in performing site-specific antibody conjugations.
3. To determine the efficiency, yield of conjugation, ease in performing the dye-antibody conjugations and financial cost involved in such procedures.
4. To illustrate the advantages and disadvantages related to each of the dye-antibody conjugation methodologies.

Membrane distribution of CD1d proteins

1. General features of CD1d distribution in the plasma membrane of B lymphocytes.
2. Relationship between CD1d and MHC proteins in the plasma membrane.
3. Role of cholesterol in the organization of CD1d proteins in the plasma membrane.
4. To characterize CD1d enriched regions in the plasma membrane of B cells.

5. MATERIALS AND METHODS

5.1. Antibodies and dyes

In our study, we used the following Mabs: the pan-MHC I W6/32 (recognizes MHC I-HC in complex with β_2m, IgG2a) (144, 145), HC-10 (recognizes free MHC I-HC, IgG2a) (145-148), L368 (anti-β_2m, IgG1) (149), L243 (anti-MHC-DR, IgG2a) (150), P2A4 (anti-intercellular adhesion molecule (ICAM1), IgG1) (151), OKT9 (anti-transferrin receptor (TfR), IgG1) (152), 51.1.3 (anti-CD1d, IgG2b) (93), and 27.1.9 (anti-CD1d, IgG1) (93). Antibodies were purified from supernatants of the hybridoma cell lines by Sepharose A affinity chromatography. Various functional derivatives: succinimidyl ester, maleimide and hydrazide derivatives, of Alexa 546 or Alexa 555 or Alexa 647 dyes were used for labeling the antibodies. All dyes were purchased from Life Technologies/Invitrogen (Budapest, Hungary). MEM75 antibody, against TfR (153) was a kind gift from Václav Horejsí (Institute of Molecular Genetics, Academy of Sciences, Prague, Czech Republic).

5.2. Chemicals

Most chemicals, like NaIO4, sodium azide, ethylenediaminetetraacetic acid (EDTA), MEA, DTT and N-ethylmaleimide (NEM) dimethyl sulfoxide (DMSO), were purchased from Sigma-Aldrich Kft (Budapest, Hungary) unless otherwise stated.

5.3. Dye-antibody conjugation protocol

Dyes were dissolved in a limited amount of DMSO and aliquots were prepared and kept in -20°C to protect the reactivity of dyes from repeated freeze-thaw cycles.

5.3.1. Succinimidyl ester-amine reaction to form carboxamide bond

Conjugates of succinimidyl ester dyes and antibodies were prepared by adding DMSO dissolved dyes to a solution of antibody, which was prepared in the phosphate buffer (pH 7.4). However, to facilitate / accelerate the reaction, sodium bicarbonate was also added into the mixture such that the pH was raised to ~9.1. The mixture of dyes and antibodies was incubated for 45 min at room temperature with gentle mixing in a shaking rotator. Unconjugated dyes were removed from the

mixture by gel filtration using sephadex G25 columns. To obtain different fluorophore to protein (F/P) ratios, the molar concentration of the dye was adjusted while the concentration of the antibody was kept constant at 1 mg/ml.

5.3.2. Maleimide-thiol group reaction to give thioether bond

To produce maleimide-thiol conjugates; first of all, antibodies were reduced with MEA (see **Table 2** for concentrations) in 5 mM EDTA containing phosphate buffer (pH 7). The incubation was generally for 90 min (see also **Table 2**) at 37°C. After the incubation, the unreacted MEA was removed from the samples with the help of 50 kDa MWCO (molecular weight cutoff) amicon spin concentrator tubes (Millipore Kft., Hungary). Thorough washing was required such that the concentration of the MEA was almost negligible in the sample. Thereafter, maleimide dyes were added to the solution of antibody adjusted to 1 mg/ml. Incubation was generally carried out for one hour at room temperature. Separation of dye-antibody conjugates was done by using sephadex G25. It is important to maintain an inert atmosphere in the labeling and washing buffer. In our case, we used nitrogen (N_2) purged PBS buffer during the whole procedure.

Table 2.

Antibody	Conjugation Method	Fluorophore/ protein (F/P)
W6/32	-SH	0.69 (50mM MEA/90 minutes)
		1.11 (5mM MEA/90 minutes)
		1.5 (25mM MEA/90 minutes)
		1.7 (10mM MEA/90 minutes)
	-CHO	0.83 (10 mM $NaIO_4$)
		1.74 (10 mM $NaIO_4$)
		1 (5mM $NaIO_4$)
L243	-SH	1.47 (25mM MEA / 90 minutes)
		2.15 (50mM MEA / 60 minutes)
		2.4 (50mM MEA / 60 minutes)
	-CHO	1.43 (10 mM $NaIO_4$)
		1.6 (10 mM $NaIO_4$)
P2A4	-SH	0.95 (5mM MEA /90 minutes)
		1.3 (10mM MEA/90 minutes)
		2.3 (25mM MEA/90 minutes)
		2.9 (50mM MEA/90 minutes)
	-CHO	2.5 (10 mM $NaIO_4$)
		1.5 (2mM $NaIO_4$)
51.1.3	-SH	1.77 (25mM MEA / 30 minutes)
		2.43 (50mM MEA / 60 minutes)
		2.55 (50mM MEA / 30 minutes)
		2.85 (50mM MEA / 60 minutes)
	-CHO	1.9 (2mM $NaIO_4$)

5.3.3. Hydrazide-aldehyde reaction to form hydrazone bond

To create aldehyde residues in antibodies, oxidation was carried out with $NaIO_4$ (see **Table 2** for concentrations) for 3 h at 37°C in a phosphate buffer (pH 5.6). The oxidized antibodies were passed through sephadex G25 gel filtration column followed by washing using 50 kDa MWCO amicon concentrator tubes, exactly like in the case of MEA removal. After washing, hydrazide dyes were mixed with the antibodies (0.5 mg/ml) at the ratio of 20:1 together with aniline (100 mM). Incubation was done overnight at room temperature with gentle rotation. The gel filtration method of separating free dyes from the antibody conjugated dyes was similar to the above methods. No clear distinction between the fronts of free dye and dye conjugated antibody was observed; therefore, 50 kDa MWCO concentrator tubes were used to eliminate any residual dye present in the solution, prepared after pooling the antibody positive fractions from the collection volume. In addition, N_2 purged PBS buffer was used during the entire labeling procedure.

5.4. Fluorophore per protein (F/P) calculation

For calculating the F/Ps, absorbance of the dye-antibody solution was taken at 280 nm and at the maximum absorption wavelength of the respective dyes using spectrophotometry (Nanodrop, Wilmington, USA). Compensation for the contribution of the dyes to the final concentration of the antibody was performed using recommended correction factors from Molecular Probes (Invitrogen).

The following formula was used to calculate the F/P:

$$\text{Concentration of antibody (mg/ml)} = \frac{A_{280} - (A_{dye} \times CF)}{1.4} \text{ mg/ml}$$

$$\text{Concentration of antibody (Molar)} = \frac{\text{Concentration of antibody (mg/ml)}}{\text{Molecular weight of antibody}}$$

$$\text{Concentration of dye (Molar)} = \frac{A_{dye}}{\varepsilon}$$

$$\text{F/P} = \frac{\text{Concentration of the dye (Molar)}}{\text{Concentration of antibody (Molar)}}$$

(A_{dye} – Absorbance of Alexa dyes at a maximum absorption wavelength; Correction factor (CF) for Alexa dyes at 280 nm; A_{280} – Absorbance of protein at 280 nm, ε – Molar extinction coefficient of Alexa dyes at a maximum absorption wavelength; MW of antibody – 150 kDa (For sulfhydryl labeling, 112.5 kDa was used as MW, an average of 75 and 150 kDa fragment of antibody, because MEA treatment of IgG produces a mixture of small and large fragments of antibody.)

5 .5. Cell line

A B lymphoid cell line, C1R-CD1d, a kind gift of Mark Exley, Harvard Medical School, Boston, USA, was used in these studies (154). This cell line stably expresses full-length CD1d and has been characterized in a previous paper (155). For our purpose, we sorted these cells using 27.1.9 CD1d antibody and pan anti-mouse secondary antibody conjugated magnetic dynabeads (Life Technologies/Invitrogen, Budapest, Hungary) to obtain uniform CD1d expression. The membrane proteins of interest for us have been found to be expressed at good levels in this cell line: MHC I (154), β_2m (80), MHC II (112), ICAM1 (156), and CD1d (80). C1R-CD1d cells were sub-cultured every second day in 10% newborn calf serum (NCS) RPMI media containing 300 µg/ml G418 unless stated otherwise.

5.6. Cell labeling

Cells ($1x10^6$) were labeled in 50 µl volume of PBS buffer (pH 7.4) containing 1 mg/ml BSA and 0.01% sodium azide. Dye-conjugated / or unconjugated antibodies were added to these cells at specific concentrations depending on the requirement (for FRET experiments predetermined saturating concentration of the dye-antibody conjugates was used). Following antibody addition, the mixture was incubated in a dark environment for 30 min on ice. Once incubation was over, samples were washed twice with ice-cold PBS buffer in order to remove unbound antibodies. If unconjugated primary antibody was used, then a secondary antibody $F(ab')_2$ conjugated to Alexa Fluor 647 dyes (10 µg/ml) was added to the cells and was reincubated in ice and dark for another 20 min. The samples were washed again using ice-cold PBS. Finally, the cells were suspended in 1% formaldehyde solution, and they were kept at $4^{\circ}C$ until the measurements were performed in a flow cytometer or a confocal microscope.

5.7. Flow cytometry and data analysis

Depending on the type of studies, fluorescence intensities were measured using FACScan or FACSCalibur or FACSArray flow cytometers (Becton Dickinson, Franklin Lakes, NJ). The instruments are equipped with various combinations of lasers: FACScan (Blue, 488 nm), FACSCalibur (Blue, 488 nm and Red, 635 nm) and FACSArray (Green, 532 nm and Red, 633 nm). FACSArray was used for the study involving the analysis of methods of dye-antibody conjugation.

Alexa 647 dye was specifically used for this purpose to minimize the contribution of autofluorescence. For the topological study of CD1d proteins, all three FACS instruments were used. Flow-cytometric FRET experiments (FCET) were performed in FACSArray flow cytometer. Cells were labeled with Alexa 546 / Alexa 555 and / or - 647 dye conjugated probes and/or antibodies. Fluorescence signals were collected using 575+/-25 BP filter for donor, 650 LP for transfer and 650+/-10 BP for acceptor molecules. In all the cases, 20,000 cells were collected for each sample. Thereafter, the FCS data files for both FRET and non-FRET data were evaluated using ReFleX software as described before (157). For two-color three-protein FCET experiment, similar protocol was used as above except the inclusion of the third protein as a donor or as an acceptor. The conventional FRET has two proteins as a FRET pair but this modified two-color three-protein FRET has three proteins as FRET pair, and two of these proteins are combinedly used as a donor or acceptor molecules. This means two Mabs against two proteins are conjugated to same Alexa dyes separately. However, they are mixed during cell-labeling and are used as either donor or acceptor. Thus, two Mabs conjugated to same Alexa dyes behave together as a unit representing either donor or acceptor species.

5.8. Antibody saturation curve determination

The concentration dependence of fluorescence intensities was the basis for determining the saturation curves for each antibody. For this purpose, C1R-CD1d cells were surface labeled with various concentrations of antibodies (conjugated/ non-conjugated) following the protocol described above. Measurements were performed and the data were analyzed by ReFleX software. The derived data were used for plotting a graph of fluorescence intensity versus concentration of the antibody (conjugated/non-conjugated) using Sigma Plot Version 10. The data were fitted with the help of a single ligand-binding module of the software which after processing provides the equilibrium dissociation constant (Kd) of the antibodies based on the equation as described below. Kd values were determined from at least three sets of independent experiments for each antibody conjugates.

$$Y = \frac{B_{max}\, X}{K_d + X} + N_x$$

The above equation fits the total binding concentration (Y) of the ligand as a function of ligand concentration (X). The extra term (N_x) represents non-specific binding.

5.9. Sodium dodecyl sulfate polyacrylamide gel electrophoresis (SDS-PAGE)

For SDS-PAGE, a mixture was prepared from 10 µg of sample and 5X sample buffer (0.25 M Tris-HCl, pH 6.8, 8% SDS, 40% glycerol, and 0.01% bromophenol blue). It was also supplemented with either 100 mM DTT or 25 mM NEM (158). Thereafter, the mixture was incubated at room temperature for approximately 30 min, followed by heating at 95 °C for 10 min. It was centrifuged at 16,000 RCF for 15 min. Finally, (3-5 µg) of each sample was used for loading into the wells of an 8% poly-acrylamide gel. The gel was run at 50 V for stacking then was shifted to 75 V until the run was completed.

5.10. Quantitation of membrane proteins

QIFIKIT (Dako Cytomation, Glostrup, Denmark) was used for quantifying the membrane proteins according to the manufacturer's instructions. The kit consists of a series of beads coated with known quantities of Mabs resembling cells with defined antigen densities. It is an indirect immunofluorescence based quantitative method. Briefly, cells were labeled with primary mouse Mab at saturating concentrations followed by incubation with FITC dye tagged polyclonal anti-mouse secondary $F(ab')_2$ with washing steps in between. The QIFIKIT beads were also prepared in the similar fashion simultaneously. Fluorescence intensities were measured using 530+/-30 BP filter on a FACSCalibur instrument. The data were analyzed using ReFleX software. The calculated data were used for plotting the curve of fluorescence intensity of the individual bead populations versus the number of Mab molecules on these beads. The number of each membrane proteins was then calculated from the obtained curve by interpolation.

5.11. Confocal microscopy

Microscopy was performed on a Zeiss LSM 510 confocal laser scanning microscope (Carl Zeiss AG, Jena, Germany) with a Plan-Apochromat 40 X (NA= 1.2) water immersion objective. Horizontal optical slice (512 × 512-pixels) of 1.5 µm thickness, four-times averaged, was recorded in line mode from the top of a cell for co-localization experiments. A multitrack option was also followed to avoid any possible crosstalk between the detection channels while acquiring images in the microscope.

5.12. Co-localization study of the proteins:

The vicinity of membrane proteins was determined by image cross-correlation. For this purpose, images were acquired from the top of the cells which were doubly or triply labeled against specific markers by respective probes tagged with spectrally different fluorophores. Cross-correlation coefficient (C) from the image pairs were determined using a custom written program in LABVIEW platform using the formula described below (159, 160).

$$C = \frac{\sum_i \sum_j (x_{i,j} - \langle x \rangle)(y_{i,j} - \langle y \rangle)}{\sqrt{\sum_i \sum_j (x_{i,j} - \langle x \rangle)^2 \sum_i \sum_j (y_{i,j} - \langle y \rangle)^2}}$$

Where $x_{i,j}$ and $y_{i,j}$ represent fluorescence pixel values at co-ordinates i and j in images x and y. Image analysis was performed only on those pixels that were above the detection threshold in both images. The theoretical maximum is '1' for perfect overlap of proteins (i.e. 100% co-localization) and a negative value '−1' indicates an anti-co-localized situation of the two molecules where a pixel is bright in one channel and dim in the other.

5.13. CD1d and GM_1 ganglioside association assay

Association of CD1d with GM_1 gangliosides was determined using the following probes: cholera toxin subunit B (CTxB, Invitrogen) for GM_1 gangliosides and 27.1.9 CD1d Mab for CD1d proteins. Cross-correlation coefficient between these two molecular species was calculated in the similar fashion as described above. For co-localization study, images of Alexa 488-CTxB and Alexa 647- 27.1.9 CD1d molecules were collected using 505/550 nm BP filter and 650 LP filter. FCET between CD1d and GM_1 gangliosides were performed similarly as above using FACSArray, however Alexa 555-CTxB and Alexa 647-27.1.9 CD1d Mab were used as donor and acceptor respectively.

5.14. Flow cytometric detergent resistance (FCDR) test

Time dependent kinetic assessment of detergent tolerance by CD1d rich regions was performed following the FCDR protocol which is published elsewhere and is based on flow cytometry (161). Similar cell labeling protocol was followed except the final step where formaldehyde fixation of cells was avoided. Unlike in other cases, samples were proceeded for measurements without any delay. FACScan with a 530+/-30 BP filter option was used for this purpose. As a baseline, initially

fluorescence intensities were measured for ~50 s, thereafter, Triton X-100 (TX100) at various concentrations was added, mixed promptly then the measurements were resumed for another five minutes. The FCS files were analyzed using ReFleX software and the calculated data were used for plotting the graph of fluorescence intensity versus time using Sigma Plot V10.

5.15. Treatment of cells with MβCD or Simvastatin

Both MβCD and simvastatin were purchased from Sigma. Specific instructions from the companies were followed to dissolve the reagents. Simvastatin treatment of C1R-CD1d cells was done by incubating (4×10^6 to 10×10^6) cells with micromolar concentrations of preactivated simvastatin in 1% NCS RPMI media for 48 h at 37°C. MβCD usage was slightly different because it was a short-term treatment. Briefly, C1R-CD1d cells (5×10^6 to 10×10^6) which were grown in 1% NCS, unless otherwise mentioned, were taken in 1 ml of 0.1% NCS RPMI media and were incubated with 2 mM MβCD for 40 min or 10 mM MβCD for 15 min at 37°C. Thereafter, the cells were thoroughly washed and were labeled as described above.

5.16. Isolation of iNK T cells from peripheral blood mononuclear cells (PBMC)

For isolation of iNK T cells from human peripheral blood, ficoll density gradient based standard procedure was employed. Leukocytes are present in the buffy coat layer present between the layers of plasma and red blood cells. iNK T cells were isolated using anti-iNK T magnetic beads (Miltenyi Biotec, Bergisch-Gladbach, Germany) from these leukocytes. Special iNKT cell medium consisting of 5% AB human serum (Sera Laboratories International Ltd, West Sussex, UK), 200 ng /ml of recombinant IL2 (Shenandoah Biotechnology**,** Inc., USA) and 2µg/ml phytohemagglutinin M (PHA-M, Sigma) was prepared for growing iNK T cells. To promote the growth of iNK T cells, α-gal (KRN7000, Avanti Polar Lipids, Inc., Alabama, USA) loaded mitomycin C-arrested (50µg/ml for 45 min) C1R-CD1d cells were used as feeder cells. Briefly, 100,000 iNK T cells were cultured together with 250,000 C1R-CD1d feeder cells in the prepared special iNK T cell medium. The medium was changed with a fresh iNK T medium the next day and the growth was monitored over the period of culture. Proliferation of the cells can be identified by the formation of clusters of cells and the turning of growth media into yellow. This way iNK T cells expand several thousand folds in a period of two weeks. The concentration of IL2 was gradually decreased from 200 ng/ml to

20 ng/ml (~10 U/ml) during the period of culture. For functional assays, iNK T cells were cultured in iNK T media without PHA-M and very low amount of IL2 (20 ng/ml) for at least 24 h. The purity of the expanded iNKT cells was examined by flow cytometry using Mabs 6B11 (anti-Vα24 Jα18, IgG1, eBioscience), C21 (anti-Vβ11, IgG2a, Beckman Coulter) and OKT3 (anti-CD3, IgG2a).

5.17. Co-culture assay with iNK T cells

C1R-CD1d cells were cultured in 1% NCS RPMI medium for 48 h before being used for co-culture assays with iNK T cells. Feeding of α-gal was performed for 18 h and 4 h leading up to the completion of 48 h incubation in the case of MβCD and simvastatin studies. Simvastatin treated C1R-CD1d cells were directly proceeded to the next step, whereas, C1R-CD1d cells for MβCD studies were treated with MβCD as described before. Thereafter, C1R-CD1d cells were extensively washed and were fixed with 1% formaldehyde for 20 min on ice, in order to prevent the reassembly of cholesterol in the membrane. The cells were washed again twice with ice-cold PBS. These cells were used at the ratio of 3:1 with iNK T cells for co-culture assays. Briefly, 60,000 C1R-CD1d cells and 20,000 iNK T cells were seeded in each well of the round-bottomed 96 well plates with RPMI medium containing 5% human serum and 20 ng/ml recombinant IL2 for 48 h at 37°C. Experiments were performed in triplicates prepared from the same sample for each test.

5.18. Statistical analysis

For comparison, either an unpaired *t*-test or one-way ANOVA together with tukey posthoc analysis was performed using SigmaStat 3.5 (GmbH, Germany) depending on the number of groups. Only '*p*' values <0.05 were considered significant. Non significant '*p*' values are indicated by abbreviation 'N.S.', whereas, '*p*' values < 0.05, < 0.005, and < 0.0005 are denoted with ∗, ∗∗, and ∗∗∗, respectively on the figures.

6. RESULTS

6.1. Analysis of dye-antibody conjugation methods

The primary objective of this study was to identify the effect of dye conjugation on binding affinity of an antibody. In this aspect, we also wanted to compare several methods of dye conjugation. Additionally, we evaluated the financial aspects, the yield of conjugates and ability to produce higher dyes per antibody for each of these methods. We took advantage of dissociation constant (Kd), a suitable indicator of the strength of interaction between ligands and receptors, to determine the influence of dye coupling in antigen binding affinity of an antibody.

6.1.1. Unconjugated antibody: A reference for antibody conjugates

For comparison, the binding affinity of an unconjugated Mabs to plasma membrane proteins of a cell line was considered as a reference. Accordingly, standard Kd values were calculated for each of these unconjugated Mabs. It was determined by performing indirect fluorescence measurements in a flow cytometer. Specifically, C1R-CD1d cells were first incubated with unconjugated primary Mabs, then; the binding of these Mabs to membrane proteins were detected using dye conjugated secondary $F(ab')_2$. Since, series of concentrations were taken for each Mab, differences in fluorescence intensities were also observed. However, the concentration dependent increase in fluorescence intensity occurred only until a certain point, from where a non-linear increase in fluorescence intensity was observed followed by almost no increase /or slight inhibition in fluorescence intensities at the highest concentrations of Mabs. This could be termed as saturation point or the occupancy of entire receptors (~99%) by Mabs on the plasma membrane at these concentrations. Such observation was evident for all Mabs in this study. This helped us to deduce a graph of fluorescence intensity versus concentration of the antibody. Kd values were estimated based on such saturation curves for each antibody. Four Mabs, W6/32, L243, P2A4 and 51.1.3 CD1d were used for this study, and they bind to the epitopes of MHC I-HC, MHC II, ICAM1 and CD1d proteins respectively. Estimated Kd values were quite different for each of the Mabs. Thus, these Mabs could be broadly categorized based on the binding affinities as high-affinity and low-affinity antibodies. W6/32, L243 and P2A4 demonstrated high binding affinity whereas 51.1.3 CD1d antibody was comparatively weaker in binding affinity to their relative antigens. For some reasons, though not related to Fc receptor binding (data not shown), Mabs P2A4 and 51.1.3 also showed a larger variation in Kd value.

The (Kd ± S.D.)s were found to be (27.7± 6.7) nM, (31.1±9.1) nM, (32.8±16.8) nM and (174.2±21.8) nM for W6/32, L243, P2A4 and 51.1.3 antibodies respectively (**Figure 7 and Table 3).**

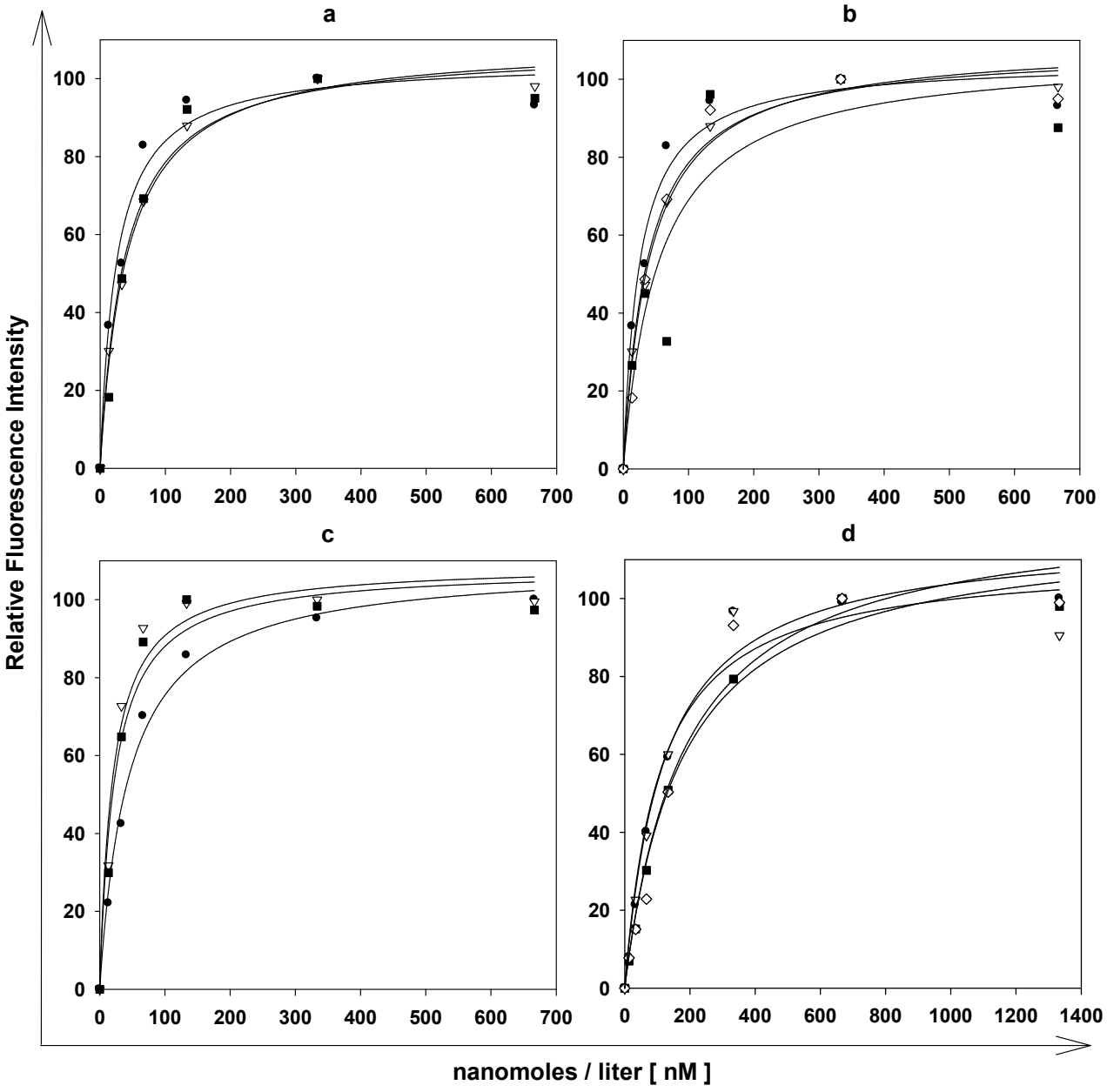

Figure 7. Kd values of unconjugated antibody by Indirect Method: **(a)** W6/32 **(b)** L243 **(c)** P2A4 **(d)** 51.1.3. Presented here are three /or four saturation curves for each Abs. Symbols represent independent experiments performed on different days.

Table 3.

Kd values of the unconjugated antibodies and antibody conjugates

Antibody	Conjugation Method	F/P	Kd ± S.D. (nM)
W6/32	Unconjugated		27.7± 6.7
	$-NH_2$	0.5	21.8±4.4
		1.1	22.1±6.9
		2.3	26.8±7.7
		3.1	25.3±3.9
		4.3	29.8±5.6
		5.8	29.1±2.9
		7.5	28.3±2.9
		8.7	55.4±7.9
	-SH	0.69	21.5±0.7
		1.11	17.0±3.7
		1.5	20.6±4.9
		1.7	16.9±2.6
	-CHO	0.83	116.5±3.5
		1.74	117.8±17.9
		1.0	26.9±10.4
L243	Unconjugated		31.1±9.1
	$-NH_2$	0.56	54.5±21.6
		0.95	37.1±7.5
		1.65	47.4±12.9
		2.2	49.2±12.1
		2.8	51.5±14.2
		4.0	42.5±8.9
		5.0	50.4±4.9
		7.7	34.8±12.7
	-SH	1.47	90.9±12
		2.15	80.5±3.1
		2.4	89.1±5.5
	-CHO	1.43	190.6±14.7
		1.6	122.5±9.9
P2A4	Unconjugated		32.8±16.8
	$-NH_2$	0.66	439.1±102.5
		1.3	51.0±0.3
		2.4	49.8±7.8
		3.3	24.4±1.3
		4.5	42.9±0.9
		6.2	58.2±10.5
	-SH	0.95	51.0±2.9
		1.3	61.1±2.7
		2.3	51.8±16.1
		2.9	62.2±5.2
	-CHO	2.5	385.9±20.2
		1.5	79.4±30.3
51.1.3	Unconjugated		174.2±21.8
	$-NH_2$	0.7	461.8±79.2
		1	552.6±39.5
		1.6	523.4±251.9
		3.2	437.6±108.5
		3.9	369.7±107.4
		4.6	304.9±17
		9.9	425.8±15
	-SH	1.77	156.0±0.2
		2.43	366.3±16.6
		2.55	668.0±41.4
		2.85	477.0±11.3
	-CHO	1.9	851.3±165.9

6.1.2. Effect of NHS ester based coupling method on the binding affinity of Mabs

Amino groups are distributed throughout the antibody structure and are also located in crucial ABS regions. Therefore, it is believed that the amine targeted approach would influence, or in the worst-case scenario destroys, the binding affinity of an antibody. The deleterious effect of $-NH_2$ method of antibody conjugation in binding affinity has also been demonstrated in previous studies (162, 163). These assessments have been made primarily from studies involving either biotinylation of antibodies or fluorophore conjugation with only few sets of antibodies. Therefore, one of our aims was to characterize antibody conjugates based on F/P ratios, especially after including different antibody isotypes. Our results suggested that although dye-coupling seems to decrease the binding affinity of an antibody, this phenomenon was not proportional to F/P ratios. There was no strict correlation between F/Ps and the decrease in binding affinity of antibody. Instead, a few of the higher F/Ps had smaller Kd values than their low F/P counterparts. The effect of increased load of dyes in binding affinity of antibody seems to be antibody dependent (**Figure 8**, **Figure 9** and **Table 3**). Low affinity antibody 51.1.3 was comparatively sensitive to dye conjugations (**Figure 9A.d** and **Table 3**) than high-affinity antibodies: W6/32 (**Figure 9A.a**) and L243 (**Figure 9A.b**). It should also be noted that although higher F/P conjugates were brighter than the lower F/P conjugates, there was no linear increase in the fluorescence intensity of the conjugates, especially above F/P>3 (**Figure 8 and Figure 9B**). Instead, the higher F/Ps > 8 showed diminished fluorescence intensities (**Figure 9B).**

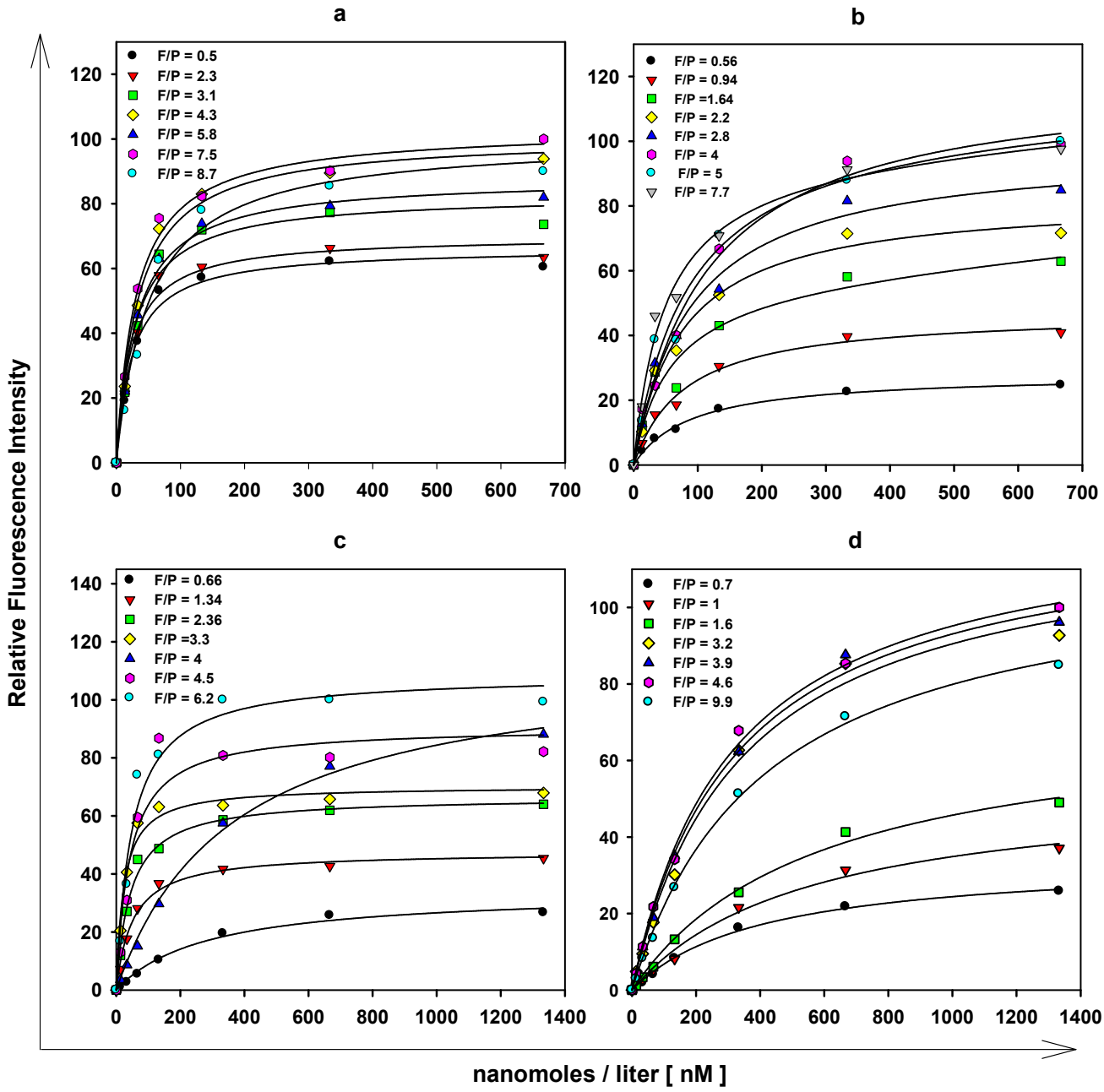

Figure 8. Saturation curves for various F/Ps obtained by -NH_2 based labeling protocol:
(a) A647-W6/32 conjugates **(b)** A647-L243 conjugates **(c)** A647-P2A4 conjugates **(d)** A647-51.1.3 conjugates. A representative curve for each set of dye-antibody conjugate is demonstrated here. The numbers of independent experiments (n) were at least 3.

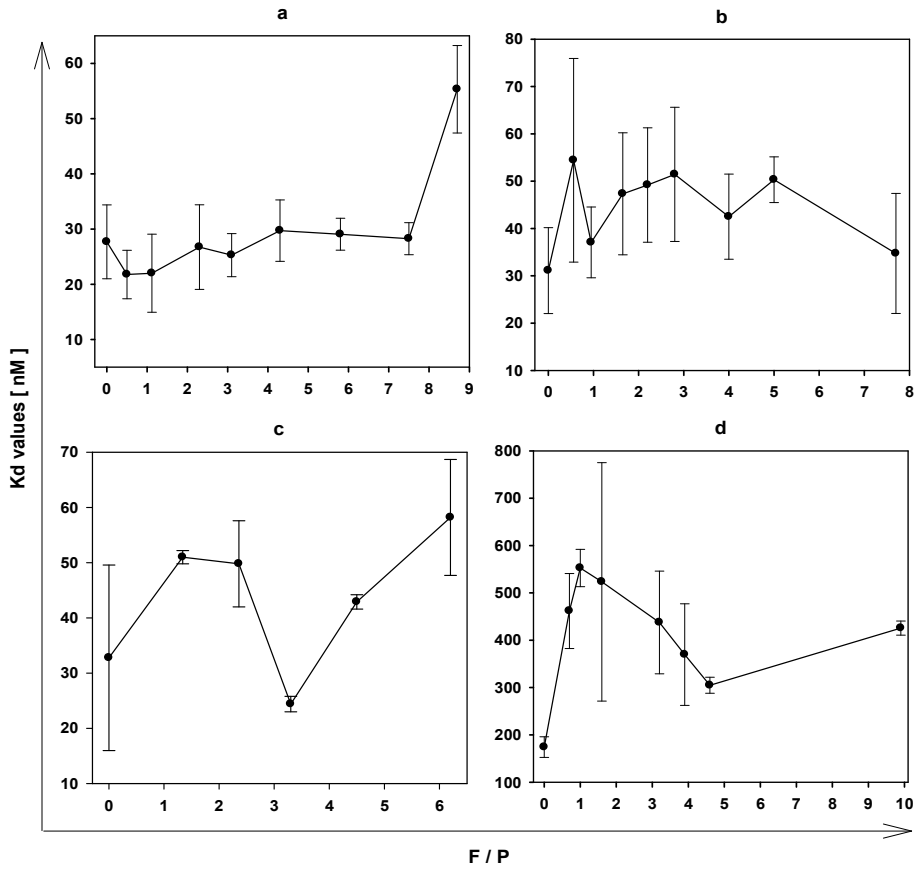

Figure 9A.

The dissociation constant (Kd) was plotted versus F/P for different antibodies.
a) A647-W6/32 conjugates
b) A647-L243 conjugates
c) A647-P2A4 conjugates
d) A647-51.1.3 conjugates

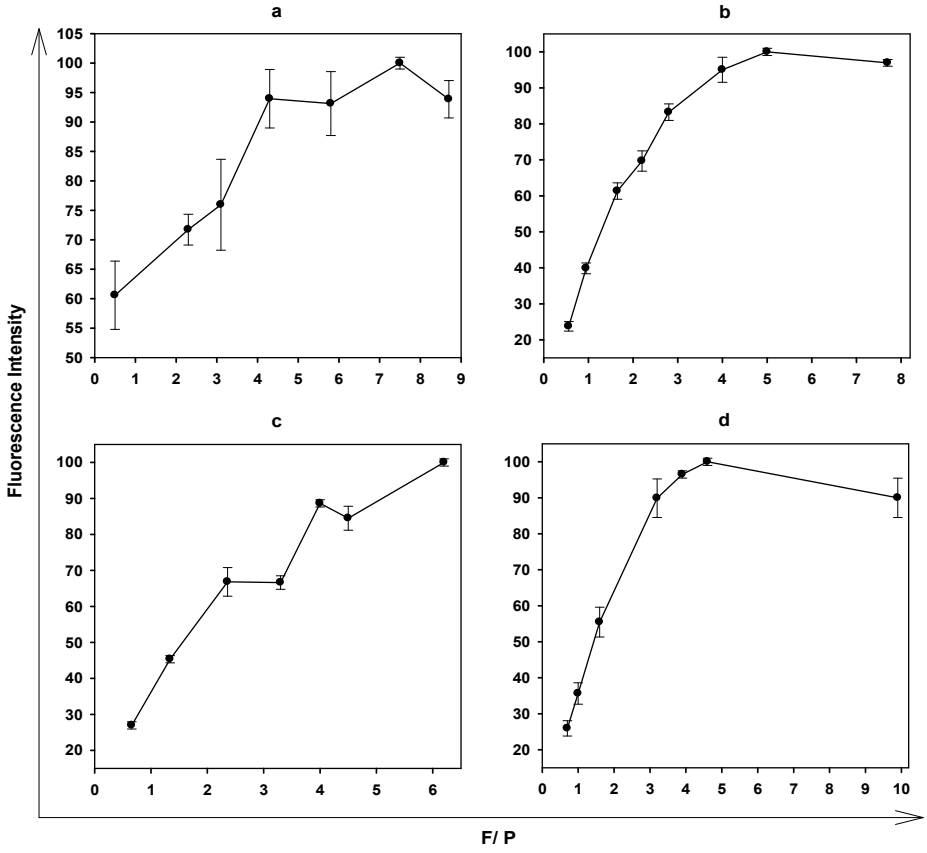

Figure 9B.
Fluorescence intensity was plotted versus F/P for different antibodies.
a) A647-W6/32 conjugates
b) A647-L243 conjugates
c) A647-P2A4 conjugates
d) A647-51.1.3 conjugates C1R-CD1d cells were labeled with saturating concentration (100 µg/ml) of respective antibodies and subsequently; the measured fluorescence signals were used to plot this graph.

6.1.3. Performance of dye-antibody conjugates generated after reduction of antibodies

The two monovalent halves of the antibody are held together by disulfide bonds, which are also responsible for maintaining its tertiary structure. Disulfide bonds are present between the "H" and "L" chains of an antibody; therefore, disruption of these bonds could render them functionless. However, if appropriately cleaved at the hinge region, then an antibody produces two equal halves with an intact antigen-binding region, thus making them attractive and easy target for sulfhydryl labeling. Studies also indicated that MEA preferentially reduced disulfide bonds at the hinge regions (9, 164). Theoretically, labeling of these specific sulfhydryl groups would be of great advantage due to the non-interference in the antigen binding activity (9). Despite the advantages conferred by half-antibodies, which would be an ideal replacement for Fab fragments in experiments, surprisingly only a limited number of studies has explored the potentiality of directly conjugating half-antibodies (165-169). Hence, we were motivated to explore the possibility of conjugating half-antibodies and compare its features with antibody conjugates prepared by amine method. Decrease in antigen binding affinity was noticed after dye-conjugation, the effect was very much similar as in the case with -NH_2 method (**Figure 10** and **Table 3**). Variation in binding affinity for 51.1.3 CD1d antibody conjugates was also noted. Apart from this antibody, the other antibody conjugates demonstrated smaller S.D. in Kd values compared to its corresponding conjugates from -NH_2 method suggesting the superior performance of -SH conjugates. As expected, the F/Ps were always less than three for all dye-antibody conjugates. This corresponds well with the number of disulfide bonds between the two "H" chains of the antibodies (**Table 3**). However, the maximum F/Ps that could be obtained, and susceptibility to MEA differed between the antibodies. IgG1 (P2A4) and IgG2b (51.1.3) conjugates yielded higher F/Ps in comparison with IgG2a conjugates. The problematic antibodies, P2A4 and 51.1.3, were also far more sensitive to MEA than the other two high-affinity antibodies under similar treatment procedures. To demonstrate this observation, W6/32 and P2A4 antibodies were reduced with similar concentrations of MEA and consequently, the obtained F/P values are presented in **Table 2**. The other two antibodies (L243 and 51.1.3) also demonstrated similar behavior towards MEA (data not shown). In comparison with -NH_2 method, -SH method consists of multiple steps, including reduction of antibody, series of washing then co-incubation with dyes. Therefore, it is a cumbersome procedure requiring effective optimization.

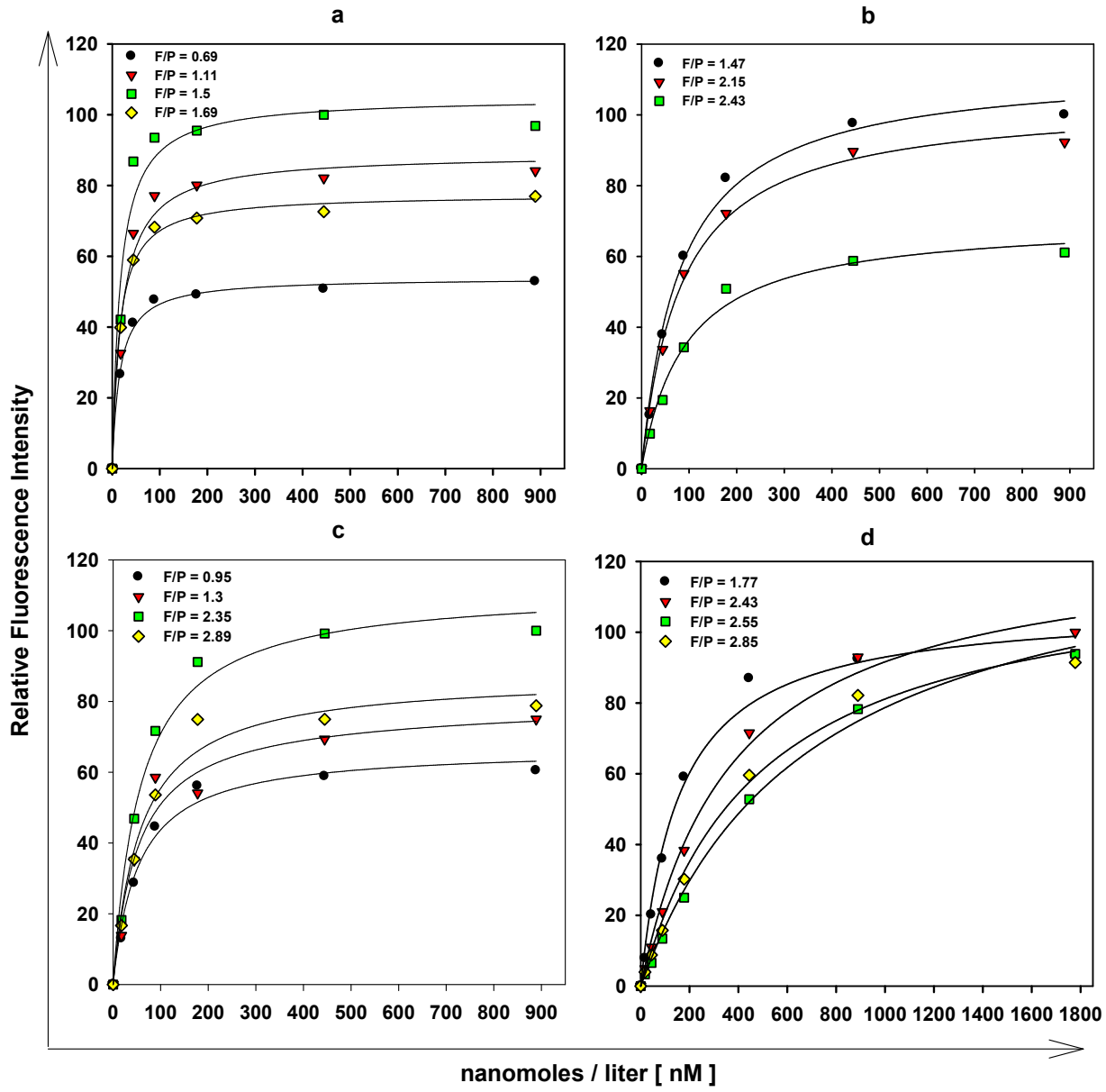

Figure 10. Saturation curves for various F/Ps obtained by sulfhydryl labeling protocol: **(a)** A647-W6/32 conjugates **(b)** A647-L243 conjugates **(c)** A647-P2A4 conjugates **(d)** A647-51.1.3 conjugates. A representative curve for each set of dye-antibody conjugate is demonstrated here, (n≥3).

6.1.4. Response of antibody after dye conjugation on the carbohydrate residues

IgGs are glycoproteins, which have heterogeneous groups of terminal sugars, including sialic acid, galactose, N-acetylglucosamine and fucose residues (170). The sugar units are mainly present on Fc site, which is far from the antigen binding region (**Figure 1**); therefore, any strategy that involves modification of this region is considered to have little or no effect on the affinity of antibody and would also allow site-specific labeling. Primarily, modifications of these oligosachharide residues are

required before initiation of any coupling reaction. The preferred strategy is to oxidize these carbohydrate residues to aldehydes. Dye conjugation at carbohydrate residues has also been demonstrated earlier on oxidation with the help of $NaIO_4$ (171). Ideally, Fc directed conjugates should have been favored by researchers; however, only a few literatures are present documenting the application of this strategy in dye-antibody conjugate preparation. Rather, it is widely used in bio affinity applications (172) and enzyme-antibody conjugate preparations (173-176). Paradoxically, in previous studies it was suggested that $NaIO_4$ mediated antibody oxidation would lead to decline or even a loss in the biological activity of an antibody (173). Out of these curiosities, we were interested in identifying the discrepancies associated with this strategy. Our results indicated that $NaIO_4$ is the sole determinant in the variation of binding affinity related to this methodology. Interestingly, different antibody isotypes and antibody with different binding affinities responded differently to $NaIO_4$. Therefore, the concentration of $NaIO_4$ needs to be optimized beforehand for each antibody. Corroborating the role of aniline in facilitating the chemical reaction between hydrazide dyes and oxidized antibodies (-CHO), we observed that the dye-antibody conjugate formation only occurred after the addition of aniline (10-100) mM in the reaction mixture. Furthermore, dye-antibody conjugate formation required at least 20 folds higher dyes than antibodies. The temperature at which $NaIO_4$ mediated oxidation was carried out also influenced the degree of labeling. In fact, $NaIO_4$ (10 mM) oxidation of antibodies at room temperature (~20°C) could only produce antibody conjugates with F/P <1 especially for high-affinity antibodies (W6/32 and L243). The shift in the oxidation temperature to 37°C yielded products with F/P>1 consistently (**Table 3**). Therefore, higher temperature favors oxidation of antibodies. We also examined the effect of sodium borohydride ($NaBH_4$), which is considered to play an important role in stabilizing the hydrazone bond (177), in the dye-antibody conjugate formation. We observed that only a few hundred μM quantities of this chemical were enough to quench the dye. Since, $NaBH_4$ was not found to be essential for conjugate formation; it was not used further in our studies. One of the antibodies, 51.1.3, got inactivated on oxidation following the above protocol while similar conditions only decreased the binding affinity of the other antibodies. At room temperature, 51.1.3 could tolerate 10 mM NaIO4 (data not shown) but not at 37°C, therefore higher temperature, although supported oxidation process, it was detrimental to antibodies as well. Likewise, lowering the concentration of $NaIO_4$ to 2 mM from 10 mM at 37°C gave functional 51.1.3 antibody conjugates (**Figure 11** and **Table 2**). Therefore, high-affinity antibodies seemed to tolerate $NaIO_4$ better than low-affinity antibodies. This was also evidenced in the form of F/Ps where high-affinity antibodies always yielded conjugates with low F/Ps at similar treatment

conditions. Similarly, higher concentration of $NaIO_4$ although produced antibody conjugates with higher F/Ps, these conjugates had a lower binding affinity in comparison with the conjugates prepared from lower concentrations of $NaIO_4$. Such differences in oxidation and F/Ps were observed for all the tested antibodies (**Figure 11**, **Figure 12**, **Table 2** and **Table 3**). Besides, other problems related to gel filtration were also visible for -CHO based conjugates. In the $-NH_2$ and -SH based methods of labeling, the free dye clearly separated from the conjugated dye-front during the gel filtration, but this phenomenon was not evident in -CHO based labeling method. Among the three dye-conjugation methods discussed in this unit, -CHO method was the most difficult one requiring rigorous optimization, longer incubation hours, higher financial cost and lower yield of desired products.

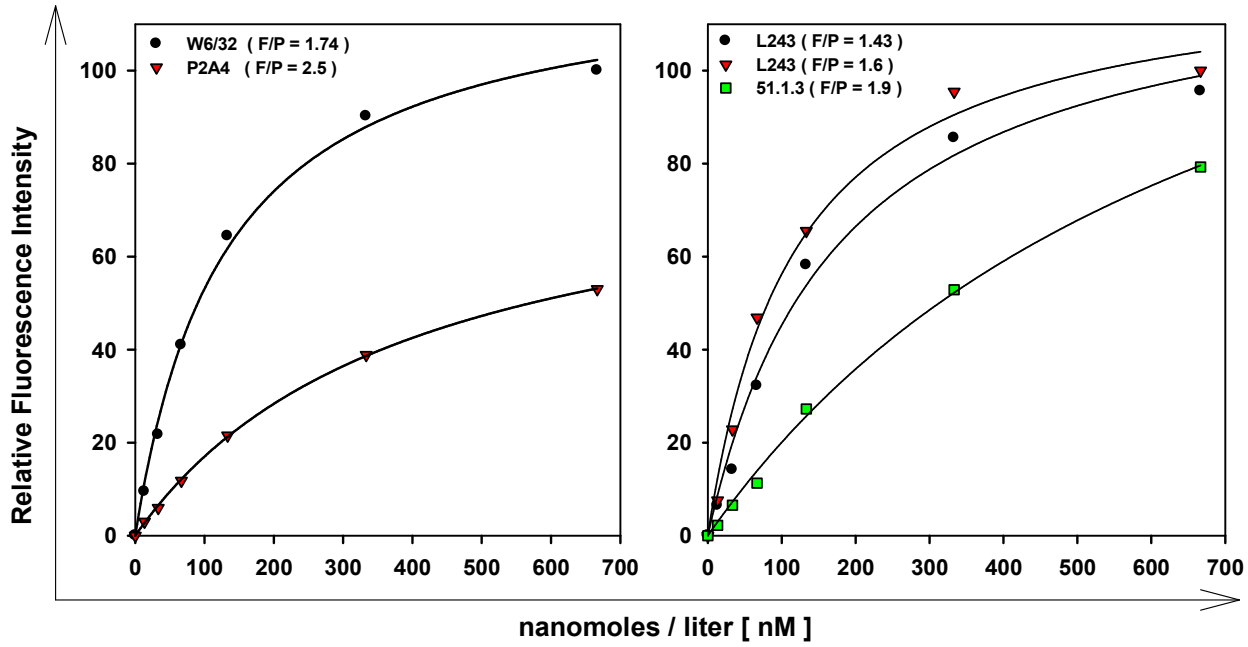

Figure 11. Saturation curves for various F/Ps obtained by carbohydrate oxidation method. A representative curve for each set of dye-antibody conjugate is demonstrated here, (n≥3).

6.1.5. Dissimilar fluorescence intensities of dye-antibody conjugates from the three methods

In the beginning, independent fluorescence studies were carried out for the dye-antibody conjugates from each of the three methods. During the investigation, we realized that the fluorescence intensities were not equivalent for similar F/P variants from the three methods. Therefore, we planned to compare the fluorescence intensities of dye-antibody conjugates with similar F/Ps from each of these methods simultaneously. In our study, we had always obtained dye-antibody conjugates with F/Ps < 3 from -SH and -CHO methods; therefore, comparison of the antibody conjugates had to be pursued

accordingly considering F/P values. We found that -NH_2 based conjugates always produced higher fluorescence signals in comparison with -SH and -CHO based conjugates. The fluorescence intensities of the dye-antibody conjugates prepared by -SH and -CHO methods were between (30-80) % of the signals from conjugates prepared by -NH_2 method. This feature was noticeable for all the four selected antibodies (**Figure 12**). This was further confirmed by confocal microscopy where -SH and -CHO based antibody conjugates produced less bright images of membrane proteins at similar microscopic recording parameters (data not shown).

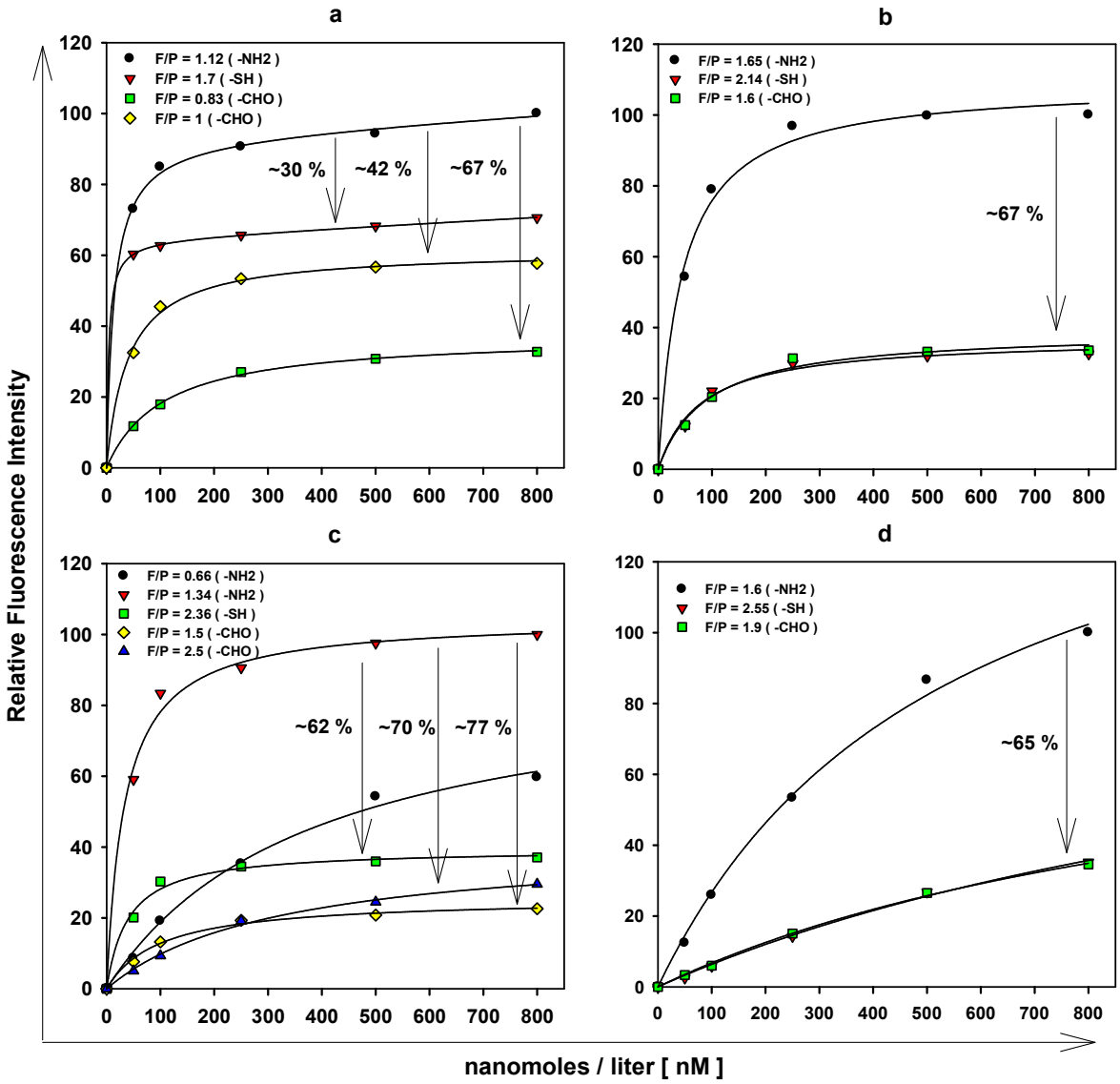

Figure 12. Comparison of dye-antibody conjugates prepared by several methods.
A representative curve for each set of dye-antibody conjugate is demonstrated here, (n≥3). **(a)** A647-W6/32 conjugates **(b)** A647-L243 conjugates **(c)** A647-P2A4 conjugates **(d)** A647-51.1.3 conjugates. The arrows on the figure indicate the approximate differences in the fluorescence intensities between the two curves which are at the head and the tail of the arrow at saturating concentrations of the dye-antibody conjugates.

6.1.6. Comparison of functional dye-antibody conjugate formation by SDS-PAGE

It was clear from the flow-cytometric histograms of dye-antibody conjugates that the performance of the conjugates from three labeling methods was not equivalent. We did not use any exogenous chemical to modify the antibodies in the case of -NH_2 method, whereas, chemical treatment was required to produce reactive functional groups in -SH and -CHO based methods. Therefore, we assumed that the observed differences could have been originated from chemical treatments. In order to identify the effects of reducing agent, MEA, and oxidizing agent, $NaIO_4$, we performed non-reducing SDS-PAGE. Under non-reducing conditions, without DTT in the sample buffer, an antibody molecule should remain intact thus should display a single band in the gel. MEA was used in -SH method to reduce antibodies; therefore, we expected predominantly half-antibodies, whereas, whole antibodies were anticipated from -NH_2 and -CHO methods. Consistent with our assumption, we detected an intense single band in the case of -NH_2 and -CHO based dye-antibody conjugates. However, -SH based dye-antibody conjugates displayed several smaller fragments of dissimilar sizes, including half-antibodies and whole unfragmented antibodies. Faint bands were also observed above and below the antibody monomer band region in the case of -CHO method (**Figure 13).**

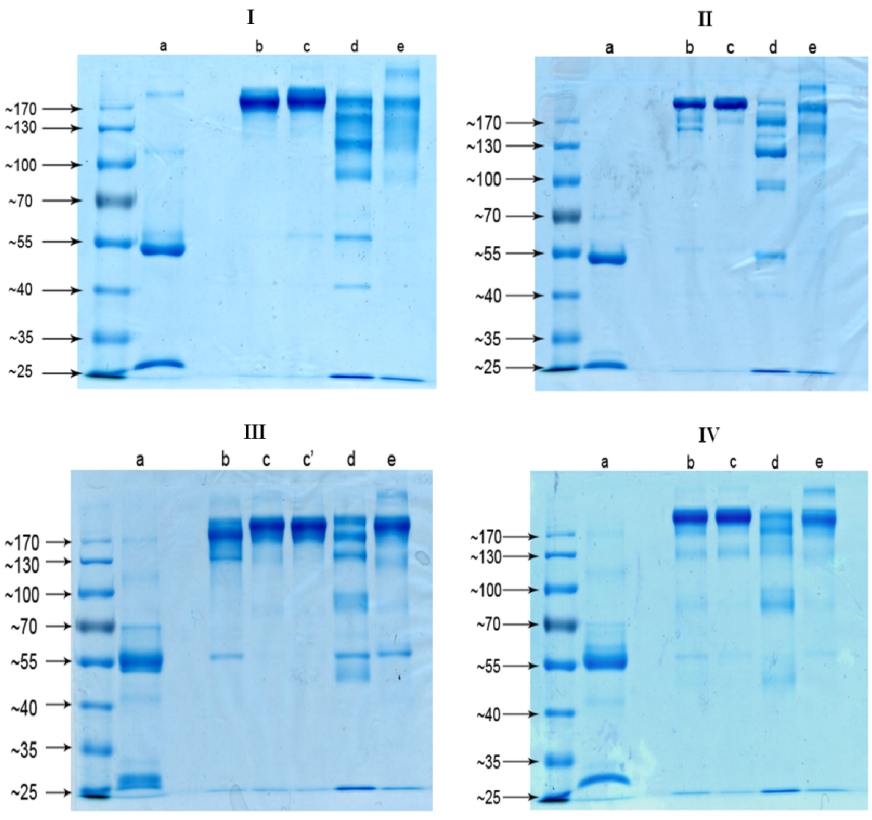

Figure 13.
Non-reducing SDS PAGE of unconjugated and fluorophore conjugated antibodies, having similar F/Ps, prepared by three different methods:

I) W6/32 conjugates
II) L243 conjugates
III) P2A4 conjugates
IV) 51.1.3 conjugates

In the figure, the lanes represent (a) DTT treated unlabeled antibody (b) NEM treated unlabeled antibody (c/c') NEM treated sample from -NH_2 method (d) NEM treated sample from -SH method and (e) NEM treated sample from -CHO method. The dye-antibody conjugates used for this study were the same as the one used for flow-cytometric comparative study (**Figure 12**).

6.2. Enigma of CD1d protein distribution on the plasma membrane of human B cells

The purpose of this study was to use fluorescence antibody conjugates in order to unravel the plasma membrane distribution features of CD1d proteins.

6.2.1. Evaluation of expression level of membrane proteins in C1R-CD1d cells

We wanted to evaluate the relationship of CD1d with MHC molecules on the membrane of B lymphocytes. For this objective, we selected a B lymphoid cell-line, C1R-CD1d which was used in various pull-down experiments previously in an attempt to identify protein interaction partners of CD1d from both plasma membrane and intracellular compartments (80, 102, 112). We also sought to verify these molecular partners of CD1d through biophysical approaches here. The original batch of CD1d transfected C1R cells was a mixture of CD1d "+ve" and CD1d "-ve" C1R cells. A rapid disappearance of CD1d "+ve" cells in a short period of culture was evident when cells were grown in such a mixed population. Additionally, FRET estimation in the lower amount of CD1d "+ve" cells, (15 – 20) % of the population, was always troublesome. Therefore, a magnetic sorting of C1R cells for the CD1d "+ve" population was performed firstly. After separation, ~99% of the cells were positive for CD1d expression, and the earlier problems declined considerably. Next, the level of expression of various proteins on the membrane of this cell line was examined by flow cytometry. Fluorescence histograms indicated that MHC II was the highest in expression, followed by CD1d, β_2m and MHC I-HC proteins in the plasma membrane (**Figure 14**). MHC I-HC was almost three and half-fold lower in expression in comparison with MHC II proteins in C1R-CD1d cells. The data obtained from the fluorescently labeled C1R-CD1d cells, after taking into account dyes-to-antibody ratios, also suggested that the expression level of β_2m was higher than that of MHC I-HC molecules in the plasma membrane (**Figure 14).**

6.2.2. Giving definite numbers to the membrane proteins

Essentially the number of proteins, stoichiometry of proteins and intermolecular distance between the proteins are the determining factors of FRET efficiency. Therefore, to further verify the expression level of membrane proteins, quantitative estimation of these proteins was performed by Qifikit analysis. The obtained results were similar to the one from general fluorescence staining by flow-cytometry. It confirmed that the most abundant protein was indeed MHC II in the membrane of C1R-CD1d cells. In addition, the amount of β_2m was higher than that of MHC I-HC by

approximately 18,000 molecules/cell. Previous studies have shown that MHC I-HC can also exist as self-clusters (oligomers) on the cell surface (178, 179). Therefore, to differentiate between β_2m-bound and β_2m-free MHC I-HC, we employed Mabs capable of identifying these two isoforms of MHC I-HC. W6/32 antibody recognizes a conformation of MHC I-HC in complex with β_2m, whereas, HC-10 recognizes β_2m-free MHC I-HC, HLA-B and -C isoforms only (145). Fluorescence intensity due to HC-10 antibody was very low, which when quantified equaled to only a few hundreds of proteins. Therefore, the majority of MHC I-HC in C1R-CD1d cells seems to exist in the β_2m-bound form. Likewise, similar level of expression was found for CD1d proteins using two antibodies, 27.1.9 and 51.1.3 hybridoma clones, against CD1d protein (**Figure 14b**). These results also suggested indirectly that most CD1d is independent of β_2m in the plasma membrane.

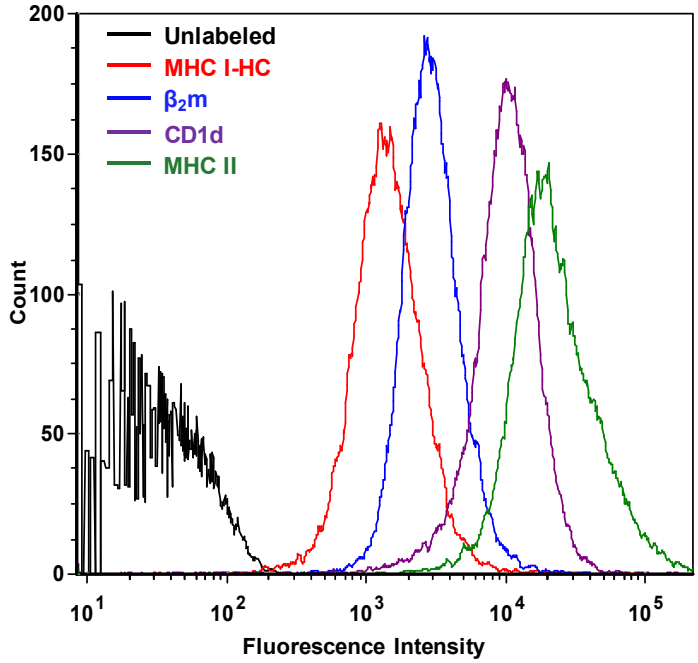

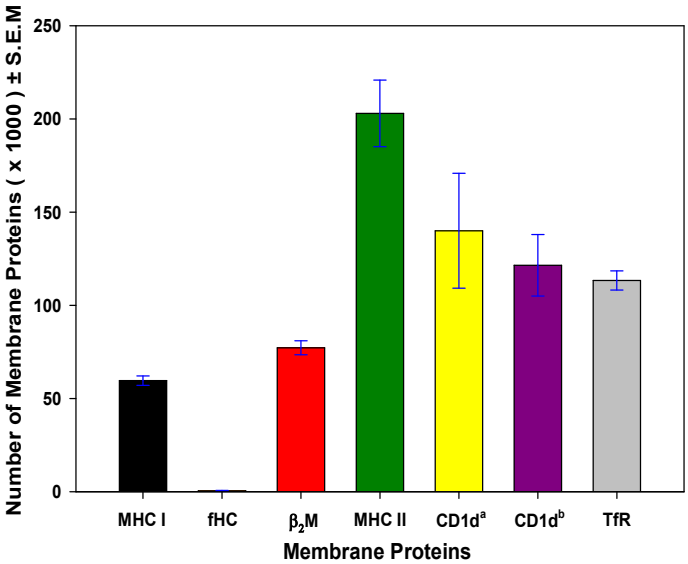

Figure 14.
a) Comparison of expression of various proteins on the surface of C1R-CD1d cells: C1R-CD1d cells were labeled with A647 dye conjugated specific Mabs against MHC I-HC (W6/32) red, β_2m (L368) blue, CD1d (27.1.9 clone) violet, MHC II (L243) green following protocols described in the materials and methods section. Measurements were performed using a FACSArray flow cytometer.

b) QIFIKIT estimation of membrane proteins:
Cells were labeled according to the protocols provided by the manufacturer. The description on labeling is also provided in the materials and method section. The sample measurements were performed immediately on FACSCalibur. The numbers of proteins are presented as Mean±S.E.M., (n=4). In the figure, CD1d^a and CD1d^b indicate staining of CD1d proteins by 51.1.3 and 27.1.9 CD1d Mabs respectively.

6.2.3. CD1d influences the plasma membrane expression of MHC proteins

With previous studies demonstrating the association of CD1d with β_2m proteins, we speculated that CD1d might be responsible for the observed increase in β_2m proteins in the cell surface. To confirm this assumption, we designed a dual color experiment to examine the effect of over expression of CD1d in the expression of MHC proteins in the plasma membrane. We had noted the disappearance of CD1d membrane expression in C1R-CD1d cells over the time of continued growth. In fact, during long-term culture, C1R-CD1d "+ve" cells turn into a mixture of CD1d "+ve" and CD1d "-ve" populations (**Figure 15a**). Therefore, we thought we could use this phenomenon for determining the role of CD1d in the membrane expression of MHC and β_2m proteins. Accordingly, we estimated the differences in the expression of MHC I, MHC II and β_2m proteins in the plasma membrane of C1R-CD1d "+ve" and C1R-CD1d "-ve" populations. We found that expression of β_2m was enhanced by ~46.7±11.5% and expression of MHC II was reduced by ~31.8±4.6% in C1R-CD1d "+ve" cells in comparison with its C1R-CD1d "-ve" counterparts. Likewise, slight up regulation in the membrane expression of MHC I-HC (~10±2.6%) was also seen in the case of C1R-CD1d "+ve" cells (**Figure 15b**). The comparison of the expression of these proteins between C1R-Mock cells and C1R-CD1d cells also revealed a similar pattern (data not shown).

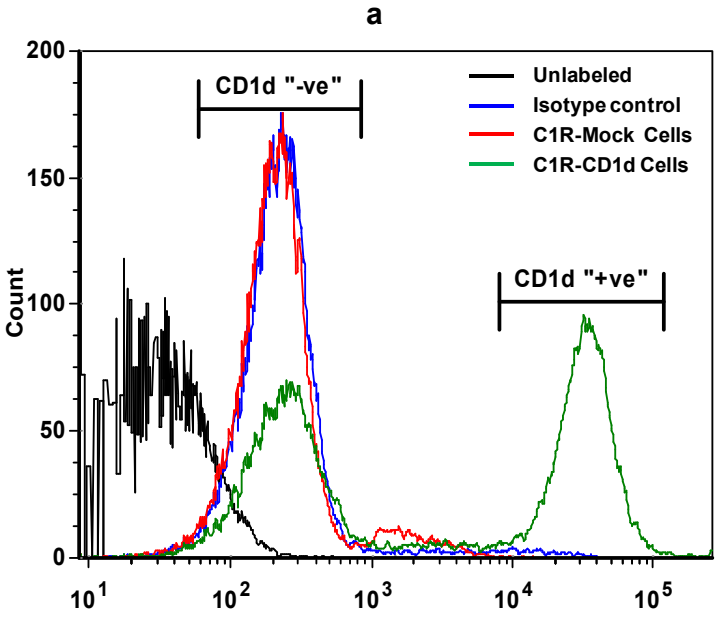

Figure 15. CD1d expression affects expression of membrane MHC proteins:
a) Histograms displaying fluorescence intensities from C1R cells with the following labeling parameters: Unlabeled (Black), Isotype control (Blue), C1R-Mock cells incubated with CD1d antibody (Red) and C1R cells containing C1R-CD1d "+ ve" and C1R-CD1d"-ve" cells (Green). The antibodies were conjugated to Alexa 647 dyes.

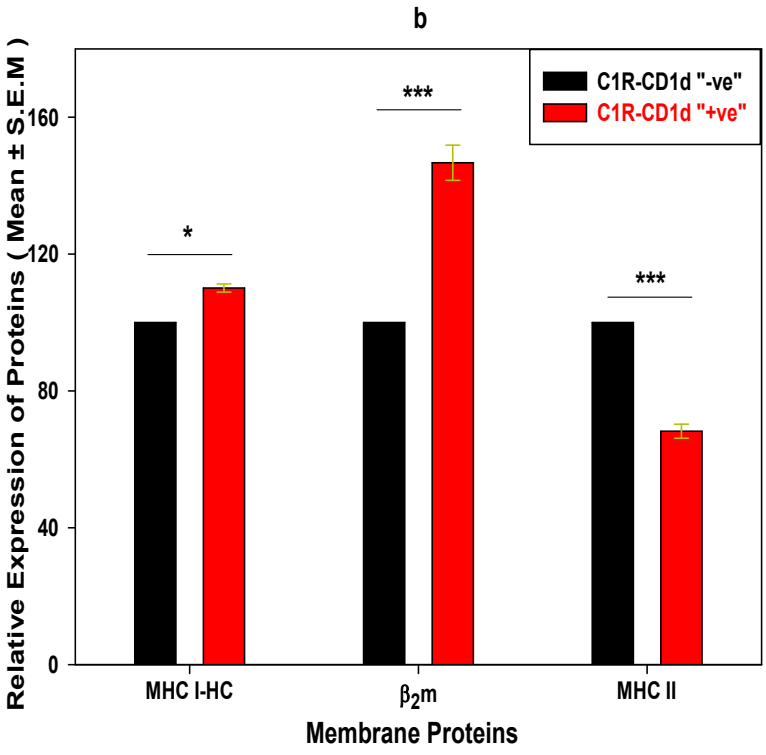

b) Differences in fluorescence signals of membrane proteins in C1R-CD1d "+ve" cells in comparison with C1R-CD1d "−ve" cells (Mean ± S.E.M., n≥6). The expression of proteins by C1R-CD1d "-ve" population was taken as 100%. A dual labeling of proteins of interest was carried out simultaneously as described in the materials and methods section. One of the labeled proteins was always CD1d protein while the second protein was among MHC I-HC, β_2m or MHC II proteins. Measurements were performed on a FACSCalibur instrument. Positive and negative populations for CD1d protein were gated carefully, and the fluorescence signals for each of the proteins in each population were quantified. Alexa 488 and Alexa 647 dyes conjugated antibodies were used for this experiment to avoid possible spectral overlap between dyes. In the figure, ∗, and ∗∗∗ indicate '*p*' values < 0.05, and < 0.0005 respectively.

6.2.4. Co-occurrence of MHC I-HC, β_2m, MHC II and CD1d in C1R-CD1d cells

Similarities in protein structure and alikeness in functional features, like antigen presentation, have been demonstrated previously between CD1d and MHC proteins (58, 80, 83, 102, 112). We and the others have also documented the co-existence of MHC I and MHC II proteins in the plasma membrane (178, 180, 181). Furthermore, both MHC I and MHC II proteins also bind to similar tetraspanin proteins on the cell surface (112, 180). Owing to such studies describing common molecular partners between CD1d, MHC I and MHC II proteins as well as the requirement of β_2m by most CD1 isoforms for plasma membrane expression; we hypothesized that CD1d and MHC proteins (I and II) might be close to each other as well. Therefore, we set up co-localization experiments. Two species of dyes, Alexa 546 and Alexa 647, conjugated to the same antibody L243, which is against MHC II was used as a positive control, whereas, GM_1 ganglioside and TfR molecules -which are considered to reside in detergent resistant and detergent sensitive membrane regions- were used as a negative control. Our results indicated a high level of co-localization between CD1d and other proteins (MHC I-HC, MHC II and β_2m). Several yellow pixels as in the case of positive control were observed between these proteins (**Figure 16a**). The confinement of these

proteins in the same region on the membrane was also corroborated by the high cross-correlation coefficient values between these proteins (**Figure 16b**).

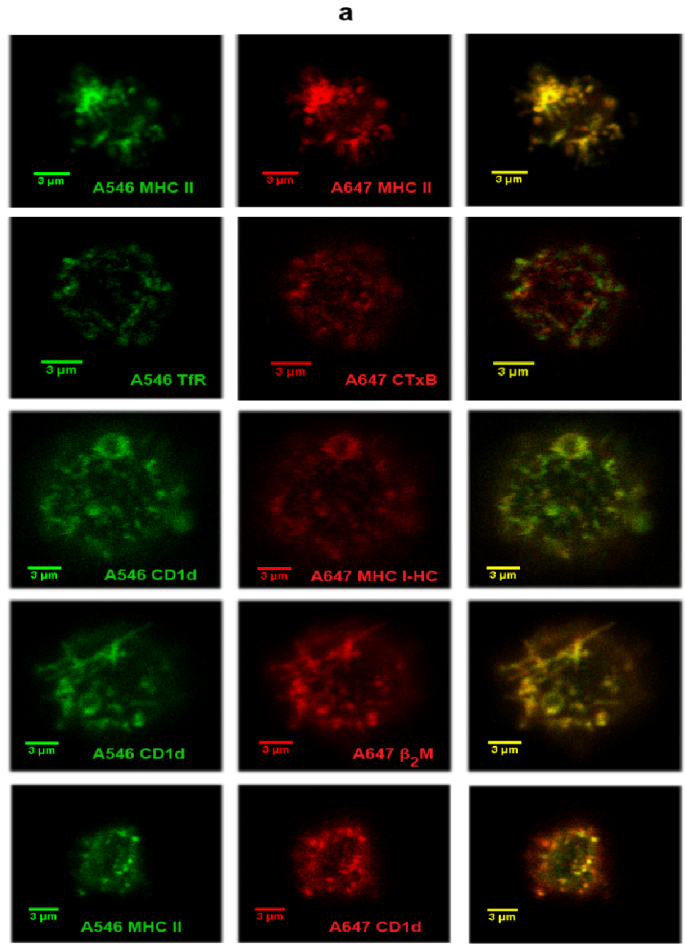

Figure 16. Co-localization of proteins:
a) Representative images for each of the proteins used in co-localization study are presented here. The images were background subtracted in this figure. The first two columns in green and red indicate the images of two different proteins in pseudo color taken in two different channels of the microscope, and the third column represents the superimposed image for these two channels. The name of the proteins which were imaged is shown on the bottom right corner of each image. For a positive control, the same L243 antibody was conjugated with both Alexa 546 and Alexa 647 dyes while CTxB and TfR were used as a negative control.

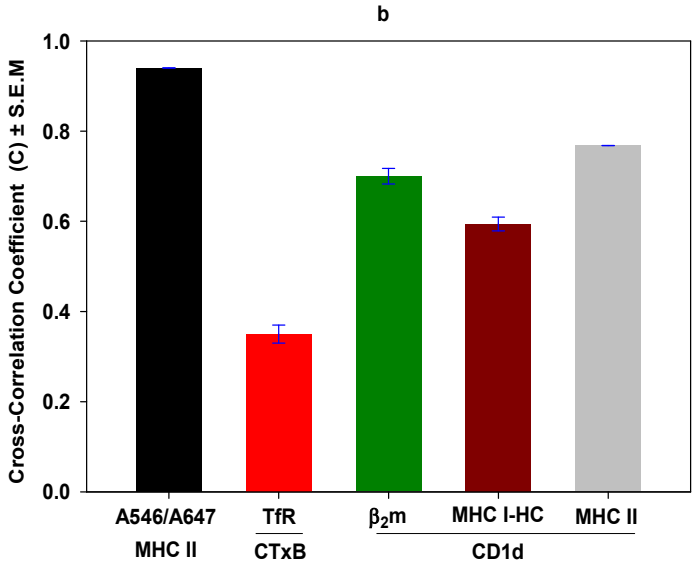

b) Cells were labeled with antibodies against each of the molecules denoted at the x-axis according to the steps described in the materials and methods section. The co-localization of the two molecules in question was calculated using a custom written program in LabView. The first and second row coloumns indicate positive and negative control respectively. The other coloumns show the 'C' values between CD1d and other molecules that were probed together. The dye conjugated antibodies used are mentioned on the right bottom of each image in **Figure 16a**. Data represent 'C' values in Mean ± S.E.M. of 15 to 20 different cells.

6.2.5. FCET determination of co-localized proteins

The resolution limit of confocal microscopy precludes the co-localization analysis from providing any information below 200 nm thus can only serve as a guidance regarding the spatial proximity of the proteins. Therefore, to illustrate physical associations of CD1d with other proteins (MHC I-HC, MHC II and β_2m), we performed a cell-by-cell FCET which has been described in detail elsewhere (157). A considerable amount of FRET efficiency was observed between CD1d and MHC I-HC, β_2m and MHC II proteins. Such association was also detected by the acceptor photobleaching FRET (data not shown). Likewise, FRET was also observed between MHC II and MHC I-HC and β_2m proteins. Interestingly, significant FRET efficiency was also detected between the same proteins when labeled proportionally with mixtures of different dye conjugates of the same antibody (independent donor and acceptor conjugates), also called as homoassociation FRET, suggesting that CD1d and MHC II also existed as self-clusters on the plasma membrane. However, the fluorescence signals were not enough to measure homoassociation FRET for MHC I-HC and β_2m proteins reliably (**Figure 17).**

6.2.6. Proximity relationship of CD1d and GM_1 ganglioside

Localization of MHC proteins in membrane micro domains, like rafts, has been demonstrated in various types of cells (182-188). Importantly, raft pre-association of MHC II was found to play a significant role in antigen presentation (185). Since, CD1d showed strong association with MHC II, we presumed that CD1d might also favor specific regions in the plasma membrane. We used CTxB, a universal marker for the raft that recognizes GM_1 ganglioside, to identify such an association between CD1d and GM_1 ganglioside. The cross-correlation coefficient value was significantly high (~0.72) between CD1d and GM_1 ganglioside on co-localization analysis, suggesting a specific preference of GM_1 rich regions by CD1d in the plasma membrane. An example is presented in **Figure 18**, demonstrating CD1d rich GM_1 regions in pink.

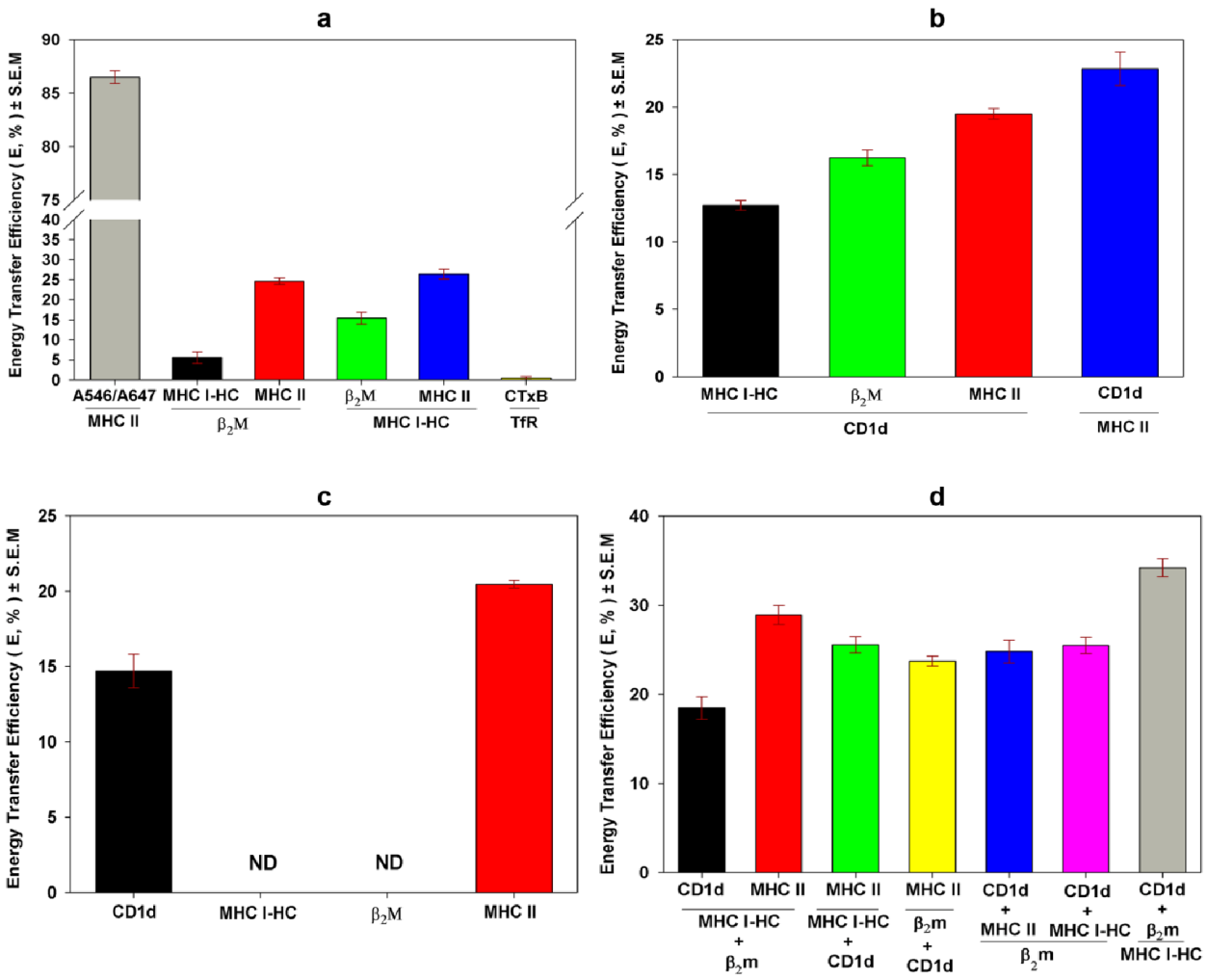

Figure 17. Flow Cytometric FRET (FCET)
FRET efficiency data is demonstrated as Mean ± S.E.M., (n = 5).
a) Flow cytometric FRET energy transfer between the proteins:
Bars from left to right: Positive control (Gray)- Both A546 and A647 dyes were conjugated to the same L243 antibody; β_2m served as a donor while MHC I-HC (Black) or MHC II (Red) served as an acceptor; MHC I-HC served as a donor while β_2m (Green) or MHC II (Blue) served as an acceptor; CTxB served as a donor while TfR served as an acceptor (Yellow). The FRET pair was always Alexa 546 and Alexa 647 dyes conjugated Mabs except for negative control where Alexa 555-CTxB probe was used as donor.
b) Flow cytometric FRET energy transfer between the proteins:
Bars from left to right: CD1d served as an acceptor while MHC I- HC (Black) or β_2m (Green) or MHC II (Red) served as a donor; MHC II served as an acceptor while CD1d (Blue) served as a donor.
c) Homoassociation Flow cytometeric FRET energy transfer between the proteins: The proteins are described in the x-axis.
d) Flow cytometric FRET energy transfer among three proteins:
Bars from left to right: (MHC I- HC + β_2m) served as a donor while CD1d (Black) or MHC II (Red) served as an acceptor; (MHC I- HC + CD1d) served as a donor while MHC II (Green) served as an acceptor; (β_2m + CD1d) served as a donor while MHC II (Yellow) served as an acceptor; β_2m served as a donor while (CD1d + MHC II) (Blue) or (CD1d +MHC I- HC) (Pink) served as an acceptor; MHC I- HC served as a donor while (β_2m + CD1d) (Gray) served as an acceptor. (Note: Proteins with '+' mark means they were conjugated to same Alexa dyes. For example 'MHC I- HC + β_2m' means MHC I- HC and β_2m were conjugated to Alexa 546 independently and were combinely used as donors in the first columns from left. The same case is also true for two proteins when used as acceptors except that the dyes were Alexa 647.

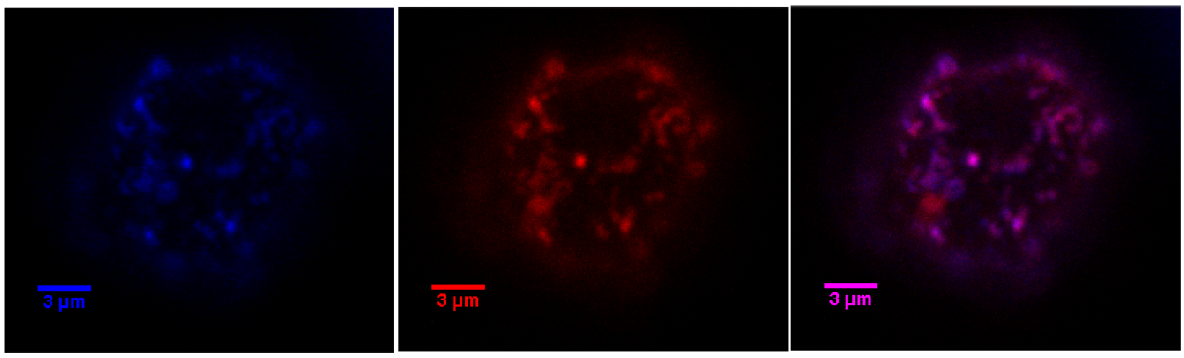

Figure 18. CD1d and GM_1 ganglioside co-localization:
Representative image of the distribution of CD1d and GM_1 gangliosides.
GM_1 gangliosides were labeled with Alexa 488-CTxB (Blue) and CD1d was labeled with Alexa 647-27.1.9 (Red). The overlay image is presented in the third column with pink pixels indicating co-localization.

6.2.7. CD1d enriched membrane regions: Mildly sensitive to cholesterol depletion but highly susceptible to low concentration of TX100

To unravel the specific nature of CD1d enriched membrane regions, we intended to calculate FRET between CD1d and GM_1 subunits. Further, we investigated whether these CD1d rich regions were influenced by cholesterol or not. For this purpose, two drugs were considered: MβCD, which extracts cholesterol, specifically from membrane (189) and simvastatin, which is an effective inhibitor of cholesterol biosynthesis (190). To optimize the concentration of the drugs, we analyzed the effect of drugs. We did not observe any significant difference in cell viability between control samples, and reagent treated samples, except for 10 mM MβCD, which led to compromised membrane integrity, based on annexin-propidium iodide FACS analysis (data not shown). With optimized parameters, we performed FRET between CD1d and GM_1 subunits. We found very high FRET efficiency between CD1d and GM_1 subunits in these cells at a resting state. Interestingly, both MβCD and simvastatin had non-significant effect on the association of CD1d with GM_1 ganglioside at the used conditions although the tendency of decrease in FRET efficiency was observed (**Figure 19**). Therefore, we thought to perform FCDR experiments, which can analyze the detergent tolerance capability of the raft associated proteins, using detergent TX100. We found that the susceptibility of CD1d enriched regions to detergent TX100, was worse than that of a TfR, a non-raft marker (**Figure 20A.c** and **20A.d**). In contrary, MHC II proteins, which partially reside in rafts, demonstrated superior resistance to TX100 than by TfR proteins (**Figure 20A.b, 20A.c** and **20B**). Furthermore, as expected the raft marker GM_1 ganglioside showed the highest degree of resistance to TX100 treatment, which is consistent with the detergent resistance feature of rafts. The effect of TX100 on the decline

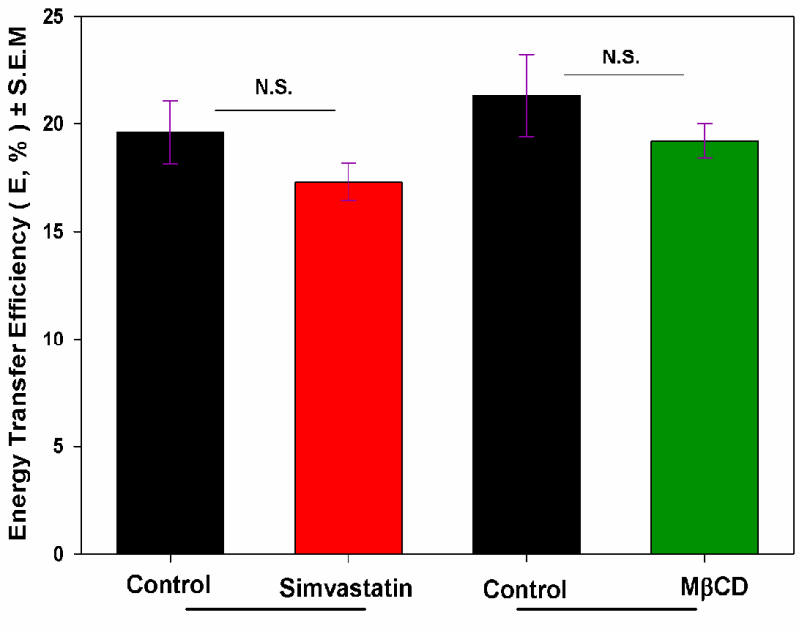

Figure 19.
Effect of MβCD and Statin in the relationship between CD1d and GM_1 ganglioside:
C1R-CD1d cells were treated with MβCD and simvastatin as described in the materials and methods section. Thereafter, the cells were labeled with saturating concentrations of CD1d antibodies and CTxB molecules for FCET experiments. CTxB was used as a donor while CD1d protein was used as an acceptor for FRET. Data demonstrate FRET efficiency values in Mean ± S.E.M., (n=6). Statistically non-significant "*p*" value is indicated as "N.S." in the figure.

of fluorescence intensity of CD1d was dose dependent (**Figure 20**) and the effect could be observed on CD1d proteins at detergent concentration as low as 0.01%, the concentration at which none of the other molecular species that were probed demonstrated any major changes. However, a marked reduction in fluorescence intensity of CD1d was observed starting from 0.013% TX100. At this concentration, the fluorescence intensities of the probed molecular species reduced to the following level in percentage relative to the initial fluorescence intensities within three minutes: CD1d decreased to ~15%, TfR decreased to ~70%, MHC II decreased to ~80% and that of GM_1 decreased to ~95% (**Figure 20**). The maximal decline in fluorescence intensity was observed for CD1d proteins. Therefore, mild detergent sensitivity is a specific feature of CD1d proteins on the membrane of B lymphocytes.

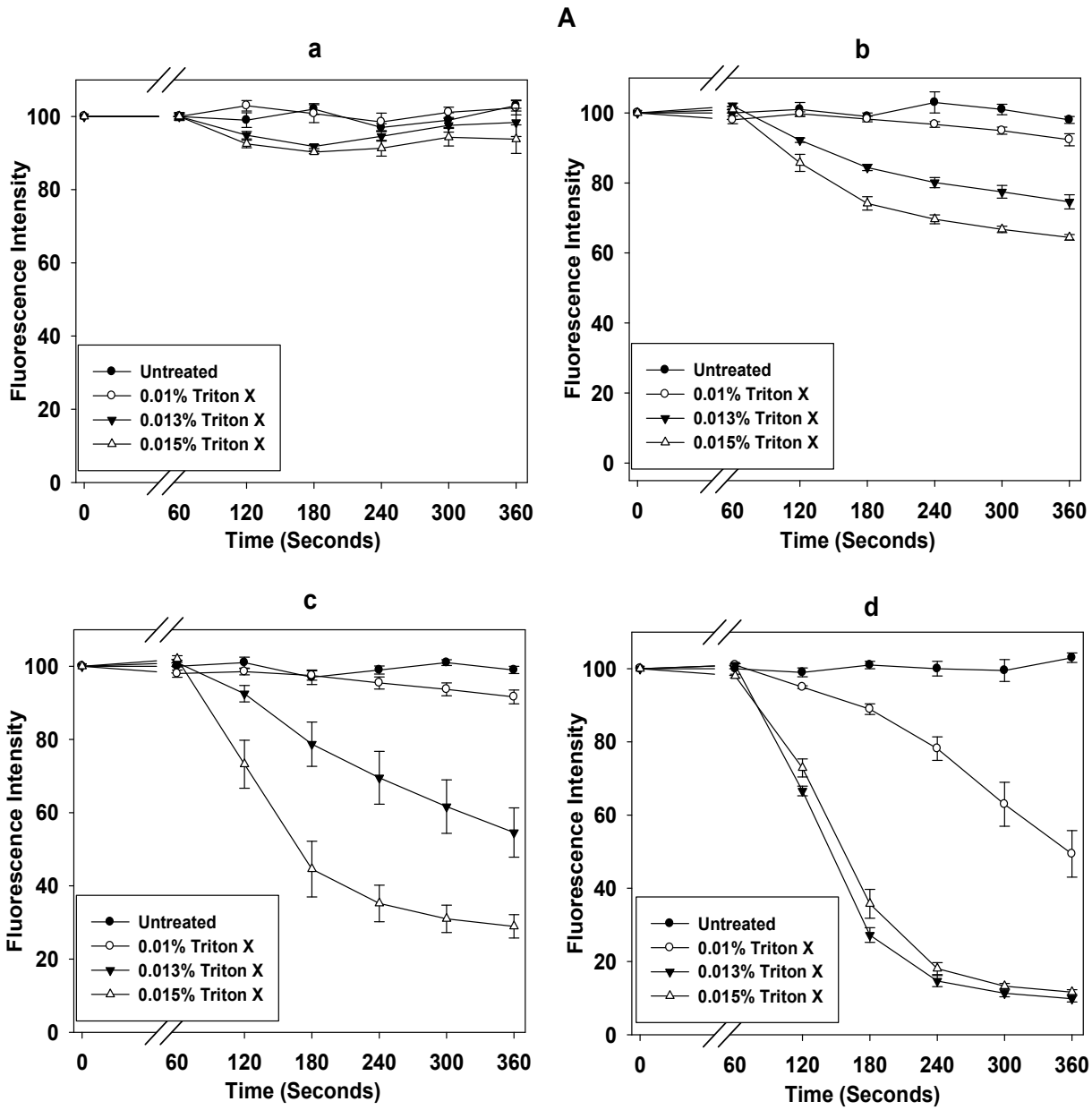

Figure 20.

A. Flow cytometry based detergent resistance analysis:

The response of various surface molecules to TX100 treatment is presented as fluorescence intensity versus time. The samples were prepared by incubating cells with respective probes independently (see materials and methods also). Non-fixed samples were processed for the measurements. Signals from the TX100 untreated samples were measured for approximately 50 s, then, ice-cold TX100 at various concentrations (untreated, 0.01%, 0.013% and 0.015%) was added to the samples, thereafter, the measurement was continued for approximately 5 min. **a)** GM_1 subunits **b)** MHC II proteins **c)** TfR **d)** CD1d proteins e) GM_1, MHC II, TfR and CD1d species at 0.013% TX100. The fluorescence intensities were averaged for every 60 s except for the first minute where it was averaged for 45 s. The break in the graph (from 45 to 50 s) represents the point of addition of TX100 except for untreated samples where continuous measurements for 6 min were performed. The data for each value is calculated from at least three sets of independent experiments and is presented as Mean±S.E.M.

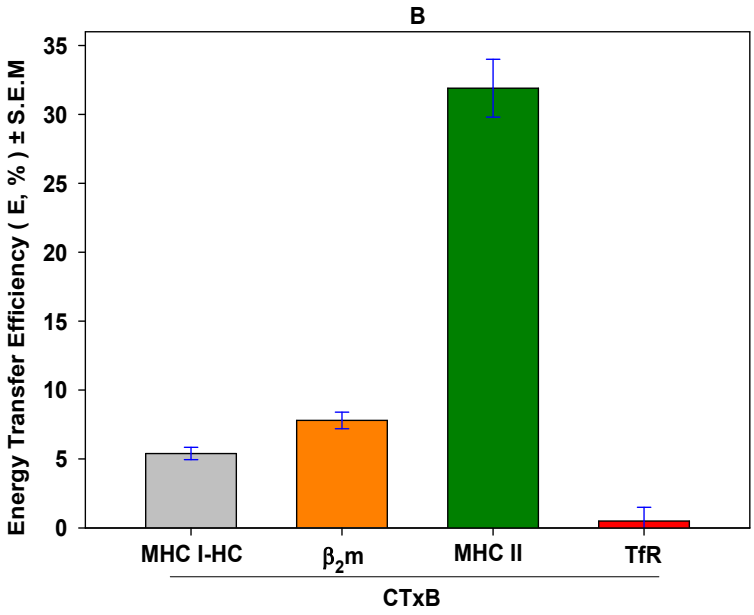

B. GM_1 ganglioside and MHC protein FCET study
One of the proteins (MHC I-HC or β_2m or MHC II or TfR) and GM_1 gangliosides were labeled on the membrane of C1R-CD1d cells. GM_1 ganglioside was always used as a donor molecule for this purpose. Procedures for probe labeling and FCET calculations were similar to the one that is described for CD1d- GM_1 FCET experiments in the materials and methods section. Data demonstrate FRET efficiency values in Mean ± S.E.M., (n≥4).

6.2.8. Effect of MβCD and Simvastatin on C1R-CD1d cells in iNK T cell activation

Dissimilar observations have been made in previous studies based on MβCD treatment of APCs: one study suggested the importance of the raft localization of CD1d in APCs as an essential element in signaling through TCR of NKT cells (132), whereas, another study concluded only a modest effect of MβCD treatment of APCs on the CD1d mediated antigen presentation (136). The application of simvastatin to APCs was also found to negatively affect NK T cell activation with significant down regulation in secretion of cytokines by NK T cells (136). To re-examine these observations, we thought to perform similar experiments but in human cells. In our case, we found that treatment of C1R-CD1d cells with 10 mM MβCD (15 min) reduced the membrane expression of CD1d proteins (28.8±2.3%, Mean±S.E.M) in C1R-CD1d cells (**Figure 22B.a**); however, this was accompanied by a greater decrease in the production of both cytokines (IFNγ up to 42% and IL4 up to 33%) from iNK T cells. In contrary, 2 mM MβCD treatment was well tolerated by C1R-CD1d cells and did not alter the membrane expression of CD1d in C1R-CD1d cells. Nevertheless, 2 mM MβCD treatment of C1R-CD1d cells had only modest inhibitory effects on the release of IFNγ and IL4 by iNK T cells (**Figure 21a** and **21b**). Notably, we did not observe any reduction, rather observed a slight up regulation, in cytokines release by iNK T cells due to treatment of C1R-CD1d cells by simvastatin (**Figure 21c** and **21d**) in contrast to studies showing negative effects of simvastatin in APCs in reducing the cytokine release by NK T cells (136). In addition, in our trials we could only measure a small amount of IFNγ but not IL4 in the supernatant of co-culture assays between lipid non-loaded

C1R-CD1d cells and iNK T cells (data not shown). Therefore the cytokine productions by iNK T cells were almost entirely in response to lipid loading of CD1d in C1R-CD1d cells.

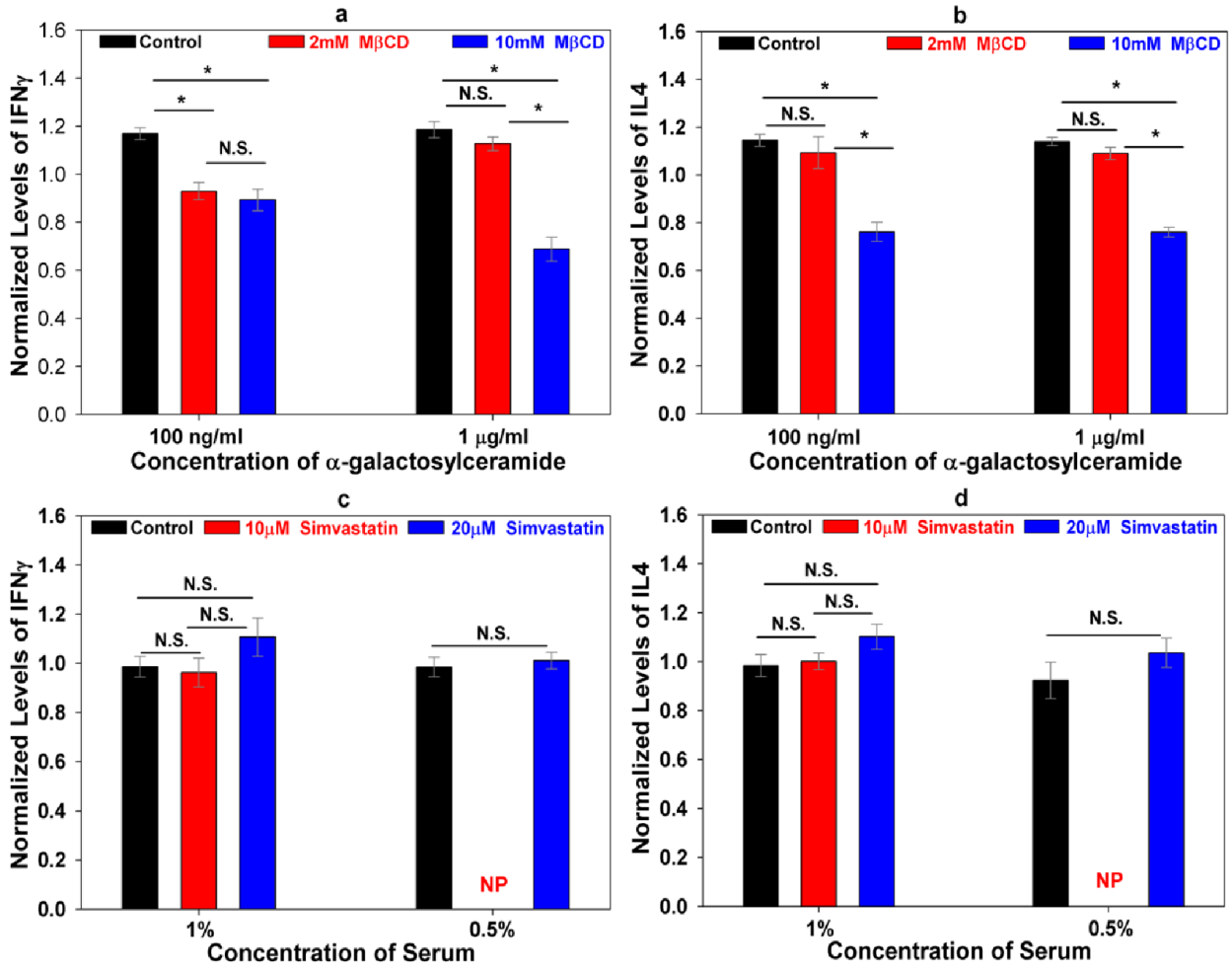

Figure 21. Effect of MβCD and simvastatin on C1R-CD1d cells in terms of iNK T cell cytokines release: One-way Anova with tukey post-hoc analyses or unpaired t-test was performed for statistical analysis. N.S. and '∗' represent non-significant or significant ('p'<0.05) values respectively. Each datum was normalized by the average of all data-set values from a particular independent experiment, including values from both control and treated samples,and is represented as Mean±S.E.M . Experiments were performed in triplicates for three or more times.

Study with MβCD treatment

C1R-CD1d cells were loaded with either 100 ng/ml or 1μg/ml α-gal for 18 h. It was then treated with MβCD. Next, the samples were fixed with 1% formaldehyde for 20 min on ice and were used in the co-culture assay with iNK T cells. **(a)** Measurement of IFNγ in the medium after 48 h of co-culture. The amount of IFNγ in control samples in Mean±S. E. M were 1589±402 pg/ml (100 ng/ml α-gal culture) and 1642±412 pg/ml (1μg/ml α-gal culture). **(b)** Measurement of IL4 in the medium after 48 h of co-culture. The amount of IL4 in control samples in Mean±S.E.M were 551±153 pg/ml (100 ng/ml α-gal culture) and 604±109 pg/ml (1μg/ml α-gal culture).

Study with simvastatin treatment

C1R-CD1d cells were incubated with or without simvastatin for 48 h in 1% NCS media or 0.5% NCS media. Four hours prior to the completion of this incubation period, 250 ng/ml α-gal was added to the C1R-CD1d cells. Next, C1R-CD1d cells were washed extensively and were fixed in 1% formaldehyde for 20 min on ice and were used in the co-culture assay with iNK T cells. 'NP' means 'Not Performed' in the figure. **(c)** Measurement of IFNγ in the medium after 48 h of co-culture. The amount of IFNγ in control samples in Mean±S.E.M were 1542±407 pg/ml (1% NCS culture) and 2407±337 pg/ml (0.5% NCS culture). **(d)** Measurement of IL4 in the medium after 48 h of co-culture. The amount of IL4 in control samples in Mean±S.E.M. were 817±145 pg/ml (1% NCS culture) and 1211±236 pg/ml (0.5% NCS culture).

6.2.9. Redistribution of membrane proteins by Simvastatin and MβCD

The association of CD1d with GM_1 ganglioside was not significantly altered by MβCD and simvastatin, therefore, we examined whether these reagents would affect the association of CD1d with other proteins (MHC I-HC, β_2m and MHC II). In fact, we found that both compounds had an effect on the topological arrangement of these proteins in the plasma membrane which means that the drugs had relevant effects in the cell. Between the two drugs, simvastatin had a far more profound effect on the redistribution of proteins in comparison with MβCD. Prominently, the association of β_2m with MHC I-HC and CD1d was significantly altered by these drugs (**Figure 22A**). Changes in FRET efficiencies between the proteins complemented the observed effect on the decrease of CD1d expression in these cells due to these compounds (25.2 ± 1.9 %, Mean±S.E.M, decrease in membrane CD1d expression due to 10 µM simvastatin, **Figure 22b**).

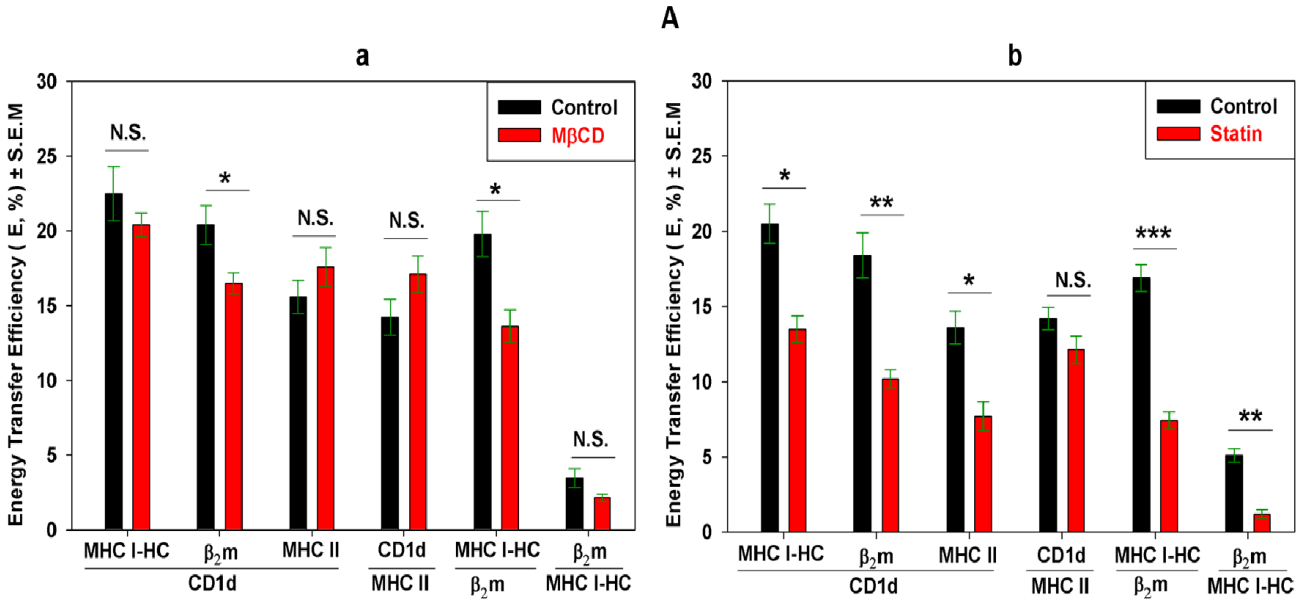

Figure 22.

A: MβCD and Simvastatin alter membrane protein distribution:
C1R-CD1d cells were treated with either MβCD (2 mM, 40 min) or simvastatin (10 µM, 48 hrs) according to the optimized protocol (see materials and methods). Thereafter, the samples were prepared for FCET experiments accordingly. Data represent FRET efficiency values in Mean ± S.E.M., (n≥6). In the figure, statistically non-significant "*p*" value is indicated as "N.S.", whereas "*p*" values < 0.05, < 0.005, and < 0.0005 are indicated by ∗, ∗∗, and ∗∗∗ symbols respectively.
a) FRET values for control samples are in black while MβCD treated samples are in red colors. Proteins mentioned just below the ticks in x-axis served as a donor while the one that is under the common line served as an acceptor for the FRET experiments.
b) FRET values for control samples are in black while simvastatin treated samples are in red colors. Proteins mentioned just below the ticks in x-axis served as a donor while the ones that are under the common line served as an acceptor for the FRET experiments.

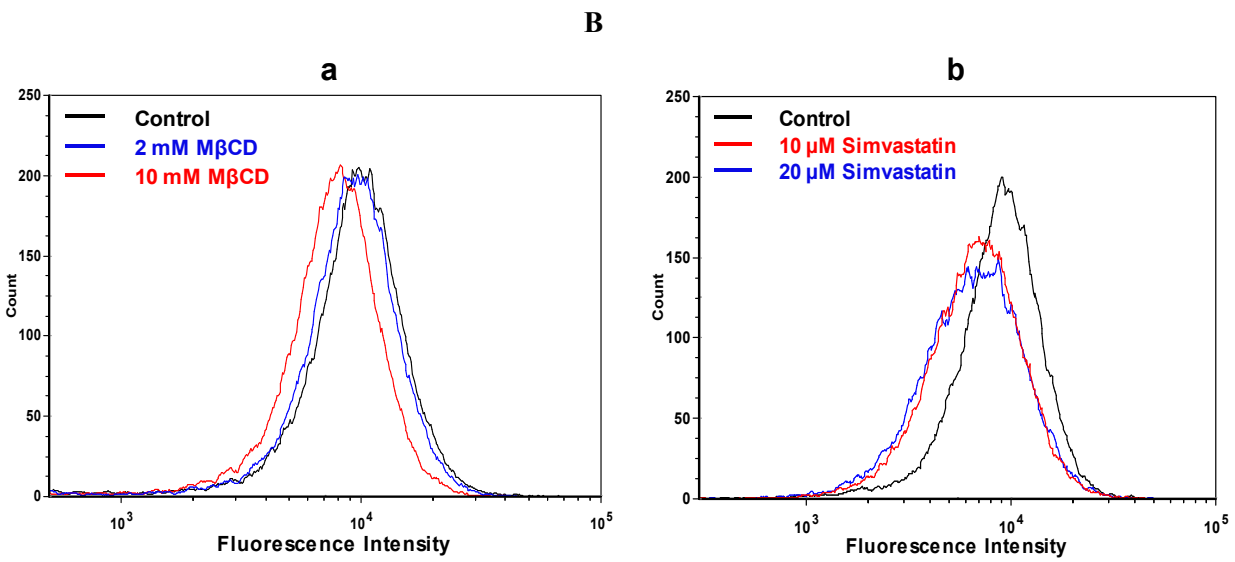

B: Effect of MβCD and Simvastatin on membrane CD1d expression.
a) Approximately (5-10) million cells, which were cultured in 10% NCS medium, were taken in 1 ml of 0.1% NCS RPMI media and were incubated with either 2 mM or 10 mM concentration of MβCD for either 40 min or 15 min at 37°C. On completion of incubation, cells were washed at least twice with PBS buffer and were labeled with saturating concentration of 27.1.9 CD1d antibody (100 µg/ml) following the protocol described in the materials and methods section. Thereafter, measurement of the prepared samples was performed using FACSArray instrument.
b) Cells ($3.5x10^6$) were cultured in 1% NCS RPMI medium for 48 hrs with or without simvastatin (10 µM or 20 µM). CD1d clone 27.1.9 Mab was used for detecting CD1d proteins. Preparation and measurement of samples were carried out like in the case of MβCD treatment as described in the materials and methods section.

6.2.10. Supramolecular complexes containing CD1d, MHC and lipid species on the membrane of C1R-CD1d cells

Based on two protein FRET system, physical association was distinctly observed between CD1d and MHC proteins as well as between MHC I and MHC II. This led us to assume that the plasma membrane of C1R-CD1d cells might contain multimolecular complexes of MHC I-HC, β_2m, MHC II and CD1d proteins. Like CD1d proteins, we also found that both MHC proteins, MHC I and MHC II, although at different degrees preferred vicinity of GM_1 gangliosides. However, comparatively MHC I-HC showed only a small FRET efficiency with GM_1 species indicating lower favorability of GM_1 species or possibly suggesting the enrichment of MHC I-HC with GM_1 gangliosides only at certain regions of the plasma-membrane (**Figure 20B**). Likewise, the co-localization of MHC I-HC with GM_1 species was not distinctive as in the case of other proteins (**Figure 23)**, although certain membrane regions showed the tendency of co-presence in accordance

to the FRET results. On performing trimolecular co-localization, we observed several predominant regions indicative of multimolecular complexes of MHC I-HC, β_2m, MHC II, CD1d and GM_1 molecules on the plasma membrane. In the **Figure 23**, such multimolecular complexes could be observed in the superimposed images as white pixels. The likelihood of the existence of multimolecular complexes on the plasma membrane was also suggested by our two-color but three-protein FCET. With this modified scheme, the FRET efficiency should increase between two proteins in comparison with conventional two protein FRET system when a new protein which is generally a part of trimolecular complex is also included in the FRET pair. In accordance with such assumptions, we observed an increase in the FRET efficiency between any two proteins with the inclusion of a third protein, mainly with MHC II as acceptor (**Figure 17d**). Thus, considering all lines of evidence, we conclude that multimolecular complexes of CD1d and other proteins (MHC I-HC, β_2m and MHC II) might also be present on the plasma membrane of these cells, preferably but not exclusively in non-GM_1 regions.

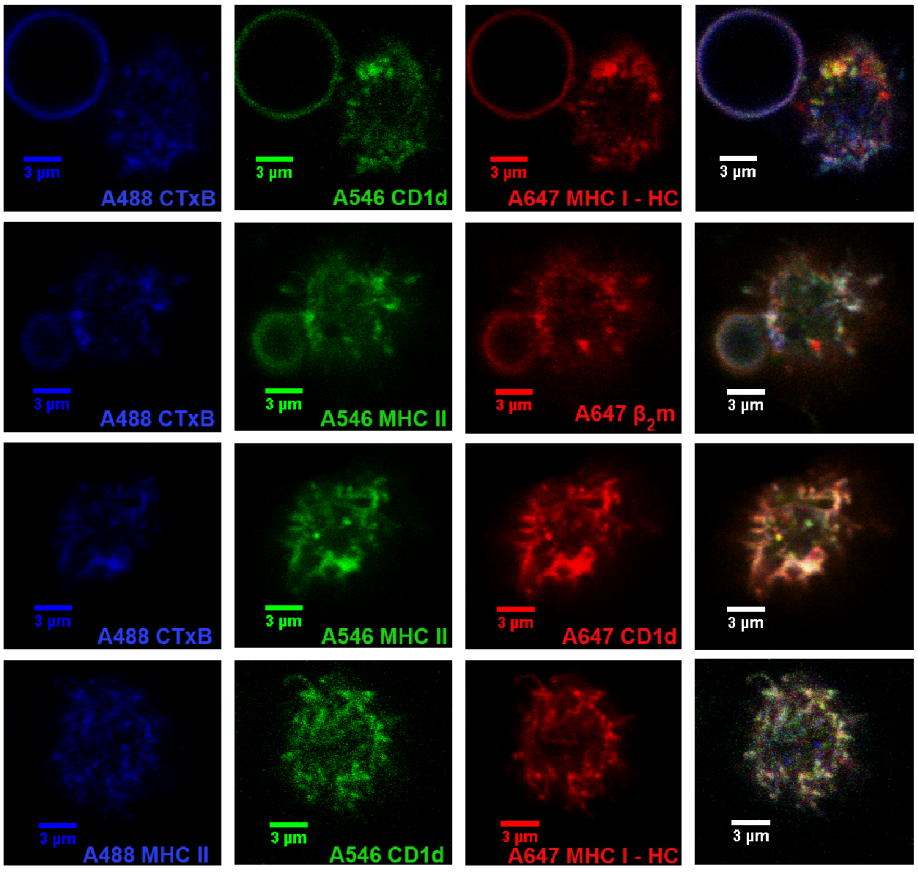

Figure 23.
Triple co-localization study: Three molecules from MHC I-HC, β_2m, MHC II, CD1d and GM_1 subunit molecules were simultaneously labeled in the similar ways as described in the materials and methods section. Once prepared, the fixed samples were washed thoroughly, thereafter; the cells were laid on poly-lysine (0.1mg/ml) coated ibidi chambers. Membrane molecules were then imaged from the top of the cell using confocal microscope. Specific dye conjugated probes were used for individual molecules, which are indicated at the right bottom of each image. The last column represents the merged image of all the three other columns.

7. DISCUSSION

7.1. Pros and cons of dye-antibody conjugation methods

A practicality of coupling fluorophores to antibody has been a significant achievement, especially in the applications related to diagnostics and biological research. In this study, three different antibody-labeling strategies were compared from the perspective of both ligation chemistry, and the financial cost involved in it. The binding affinity of dye conjugated Mabs against that of unconjugated counterparts was taken as a ruler to determine changes in the function of antibodies. Next, in each of the paragraphs below, important results will be outlined in a few words, which will then be elaborated for discussions.

7.1.1. Variation in binding affinity of antibodies

Two IgG isotypes, IgG1 and IgG2, were used for this study. IgG2a isotypes, W6/32 and L243, performed better and had low Kd values, whereas, IgG1 (P2A4) and IgG2b (51.1.3 CD1d) often showed greater variation in Kd values. IgG1, in comparison with IgG2, antibodies possess higher affinity for Fc receptors and is also an efficient inducer of antibody-dependent cellular cytotoxicity (ADCC) (191). Therefore, we speculated that the variation in Kd might be due to Fc receptor binding. However, using conjugates prepared by -NH_2 method, we found that Fc fragment of an antibody had only minimal influence on the binding affinity of these antibodies, ruling out any roles of Fc receptors on such inconsistent behavior (data not shown). Thus, the problems associated with P2A4 and 51.1.3 must be related to the intrinsic features of antibodies.

7.1.2. Fluorescence intensity and decrease in binding affinity do not correlate with F/P of dye-antibody conjugates

Our dye-antibody conjugates were functional; therefore, we assumed that dye conjugations had occurred in regions other than ABS. As it has been reported previously, dye-antibody conjugates prepared by -NH_2 method demonstrated the tendency of decrease in antigen binding affinity with the increase in F/P values. However, there was no strict linear relationship between F/Ps and the decrease in binding affinity of an antibody. In fact, F/Ps especially around 4 showed a better binding affinity in most cases. The binding affinity is influenced by both ‘V’ and ‘C’ regions of an antibody (192); therefore, appropriate conformation determines the features of binding affinity. This

also means that improved orientation of some amino acids in the three-dimensional space of the ABS could be one possible reason for the differential affinity between the low and high F/P conjugates. With the increase in F/P there should be a linear increase in fluorescence intensity at least theoretically. Nevertheless, such relationships between F/P and fluorescence intensity were only seen in the case of lower F/P variants (<3). In fact, higher F/Ps showed reduced fluorescence intensities in comparison with their preceding lower F/P variants. Such phenomenon has been described previously in a study based on confocal microscopy analysis (193). The authors suggested that the fluorescence quenching event was due to the complex spatial interactions and self-quenching processes occurring between the similar dyes lying in the FRET distance (<10 nm) of each other. In fact in a small molecule like IgG, the dye-conjugated distances would rarely be larger than 10 nm. This is because a typical length of an IgG molecule is approximately 24 nm at its 'Y' shape. Each of its arms (Fab and Fc) is about 9 nm in length and the distance between Fab and Fc is about 13 nm (194, 195). Hence, theoretically a 'Y' shape of the antibody offers only three sites where occurrence of dye conjugations can avoid possible quenching effects due to FRET. Such sites are the end of each arm of an antibody. However, dye conjugations at such sites simultaneously are almost inconceivable in -NH_2 method. This is because the conjugation of any dye at ABS would render antibodies ineffective in binding the antigen. In our case, all dye-antibody conjugates were capable of antigen recognitions; therefore, we do not see the probability of dye conjugations occurring at least at ABS. This means that most dyes after being conjugated to antibody are in a FRET distance of 10 nm especially when F/P is above 2. This distance between the dyes in an antibody would decrease with the increase in F/P ratio. Hence, we conclude that significant quenching of fluorescence intensity at higher F/P is partly due to homoFRET occurring between similar dyes conjugated to the same antibody. To further confirm this finding, we have also included an experimental study where we conjugated two dyes which are mostly used as a FRET pair, Alexa 546 and Alexa 647, to the same antibody L243 at similar F/P ratios (~4). We showed that significant FRET occurs between these two molecular species in such cases by FCET (**Figure 17**). In addition, aromatic amino acids like tryptophan, tyrosine and histidine as well as methionine present in antibodies can also act as natural quencher. Especially, the conserved nucleotide binding site (NBS) in antibodies is found to be enriched in tyrosine and tryptophan residues. These NBS regions are present in the variable domain of the Fab arm of all antibody isotypes from various species. Aromatic amino acids have been found to quench fluorescence of

organic dyes through combination of static and dynamic quenching mechanisms. Static quenching often arises when the fluorophore and quencher form a nonfluorescent ground-state complex due to stacking interactions (196, 197). Tyrosine residues, which are good electron acceptors, can also undergo photoinduced electron transfer (PET) which requires contact formation between the fluorophore and the quencher at a van der waals distance of subnanometer scale (198). Besides, fluorescence quenching can also occur via transition of a molecule from an excited singlet state to a triplet dark state, which means no fluorescence photon would be emitted thus reducing the photon yield. Alexa 647 dyes generate relatively long-lived dark states on illumination with red lasers (199). Combinedly, the diminished fluorescence intensity at higher F/Ps is due to the increased number of complex photophysical events including homoFRET, PET, static and dynamic quenching processes. In addition, another possible scenario that might be responsible for fluorescence quenching especially in a complex structure like cell membrane is the topological distribution of membrane proteins. It has been shown previously that clustering of proteins can lead to homoFRET, therefore, indirectly the molecular organization of proteins can also contribute to the reduction of fluorescence intensities of each dye-antibody conjugates. Primarily, the dyes being aligned to each other will be greater for higher F/Ps in comparison with lower F/Ps if protein clustering is to occur. Therefore, the quenching of fluorescence intensity would be larger for higher F/Ps due to protein clustering as well. In C1R-CD1d cells, MHC II and CD1d proteins were capable of forming self-clusters in the plasma membrane (**Figure 17**). Furthermore, the description of MHC I and ICAM1 homoclusters can also be found in the literature (200). However, we could not detect homoFRET for MHC I-HC due to low fluorescence signals though it does not rule out that possibility (**Figure 17**). In light of these findings, it becomes essential to consider the potential effect of intramolecular quenching and labeling sites in a protein especially if the conjugates involve quantitative measurements of fluorescence intensity.

7.1.3. Improved performance of dye-antibody conjugates prepared by -SH method over -NH_2 method

Antibody conjugates obtained from -SH method demonstrated low standard deviation in binding affinity in comparison with their -NH_2 based counterparts. It suggested that -SH based conjugates were better at preserving the ABS. Elimination of any kind of interference due to Fc receptors in the IgG isotypes, although very minimal, could be one reason for such performance. Despite this

observation, decrease in binding affinity relative to its unconjugated counterpart was still noticeable. We believe the observed effect in binding affinity is due to reduction in the avidity of antibody instead of the direct effect in binding affinity itself because only functional monovalent halves of the antibody can produce fluorescence intensities in our case (**Figure 10** and **Table 3**).

7.1.4. Differences in generation of F/P variants by IgG1 and IgG2 isotypes in -SH method

IgG1 has only two and IgG2 isotypes have four intra-heavy chain disulfide bonds connecting the two monovalent halves at the Fc region (201) of an antibody. We noticed that IgG1 (P2A4) and IgG2b (51.1.3) Mabs always produced higher F/P variants in comparison with IgG2a Mabs (W6/32 and L243) at similar dye coupling conditions by -SH method, therefore, the number of disulfide bonds between the two "H" chains does not explain the difference in the obtained F/P ratios for different isotypes of Mabs. Instead, F/P variants of Mabs might have been influenced by the presence of unconjugated fragments and conjugated inactive fragments of antibodies in the mixture. This assumption is also corroborated by our SDS-PAGE experiment where we observed the non-uniform reductive nature of MEA. Furthermore, it is also reminiscent of the observations that were made previously with MEA and DTT reduction of antibody (167, 202). We also noted that P2A4 and 51.1.3 Mabs were far more sensitive to MEA reduction than W6/32 and L243. Thus, it gives the notion that different antibody isotypes would produce completely different non-homogenous fragments of antibodies upon reduction with MEA.

7.1.5. Complications of carbohydrate targeted antibody conjugation

This method of dye-conjugation was quite tricky. It required multiple steps as in the case of -SH method. One complication that arose during the experimental optimization was the reaction kinetics thereof the reactivity of the oxidized antibody (i.e. aldehyde groups) with hydrazide dyes. It was very slow as described in the result section. However, the chemical reaction between the reactants could be significantly enhanced by including a catalyst like aniline during the incubation (203-206). Our observation is in parallel with the previous reports documenting the slow reaction kinetics of hydrazone chemistry (204, 207). It should be noted that a higher concentration of dye (≥200 folds to the antibody) was used in the previous dye conjugation study. This is ten times higher than the concentration used in our study; therefore, low F/P obtained in this study could be due to the lesser

quantity of dye (208). However, no catalyst was used in that study; therefore, the use of higher concentration of dye is also justifiable. Furthermore, low F/Ps obtained in our study might also be due to the difference in the glycosylation status of the Mabs produced by different hybridoma cell lines. Notably, binding affinity of antibody was adversely affected by this method even worse than in the case of other two methods. We presume that the effects in the antigen binding affinity of antibodies in this method are a result of over oxidation of Mabs due to $NaIO_4$. This in turn could have affected the tertiary structure of a protein (173, 174, 208) or even have had inactivated the antibodies. Interestingly, the sensitivity to $NaIO_4$ and tolerance to MEA in -CHO and -SH methods related similarly to binding affinity of the Mabs. High-affinity antibodies tolerated $NaIO_4$ better than low-affinity / or problematic antibodies. Does it convey the message of protein conformation dependent sensitivity to reducing and oxidizing agents? Yes, it could be. However, this aspect needs further investigation, especially after including antibodies of different isotypes and with different binding affinity. In all aspects, it performed worst among the three methods of dye conjugation. Separation between the free dyes and dye-conjugated antibody fronts were also not distinguishable unlike in $-NH_2$ and -SH based methods during gel chromatography probably due to oxidation-related adduct/or byproduct formation. This was clearly a reminder of the examination of this method with the capillary electrophoresis of the quantum dot-antibody conjugates where no clear baseline separation was observed between free quantum dots and antibody conjugated quantum dots (165). Aldehydes can react with amino groups; therefore cross-linking of antibodies would have occurred. In fact, such events have been reported before (208) and our SDS experiments further confirm the formation of antibody aggregates in this method.

7.1.6. Differential conjugation efficiency of the antibodies by the three methods

We mentioned that the strongest fluorescence intensities were demonstrated by the conjugates prepared by $-NH_2$ based method in comparison with the -SH and -CHO based conjugates, for similar F/Ps. Such situation would occur either due to lower yield of functional dye-antibody conjugates or fewer percentages of over-labeled antibodies. In the case of -SH based labeling, functional antibody conjugates with higher F/P (>3) is highly unrealistic owing to the limited number of disulfide bonds. Therefore, the only possibility would be the formation of the lower amount of active dye-antibody conjugates, whereas, both cases could be envisaged for -CHO based labeling method. Furthermore, the contribution from inert/inactive fragments of antibody in the -SH

method and cross-linked antibodies in the -CHO method could well be another factor in such behavior.

7.1.7. SDS-PAGE explains the inefficiency of -SH and -CHO methods

Unlike in the case of unlabeled antibodies and conjugates from -NH_2 method, single band representing intact antibodies was never obtained by -SH and -CHO methods when examined by non-reducing SDS PAGE. Therefore, we speculated that it was due to the use of chemicals, MEA and $NaIO_4$. Heterogeneity in the mixture of antibody conjugates, in fact, explains the discrepancy related to the low fluorescence intensity associated with the dye conjugates from -SH and -CHO methods. Fragments of various sizes 50, 75, 125 or >150 kDa were clearly observed due to MEA treatment indicating the generation of functional dye conjugated, functional dye unconjugated and non-functional antibody fragments. A similar effect was seen at various concentrations of MEA (data not shown). Therefore, MEA acts randomly in antibodies. Similarly, in the case of -CHO method, aggregated and fragmented antibodies were also seen, although it was in very small scale. In conclusion, our SDS-PAGE experiments suggest that only a small fraction of functional dye-antibody conjugates can be produced by -SH and -CHO methods.

7.2. Topography of CD1d proteins

The primary objective of this part of the study was to demonstrate the relative distribution of CD1d and MHC proteins on the surface of B lymphocytes. We employed various biophysical methods, including FRET, based on confocal microscopy and flow-cytometer. The possible explanations for several observations noted in the studies are thoroughly discussed in sections below:

7.2.1. Interaction between CD1d and MHC proteins in the plasma membrane

Our FCET results demonstrated that CD1d, MHC I-HC and MHC II proteins were physically close to each other in the membrane regions of C1R-CD1d cells. Thus, it confirms the findings from previous co-immunoprecipitation study where the association of CD1d with MHC II was found in B cells (112) and is also reminiscent of the association between CD1a and MHC I-HC observed in normal thymus cells (125). In fact, considering the association of CD1a with MHC II (124) and MHC I-HC (125), it can be postulated that all CD1 isoforms might interact with MHC I-HC since other common proteins from tetraspanin family also seem to associate with MHC I-HC, CD1 isoforms and MHC II proteins. This is also supported by the fact that multimolecular complexes of CD1 isoforms (CD1a, CD1b and CD1c) were also found on normal thymus cells (209, 210).

7.2.2. Quantitatively low amount of MHC I-HC in comparison with β_2m proteins in the plasma membrane of C1R-CD1d cells

Quantitatively, β_2m was higher than the level of MHC I-HC proteins in C1R-CD1d cells (**Figure 14b**). Among the proteins, MHC I-HC is the most well characterized protein that carries β_2m from the interior of a cell to the plasma membrane (211, 212). Since β_2m can also bind to CD1d and is considered important in the formation of CD1d-β_2m functional unit that specifically activates a group of T cells, we presumed that the observed differences in the expression of β_2m were due to the influence of CD1d. This speculation came out to be true when experiments were performed with CD1d "+ve" and CD1d "-ve" population of C1R cells. The lower amount of MHC I-HC in the plasma membrane in comparison with β_2m can also be explained by the FRET efficiency values between MHC I-HC and β_2m which was higher when MHC I-HC was used as a donor instead of β_2m. This is because with the increased amount of acceptors, generally the FRET efficiency increases thus it corroborates the quantitative examination of membrane proteins.

7.2.3. Exogenous expression of CD1d decreases MHC II expression and increases MHC I-HC and β_2m expression in the plasma membrane

In contrary to the enhancement of β_2m expression, reduction in MHC II proteins was found in the plasma membrane due to over expression of CD1d. This tends to suggest that either there is a competition for chaperones like an invariant chain in the intracellular compartments or alteration in trafficking behavior of MHC II proteins due to expression of CD1d somehow leading to retention of MHC II inside the cell or causing faster endocytosis of MHC II from the plasma membrane. Invariant chain was found to be associated with both MHC II and CD1d in C1R-CD1d cells (112) as well as in murine cells (111). In addition, invariant chain was found to influence the membrane expression of MHC II in a murine model (213). Considering the study in immature DCs, which suggested a higher degree of association between CD1a and invariant chain in the plasma membrane, even greater than with MHC II, it could be speculated that CD1d might also be associated with invariant chains in the cell surface. The expression of the invariant chain was also found to increase due to its ability to bind CD1a (124). Likewise, we also found a mild increase in MHC I-HC due to exogenous CD1d expression, which might be related to its ability to bind CD1d directly, thus causing a fraction of MHC I-HC to traffic together with CD1d to the plasma membrane. However, these areas would need further studies taking into account of the spatial and temporal distribution of CD1d, MHC I, MHC II and invariant chain proteins in the cell.

7.2.4. Direct and indirect association of β_2m and CD1d in the plasma membrane

We found a high FRET efficiency between CD1d and β_2m proteins. Thus, it confirmed that β_2m indeed physically interacted with CD1d as has been demonstrated before (80, 112). However, the increase in β_2m proteins relative to CD1d membrane expression was very low. Furthermore, a very low amount of free MHC I-HC proteins were present on the cell surface of C1R-CD1d cells. Therefore, the high FRET efficiency obtained between CD1d and β_2m proteins would be a result of both direct interaction of CD1d with β_2m and indirect co-occurrence of CD1d and β_2m due to the association of CD1d with MHC I-HC proteins in the plasma membrane. It should also be noted that the effect of cholesterol depletion from the plasma membrane was the significant redistribution of membrane proteins, mainly the interaction of β_2m with CD1d and MHC I-HC proteins (**Figure 22**). This further provides evidence to the notion that cholesterol dependent dissipation of MHC I-HC from the vicinity of CD1d proteins was responsible for the decrease in the FRET efficiency between

CD1d and β_2m. Hence, CD1d non-associated but MHC I-HC bound β_2m could also indirectly position itself in the vicinity of CD1d proteins.

7.2.5. High level of β_2m-free CD1d in the plasma membrane of C1R-CD1d cells

We described that β_2m expression on the plasma membrane of C1R-CD1d "+ve" cells was enhanced by ~46.7±11.5% in comparison with C1R-CD1d "-ve" cells. We also mentioned in our results that only few hundred β_2m free MHC I-HCs were found in the surface of these cells accounting for less than 1% of the total MHC I proteins in the plasma membrane of C1R-CD1d cells. Therefore, it suggests that most of the increased β_2m proteins on the surface i.e ~15% of the total CD1d proteins expressed on the plasma membrane were only bound to CD1d directly. This means that very high percentage of CD1d (~85%) in the plasma membrane of C1R-CD1d cells is present in the β_2m independent form. The interaction between β_2m and CD1d is not new and has been described before in this cell line (80) and epithelial cells (79), however, the presence of a large percentage of β_2m independent CD1d isoforms is something that is quite surprising. Since, β_2m independent CD1d is considered to be partially glycosylated, most of these proteins might be immature in nature (80). It would need specific probes, which is lacking right now, to demonstrate the two-dimensional spatial distribution and CD1d isoform co-operation events in the plasma membrane of these cells. Nevertheless, the occurrence of both isoforms capable of activating T cells has been reported in mouse B cells (214). Thus, the identified different isoforms of CD1d might have distinct functional roles in the activation of T cells.

7.2.6. Endogenous clusters of CD1d proteins on the cell surface

In this study, for the first time we demonstrated that CD1d could also form endogenous self-clusters in the plasma membrane. Homo clusters of CD1d proteins have been described previously on a monocytic cell line, THP1, using atomic force microscopy (AFM) (215). However, there are some major differences between our study and the aforementioned AFM study of CD1d proteins. First of all, iNK T TCRs were used to map the distribution of CD1d in THP1 plasma membrane. As have been known, TCRs would only be able to detect cognate lipid-loaded CD1d proteins. In addition, antigenic lipid ligand loading of APCs have been shown to facilitate the entry of CD1d proteins to detergent resistant membrane regions (131). Hence, the AFM recognition CD1d mapping study

might have detected the modified topography of CD1d proteins in the plasma membrane of THP1 cells. Since, we used Mab (27.1.9 clone) that can detect both empty or lipid loaded CD1d proteins, our study is thus first of its type to demonstrate endogenous distribution of CD1d proteins in the plasma membrane of B cells. Besides, the cells of monocytic and lymphoid lineage might also inherently differ in their ability to organize CD1d proteins in the plasma membrane.

7.2.7. Mild effect of cholesterol depletion in CD1d association of GM_1 ganglioside in C1R-CD1d cells and concomitant iNK T cell activation

From our studies, it was obvious that CD1d proteins were abundantly present in the proximity of GM_1 gangliosides of the plasma membrane. However, unlike MHC I and MHC II which are partially present in rafts and show cholesterol dependent residence in membrane microdomains/rafts (34, 159, 184, 188, 216), CD1d was shown to be influenced very little by cholesterol in its ability to associate with GM_1 subunits. The cholesterol depleting agents, MβCD and simvastatin, had only minimal effect on the association of CD1d with GM_1 ganglioside based on FRET. This observation was supported by a co-culture assay between MβCD/simvastatin treated C1R-CD1d cells and iNK T cells implying a minor role of cholesterol in CD1d mediated iNK T cell activation. Notably both of these chemicals reduced the plasma membrane level of cholesterol by greater than 30% when examined by filipin staining. Thus, it argues that either CD1d was present in the low cholesterol containing regions on the periphery of GM_1 gangliosides or the GM_1 enriched membrane microdomains proximal to CD1d were different from conventional rafts. Unlike MβCD, the effect of simvastatin might also be related to alteration in isoprenoid pathways. In fact, previous studies demonstrated that simvastatin had a negative impact on both peptide (MHC II) and lipid (CD1d) mediated antigen presentation. The diminished antigen presentation activity of the cells was attributed to secondary effects of simvastatin instead of reduction in cholesterol production (135, 136). In our study and with our experimental conditions, we did not really observe any reduction in cytokine secretion by iNK T cells in contrast to previous studies with simvastatin treatment of APCs. It was not due to the inactivation or non efficiency of simvastatin because the effect of simvastatin could be noticed morphologically in the treated cells. Furthermore, the same concentration of simvastatin leads to redistribution of proteins in the plasma membrane. Rather interestingly, simvastatin increased the GM_1 ganglioside surface expression (data not shown) suggesting secondary effects of simvastatin as well as a possible change in membrane fluidity.

Furthermore, simvastatin has been reported to alter the function of small GTPases (217-219) and disrupt the actin cytoskeleton (220, 221) in numerous studies. Actin destabilizing agent and rho kinase inhibitors are also found to enhance antigen presentation by CD1d in murine cells (222). Therefore, the effects of simvastatin on antigen presentation due to decrease in CD1d membrane expression and cholesterol depletion could have been negated by the ability of simvastatin to modify rho kinase functions and disrupt the actin cytoskeleton. However, it would need further investigation to verify such a hypothesis. We are also currently examining the roles of isoprenoid pathways in our cellular models to identify the importance of prenylation in CD1d mediated antigen presentation.

7.2.8. Detergent sensitivity and limited presence of cholesterol: Possibly, a new raft subtype where CD1d resides

Having been surprised by the features of CD1d in the plasma membrane, we decided to apply the detergent resistance test to CD1d proteins. Operationally, the hallmark feature of raft and raft-resident proteins is their resistance to high detergent concentration. Detergent sensitivity is considered as a feature of non-raft resident proteins like TfR only (159, 161, 223). A flow-cytometric version of detergent resistance test was also described by Gombos *et al* (161), and is comparatively easier to follow and quicker to apply than the biochemical method of detergent resistance test. On characterizing CD1d with FCDR, we realized that the detergent resistance capability of CD1d enriched regions was far lower than that of TfR, whereas, GM_1 and MHC II, which are considered to reside in detergent resistant regions of the membrane, displayed strong resistance to TX100. The non-raft residence of TfR was also confirmed by FRET (**Figure 20B**). Thus, it was intriguing because this was quite unlike that of raft-resident proteins. Sensitivity to detergents by CD1d enriched regions has also been demonstrated in other cell types (131, 133). Therefore, susceptibility to low concentration of detergents seems to be a specific feature of CD1d rich regions. However, cholesterol depletion had a mild but non-significant effect on the association between CD1d and GM_1 ganglioside in the plasma membrane. Therefore, our results suggest that the CD1d enriched detergent sensitive membrane regions of the plasma membrane, which seems to contain low cholesterol, could be a distinct raft subtype. Interestingly, a previous study also demonstrated that MHC I enriched regions in the plasma membrane of B cells has similar features of low cholesterol enrichment (184), thus resembling CD1d rich regions; however, unlike MHC I

which was very weakly associated with GM_1 gangliosides; CD1d showed strong GM_1 association, a feature of MHC II proteins in the plasma membrane. Several studies using various detergents advance the notion that different types of rafts/ or detergent resistant membrane regions might exist (184, 224, 225). The possible presence of cholesterol dependent and cholesterol independent raft subtypes were also documented using biophysical methods for the epidermal growth factor receptor (226). In addition, presence of cholesterol independent sphingolipid domains, ~200nm in diameter, was documented recently in the plasma membrane of fibroblasts. The underlying cytoskeletal structures were mainly responsible for maintaining these sphingolipid domains rather than cholesterol in these cells (227). Thus, the nature of CD1d enriched membrane regions needs further characterization, especially by comparing it with MHC enriched domains and other raft like structures.

7.2.9. Multimolecular complexes of CD1d, MHC and lipid species on the cell surface

Our co-localization and FRET experiments revealed that CD1d, MHC and GM_1 would co-exist in the plasma membrane. Furthermore, our triple co-localization and a modified two color three protein FRET set up additionally corroborated such possibilities. MHC II and CD1d showed markedly high presence in GM_1 rich regions, whereas, MHC I and CD1d scantily co-distributed in GM_1 regions by triple co-localization. In line with this observation, the FRET efficiency between any two proteins by the modified FRET set-up was always higher than the values from a conventional two protein system on inclusion of the third protein. Similarly, several tetraspanin proteins (CD82 and CD9) (112, 124, 228-230) and invariant chain proteins (124) are found to be associated with both MHC and CD1 proteins. Therefore, we speculate that these molecules as a supramolecular complex would also be present on the plasma membrane of these cells, although differences might occur in the abundance of these clusters in GM_1 rich and non-GM_1 regions.

7.2.10. Potential physiological implications of physical association of proteins and lipids on the cell surface

One of the surprising findings from our study was the presence of relatively high level of β_2m independent CD1d in the plasma membrane of these cells. Although, presence of β_2m independent CD1d is not a new finding, abundance in such a high amount is quite striking. Furthermore, CD1d seems to form self clusters in the plasma membrane which might be primarily

formed by these β_2m independent CD1d isoforms. It has been shown before in B cells that soluble extracellular β_2m would dissipate the homoclusters of MHC I proteins in the plasma membrane and thus makes them an efficient target for cytolysis (179), we hypothesize that similar situation might also occur in the case of CD1d proteins. Such a feature would be of physiological relevance in cases of multiple myeloma, hodgkin lymphomas or some autoimmune diseases where elevated levels of serum β_2m is observed. In fact, administration of lipid ligands may enhance the therapeutic outcome in such cases by enhancing the activity of NK T cells. Recently, it was also shown that association of MHC I-HC with CD1d would inhibit expression of functional CD1d proteins in the plasma membrane and thereby would inhibit CD1d antigen presentation in murine cells (231). Likewise, the association of CD1d with MHC II was found to enhance an exogenous antigen presentation by CD1d mainly by inducing increased endocytosis of CD1d to endolysosomal compartments through invariant chain (232). iNK T cells secrete large amount of cytokines like innate cells on activation, therefore, uncontrolled stimulation of these cells might exacerbate cases like autoimmune diseases. In summary, the physical association between MHC and CD1d proteins in the plasma membrane of cells might help in keeping the activity of immune cells in balance. Though not clear yet in our system, such interactions between these molecules would either enhance or inhibit CD1d mediated antigen presentation or vice versa. Similarly, the association of CD1d with lipid species like GM_1 gangliosides might be critical in situations when there is a limited amount of antigens present in the environment. Such an association possibly would increase the local concentration of CD1d/antigen complexes that might be optimal for TCR stimulation especially in the contact regions between that of APCs and iNK T cells.

8. GENERAL CONCLUSIONS AND FUTURE PERSPECTIVES

8.1. A compromise between necessity and severity

The ability to conjugate antibodies to another protein has been a milestone in the success and evolution of protein biology. Any aspects of antibody conjugation should demonstrate the hybrid features of both antibody and the conjugated element, like dyes, with minimal effect on the independent features. Theoretically, it is possible to envisage the preservation of remarkable features of two proteins coming into splicing; however, it does not necessarily happen. Therefore, a right approach should help to minimize the detrimental effects due to bioconjugation. In the case of antibody conjugation, the appropriate chemistry should yield the products with the best possible retention of antigen binding activity. Among the three most common strategies employed in antibody conjugation, we found that -NH_2 based method was hassle free and easy to perform approach. It included fewer steps with faster reaction kinetics thus permitting higher yield of dye-antibody conjugates at lower cost. Next to -NH_2 method was -SH method due to its advantage in generating functional half-antibodies with minimal non-specific binding and preservation of antigen binding function. However, issues pertaining to the yield of dye-antibody conjugates have to be addressed. The performance was below par in contrary to its assumptions of preserving antibody binding function in the case of -CHO method. Especially, the use of reagents like $NaIO_4$ seems to alter the binding affinity of antibody. Furthermore, the reaction kinetics in -CHO method is also very slow; therefore, selective chemical reagents that can have defined effect in the antibody should be explored or biological approach, like the use of special enzymes, for instance, galactosidase, neuraminidase, etc., should be critically evaluated (233, 234). In summary, based on the yield of conjugates, ease of operation, experimental optimization and finance, the performances of three antibody conjugation methods were in the following order: -NH_2 >-SH>-CHO. Thus, despite the challenges posed by -NH_2 and -SH methods of labeling due to their susceptibility to hydrolysis under conditions of bioconjugation, the advantages offered by these methods outweigh the inadequacies and are better than -CHO based labeling strategy.

8.2. Finer landscapes of CD1d distribution in the plasma membrane

With our microscopic and flow-cytometric studies, we are able to show that CD1d harbors a close relationship with MHC and GM_1 gangliosides on the plasma membrane. Some features were quite

distinct for CD1d proteins. β_2m association is indispensable for MHC I-HC plasma membrane expression whereas most CD1d seems to be independent of β_2m on the cell surface. Similarly, CD1d seems to be tightly associated with GM_1 gangliosides, a raft marker, based on FRET, however, detergent resistance analysis of CD1d enriched regions suggested otherwise. Interestingly, cholesterol depletion had mild but non-significant effect on the association of CD1d and GM_1 gangliosides, therefore, CD1d enriched regions in the plasma membrane seem to be low in cholesterol. Such a feature is also supported by the fact that CD1d rich regions in the plasma membrane of B cells only had a mild dependence on cholesterol during iNK T cell activation. In our study, we used flow cytometry which provides statistically robust data; however, it does not offer any distinctive information regarding the spatial regions that generally differ in the distribution of proteins in the plasma membrane of a cell. Likewise, confocal microscope suffers from the diffraction limit thus has a spatial resolution of about >200 nm in XY plane. Emergence of novel super-resolution optical microscopes (or nanoscopies) such as stimulated emission depletion microscopy (STED) or fluorescence photoactivation localization microscopy (fPALM)/ direct stochastic optical reconstruction microscopy (dSTORM) or near-field scanning optical microscope (NSOM) etc has helped to overcome such limitations. Most of these microscopes allow far greater resolution with a feasibility of imaging molecular distribution below 100 nm in living cells thus confer several advantages over confocal microscopes (235-237). Such advantage renders nanoscopes with an ability to provide far greater insights into the active physiological processes occurring in the plasma membrane of a cell. Since plasma membrane is not static rather it is a dynamic yet structured assemblies of proteins and lipids. Therefore, studies using such nanoscopies would provide significant details on the features of CD1d proteins. Particularly, fluorescence methods, like fluorescence correlation spectroscopy, using nanoscopies would be able to shed light into the lateral homotypic and heterotypic cis-interactions occurring between proteins and lipids over different scales of time and space (235). The diffusion features of a molecular species depend upon the environment it resides within the plasma membrane. A monomer diffuses faster than the multimolecular blocks of the same protein. Furthermore, organization of proteins in the membrane is critical in defining the biological events; therefore, studying the assembly, organization and interaction dynamics of CD1d would significantly advance our understanding of the signaling pathways mediated by this protein. Thus, it would pave the ways for the development of therapeutic opportunities exploiting CD1d immune axis.

9. SUMMARY

In the first part of the thesis, we generated dye-antibody conjugates by three different strategies which are commonly employed in most research laboratories (amine, sulfhydryl and carbohydrate targeted approaches) so that it could be used for studying membrane protein dynamics. The goal was to obtain conjugates which retained the maximum antigen recognition features and that produced the highest fluorescence intensities. We found that only amine targeted approach could produce higher dye per antibody variants (>3) with a maximum yield of antibody conjugates. Sulfhydryl and carbohydrate targeted approaches are site-specific, however, they led to the generation of low amount of functional dye-antibody conjugates. Therefore, amine targeted approach is the best method of antibody conjugation in comparison with the other two approaches in totality.

In the second part of the thesis, our goal was to unravel the topological features of a membrane protein termed cluster of differentiation 1d (CD1d). These proteins are involved in lipid-based antigen presentation. We wanted to demonstrate the relationship of CD1d with peptide antigen presenters i.e. major histocompatibility complex (MHC) proteins on the cell surface. We documented using fluorescent dye-antibody conjugates and biophysical tools that CD1d harbors a close relationship with MHC I, β_2-microglobulin (β_2m), MHC II and GM_1 gangliosides on the plasma membrane of human B cells at resting state. Surprisingly, β_2m dependent CD1d constituted only ~15% of the total membrane CD1d proteins. In addition, fluorescence resonance energy transfer (FRET) studies revealed only minimal effect of membrane cholesterol depletion on the association between CD1d and GM_1 ganglioside on the cell surface. Instead, CD1d rich regions were highly sensitive to low concentration of Triton X-100. Therefore, CD1d is either located at the periphery of GM_1 gangliosides or is enriched in low cholesterol containing detergent sensitive membrane regions of the plasma membrane which could be a distinct raft subtype.

In summary, we generated dye-antibody conjugates which were suitable for studying the membrane distribution of CD1d proteins. We believe the investigated antibody conjugation approaches can provide researchers with up-to-date information in the field of bioconjugation.

Likewise the membrane topological features of CD1d discovered in our study might be immunologically relevant considering the importance of CD1d mediated lipid antigen presentation in linking the innate and adaptive immunity.

10. LITERATURE CITED

1. Tak W. Mak, and M. Saunders. 2011. Academic Press.
2. Kaufmann, S. H. 2008. Immunology's foundation: the 100-year anniversary of the Nobel Prize to Paul Ehrlich and Elie Metchnikoff. Nat Immunol 9:705-712.
3. Drews, J. 2004. Paul Ehrlich: magister mundi. Nat Rev Drug Discov 3:797-801.
4. MargiePatlak. 2009. Magic Bullets and Monoclonals: An Antibody Tale. In Breakthroughs in bioscience. Federation of American Societies for Experimental Biology (FASEB).
5. Zouali, M. 2001. Antibodies. Encyclopedia of Life Sciences:8.
6. Wols, H. A. M. 2005. Plasma Cells. Encyclopedia of Life Sciences..
7. Lipman, N. S., L. R. Jackson, L. J. Trudel, and F. Weis-Garcia. 2005. Monoclonal versus polyclonal antibodies: distinguishing characteristics, applications, and information resources. ILAR J 46:258-268.
8. Boenisch, T. 2009. Antibodies. Dako, California.
9. Hermanson, G. T. 2008. Bioconjugate techniques. Academic Press San Diego, CA.
10. Taniguchi, N. 2009. Amino Acids and Proteins. Mosby Elsevier.
11. Haugland, R. P. 1995. Coupling of monoclonal antibodies with fluorophores. Methods Mol Biol 45:205-221.
12. Betts, M. J., and R. B. Russell. 2003. Amino Acid Properties and Consequences of Substitutions. John Wiley & Sons, Ltd, West Sussex.
13. Turkova, J. 1993. Survey of the most common coupling procedures. Esevier Science Publishers B.V, Amsterdam.
14. Crisalli, P., and E. T. Kool. 2013. Water-soluble organocatalysts for hydrazone and oxime formation. J Org Chem 78:1184-1189.
15. Galy, A., M. Travis, D. Cen, and B. Chen. 1995. Human T, B, natural killer, and dendritic cells arise from a common bone marrow progenitor cell subset. Immunity 3:459-473.
16. Burrows, P. D., LeBien, T., Zhang, Z., Randall S. Davis., Cooper, M. D. 2004. The Development of Human B Lymphocytes. Academic Press Inc.
17. Kearney, J. F. 2004. Development and Function of B Cell Subsets. Academic Press Inc.
18. Trombetta, E. S., and I. Mellman. 2005. Cell biology of antigen processing in vitro and in vivo. Annu Rev Immunol 23:975-1028.
19. Evans, D. E., M. W. Munks, J. M. Purkerson, and D. C. Parker. 2000. Resting B lymphocytes as APC for naive T lymphocytes: Dependence on CD40 ligand/CD40. Journal of Immunology 164:688-697.
20. Krieger, J. I., S. F. Grammer, H. M. Grey, and R. W. Chesnut. 1985. Antigen presentation by splenic B cells: resting B cells are ineffective, whereas activated B cells are effective accessory cells for T cell responses. Journal of Immunology 135:2937-2945.
21. Rodriguez-Pinto, D. 2005. B cells as antigen presenting cells. Cellular Immunology 238:67-75.
22. Chen, X. J., and P. E. Jensen. 2008. The role of B lymphocytes as antigen-presenting cells. Archivum Immunologiae Et Therapiae Experimentalis 56:77-83.
23. Batista, F. D., and M. S. Neuberger. 1998. Affinity dependence of the B cell response to antigen: a threshold, a ceiling, and the importance of off-rate. Immunity 8:751-759.
24. Parra, D., A. M. Rieger, J. Li, Y. A. Zhang, L. M. Randall, C. A. Hunter, D. R. Barreda, and J. O. Sunyer. 2012. Pivotal Advance: Peritoneal cavity B-1 B cells have phagocytic and microbicidal capacities and present phagocytosed antigen to $CD4^+$ T cells. Journal of Leukocyte Biology 91:525-536.
25. Nakashima, M., M. Kinoshita, H. Nakashima, Y. Habu, H. Miyazaki, S. Shono, S. Hiroi, N. Shinomiya, K. Nakanishi, and S. Seki. 2012. Pivotal Advance: Characterization of mouse liver phagocytic B cells in innate immunity. Journal of Leukocyte Biology 91:537-546.
26. Todd, I. 2001. Cells of the Immune System. Encyclopedia of Life Sciences:7.
27. Hayday, A. C. 2000. γδ cells: a right time and a right place for a conserved third way of protection. Annu Rev Immunol 18:975-1026.
28. Brandes, M., K. Willimann, and B. Moser. 2005. Professional antigen-presentation function by human γδ T Cells. Science 309:264-268.

29. Stetson, D. B., M. Mohrs, R. L. Reinhardt, J. L. Baron, Z. E. Wang, L. Gapin, M. Kronenberg, and R. M. Locksley. 2003. Constitutive cytokine mRNAs mark natural killer (NK) and NK T cells poised for rapid effector function. J Exp Med 198:1069-1076.
30. Jeff Subleski, J. M. W., Robert H. Wiltrout, John R. Ortaldo. 2009. NK and NKT cells: the innate – adaptive interface including humoral responses. Academic Press.
31. Brennan, P. J., M. Brigl, and M. B. Brenner. 2013. Invariant natural killer T cells: an innate activation scheme linked to diverse effector functions. Nat Rev Immunol 13:101-117.
32. Van Kaer, L., V. V. Parekh, and L. Wu. 2013. Invariant natural killer T cells as sensors and managers of inflammation. Trends Immunol 34:50-58.
33. Subleski, J. J., Q. Jiang, J. M. Weiss, and R. H. Wiltrout. 2011. The split personality of NKT cells in malignancy, autoimmune and allergic disorders. Immunotherapy 3:1167-1184.
34. 2005. Antigen Presenting Cells: From Mechanisms to Drug Development. Wiley-VCH.
35. Blum, J. S., P. A. Wearsch, and P. Cresswell. 2013. Pathways of Antigen Processing. Annu Rev Immunol.
36. Garstka, M. A., and J. Neefjes. 2012. How to target MHC class II into the MIIC compartment. Mol Immunol.
37. Watts, C., and S. Amigorena. 2000. Antigen traffic pathways in dendritic cells. Traffic 1:312-317.
38. Li, L., S. Kim, J. M. Herndon, P. Goedegebuure, B. A. Belt, A. T. Satpathy, T. P. Fleming, T. H. Hansen, K. M. Murphy, and W. E. Gillanders. 2012. Cross-dressed $CD8\alpha^+/CD103^+$ dendritic cells prime $CD8^+$ T cells following vaccination. Proc Natl Acad Sci U S A 109:12716-12721.
39. Potter, N. S., and C. V. Harding. 2001. Neutrophils process exogenous bacteria via an alternate class I MHC processing pathway for presentation of peptides to T lymphocytes. J Immunol 167:2538-2546.
40. Pfeifer, J. D., M. J. Wick, R. L. Roberts, K. Findlay, S. J. Normark, and C. V. Harding. 1993. Phagocytic processing of bacterial antigens for class I MHC presentation to T cells. Nature 361:359-362.
41. Kjer-Nielsen, L., O. Patel, A. J. Corbett, J. Le Nours, B. Meehan, L. Liu, M. Bhati, Z. Chen, L. Kostenko, R. Reantragoon, N. A. Williamson, A. W. Purcell, N. L. Dudek, M. J. McConville, R. A. O'Hair, G. N. Khairallah, D. I. Godfrey, D. P. Fairlie, J. Rossjohn, and J. McCluskey. 2012. MR1 presents microbial vitamin B metabolites to MAIT cells. Nature 491:717-723.
42. Cobb, B. A., Q. Wang, A. O. Tzianabos, and D. L. Kasper. 2004. Polysaccharide processing and presentation by the MHCII pathway. Cell 117:677-687.
43. Cobb, B. A., and D. L. Kasper. 2008. Characteristics of carbohydrate antigen binding to the presentation protein HLA-DR. Glycobiology 18:707-718.
44. Vavassori, S., A. Kumar, G. S. Wan, G. S. Ramanjaneyulu, M. Cavallari, S. El Daker, T. Beddoe, A. Theodossis, N. K. Williams, E. Gostick, D. A. Price, D. U. Soudamini, K. K. Voon, M. Olivo, J. Rossjohn, L. Mori, and G. De Libero. 2013. Butyrophilin 3A1 binds phosphorylated antigens and stimulates human γδ T cells. Nat Immunol 14:908-916.
45. Lafont, V., J. Liautard, M. Sable-Teychene, Y. Sainte-Marie, and J. Favero. 2001. Isopentenyl pyrophosphate, a mycobacterial non-peptidic antigen, triggers delayed and highly sustained signaling in human γδ T lymphocytes without inducing down-modulation of T cell antigen receptor. J Biol Chem 276:15961-15967.
46. Porcelli, S. A. 1995. The CD1 family: a third lineage of antigen-presenting molecules. Adv Immunol 59:1-98.
47. Dascher, C. C. 2007. Evolutionary biology of CD1. Curr Top Microbiol Immunol 314:3-26.
48. Wang, C., T. V. Perera, H. L. Ford, and C. C. Dascher. 2003. Characterization of a divergent non-classical MHC class I gene in sharks. Immunogenetics 55:57-61.
49. Kruiswijk, C. P., T. T. Hermsen, A. H. Westphal, H. F. Savelkoul, and R. J. Stet. 2002. A novel functional class I lineage in zebrafish (Danio rerio), carp (Cyprinus carpio), and large barbus (Barbus intermedius) showing an unusual conservation of the peptide binding domains. J Immunol 169:1936-1947.

50. Shum, B. P., R. Rajalingam, K. E. Magor, K. Azumi, W. H. Carr, B. Dixon, R. J. Stet, M. A. Adkison, R. P. Hedrick, and P. Parham. 1999. A divergent non-classical class I gene conserved in salmonids. Immunogenetics 49:479-490.
51. Maruoka, T., H. Tanabe, M. Chiba, and M. Kasahara. 2005. Chicken CD1 genes are located in the MHC: CD1 and endothelial protein C receptor genes constitute a distinct subfamily of class-I-like genes that predates the emergence of mammals. Immunogenetics 57:590-600.
52. Baker, M. L., and R. D. Miller. 2007. Evolution of mammalian CD1: marsupial CD1 is not orthologous to the eutherian isoforms and is a pseudogene in the opossum Monodelphis domestica. Immunology 121:113-121.
53. Calabi, F., and C. Milstein. 1986. A novel family of human major histocompatibility complex-related genes not mapping to chromosome 6. Nature 323:540-543.
54. Albertson, D. G., R. Fishpool, P. Sherrington, E. Nacheva, and C. Milstein. 1988. Sensitive and high resolution in situ hybridization to human chromosomes using biotin labelled probes: assignment of the human thymocyte CD1 antigen genes to chromosome 1. EMBO J 7:2801-2805.
55. Moseley, W. S., M. L. Watson, S. F. Kingsmore, and M. F. Seldin. 1989. CD1 defines conserved linkage group border between human chromosomes 1 and mouse chromosomes 1 and 3. Immunogenetics 30:378-382.
56. Brigl, M., and M. B. Brenner. 2004. CD1: antigen presentation and T cell function. Annu Rev Immunol 22:817-890.
57. Calabi, F., J. M. Jarvis, L. Martin, and C. Milstein. 1989. Two classes of CD1 genes. Eur J Immunol 19:285-292.
58. Porcelli, S. A., and R. L. Modlin. 1999. The CD1 system: Antigen-presenting molecules for T cell recognition of lipids and glycolipids. Annual Review of Immunology 17:297-329.
59. Golmoghaddam, H., A. M. Pezeshki, A. Ghaderi, and M. Doroudchi. 2011. CD1a and CD1d genes polymorphisms in breast, colorectal and lung cancers. Pathol Oncol Res 17:669-675.
60. Oteo, M., J. F. Parra, I. Mirones, L. I. Gimenez, F. Setien, and E. Martinez-Naves. 1999. Single strand conformational polymorphism analysis of human CD1 genes in different ethnic groups. Tissue Antigens 53:545-550.
61. Han, M., L. I. Hannick, M. DiBrino, and M. A. Robinson. 1999. Polymorphism of human CD1 genes. Tissue Antigens 54:122-127.
62. Gan, L. H., Y. Q. Pan, D. P. Xu, M. Li, A. Lin, and W. H. Yan. 2010. Polymorphism of human CD1a, CD1d, and CD1e in exon 2 in Chinese Han and She ethnic populations. Tissue Antigens 75:691-695.
63. Tamouza, R., R. Sghiri, R. Ramasawmy, M. G. Neonato, L. E. Mombo, J. C. Poirier, V. Schaeffer, C. Fortier, D. Labie, R. Girot, A. Toubert, R. Krishnamoorthy, and D. Charron. 2002. Two novel CD1 E alleles identified in black African individuals. Tissue Antigens 59:417-420.
64. Tourne, S., B. Maitre, A. Collmann, E. Layre, S. Mariotti, F. Signorino-Gelo, C. Loch, J. Salamero, M. Gilleron, C. Angenieux, J. P. Cazenave, L. Mori, D. Hanau, G. Puzo, G. De Libero, and H. de la Salle. 2008. Cutting edge: a naturally occurring mutation in CD1e impairs lipid antigen presentation. J Immunol 180:3642-3646.
65. Zimmer, M. I., H. P. Nguyen, B. Wang, H. Xu, A. Colmone, K. Felio, H. J. Choi, P. Zhou, M. L. Alegre, and C. R. Wang. 2009. Polymorphisms in CD1d affect antigen presentation and the activation of CD1d-restricted T cells. Proc Natl Acad Sci U S A 106:1909-1914.
66. Jones, D. C., C. M. Gelder, T. Ahmad, I. A. Campbell, M. C. Barnardo, K. I. Welsh, S. E. Marshall, and M. Bunce. 2001. CD1 genotyping of patients with Mycobacterium malmoense pulmonary disease. Tissue Antigens 58:19-23.
67. Caporale, C. M., F. Papola, M. A. Fioroni, A. Aureli, A. Giovannini, F. Notturno, D. Adorno, V. Caporale, and A. Uncini. 2006. Susceptibility to Guillain-Barre syndrome is associated to polymorphisms of CD1 genes. J Neuroimmunol 177:112-118.
68. Kuijf, M. L., K. Geleijns, N. Ennaji, W. van Rijs, P. A. van Doorn, and B. C. Jacobs. 2008. Susceptibility to Guillain-Barre syndrome is not associated with CD1A and CD1E gene polymorphisms. J Neuroimmunol 205:110-112.

69. Wu, L. Y., Y. Zhou, C. Qin, and B. L. Hu. 2012. The effect of TNF-α, FcγR and CD1 polymorphisms on Guillain-Barre syndrome risk: evidences from a meta-analysis. J Neuroimmunol 243:18-24.
70. Caporale, C. M., F. Notturno, M. Pace, A. Aureli, V. Di Tommaso, G. De Luca, D. Farina, A. Giovannini, and A. Uncini. 2011. CD1A and CD1E gene polymorphisms are associated with susceptibility to multiple sclerosis. Int J Immunopathol Pharmacol 24:175-183.
71. Jamshidian, A., A. R. Nikseresht, M. Vessal, and E. Kamali-Sarvestani. 2010. Association of CD1A +622 T/C, +737 G/C and CD1E +6129 A/G genes polymorphisms with multiple sclerosis. Immunol Invest 39:874-889.
72. McMichael, A. J., J. R. Pilch, G. Galfre, D. Y. Mason, J. W. Fabre, and C. Milstein. 1979. A human thymocyte antigen defined by a hybrid myeloma monoclonal antibody. Eur J Immunol 9:205-210.
73. Martin, L. H., F. Calabi, and C. Milstein. 1986. Isolation of CD1 genes: a family of major histocompatibility complex-related differentiation antigens. Proc Natl Acad Sci U S A 83:9154-9158.
74. Girardi, E., and D. M. Zajonc. 2012. Molecular basis of lipid antigen presentation by CD1d and recognition by natural killer T cells. Immunol Rev 250:167-179.
75. Calabi, F., and C. Milstein. 2000. The molecular biology of CD1. Semin Immunol 12:503-509.
76. Mori, L., and G. De Libero. 2012. T cells specific for lipid antigens. Immunol Res 53:191-199.
77. Bauer, A., R. Huttinger, G. Staffler, C. Hansmann, W. Schmidt, O. Majdic, W. Knapp, and H. Stockinger. 1997. Analysis of the requirement for beta 2-microglobulin for expression and formation of human CD1 antigens. Eur J Immunol 27:1366-1373.
78. Sugita, M., S. A. Porcelli, and M. B. Brenner. 1997. Assembly and retention of CD1b heavy chains in the endoplasmic reticulum. J Immunol 159:2358-2365.
79. Somnay-Wadgaonkar, K., A. Nusrat, H. S. Kim, W. P. Canchis, S. P. Balk, S. P. Colgan, and R. S. Blumberg. 1999. Immunolocalization of CD1d in human intestinal epithelial cells and identification of a beta2-microglobulin-associated form. Int Immunol 11:383-392.
80. Kim, H. S., J. Garcia, M. Exley, K. W. Johnson, S. P. Balk, and R. S. Blumberg. 1999. Biochemical characterization of CD1d expression in the absence of beta2-microglobulin. J Biol Chem 274:9289-9295.
81. Knowles, R. W., and W. F. Bodmer. 1982. A monoclonal antibody recognizing a human thymus leukemia-like antigen associated with beta 2-microglobulin. Eur J Immunol 12:676-681.
82. Amiot, M., H. Dastot, M. Fabbi, L. Degos, A. Bernard, and L. Boumsell. 1988. Intermolecular complexes between three human CD1 molecules on normal thymus cells. Immunogenetics 27:187-195.
83. Porcelli, S. A., and D. B. Moody. 2005. Antigen Processing and Presentation by CD1 Family Proteins. Wiley-VCH.
84. Garcia-Alles, L. F., G. Giacometti, C. Versluis, L. Maveyraud, D. de Paepe, J. Guiard, S. Tranier, M. Gilleron, J. Prandi, D. Hanau, A. J. Heck, L. Mori, G. De Libero, G. Puzo, L. Mourey, and H. de la Salle. 2011. Crystal structure of human CD1e reveals a groove suited for lipid-exchange processes. Proc Natl Acad Sci U S A 108:13230-13235.
85. de la Salle, H., S. Mariotti, C. Angenieux, M. Gilleron, L. F. Garcia-Alles, D. Malm, T. Berg, S. Paoletti, B. Maitre, L. Mourey, J. Salamero, J. P. Cazenave, D. Hanau, L. Mori, G. Puzo, and G. De Libero. 2005. Assistance of microbial glycolipid antigen processing by CD1e. Science 310:1321-1324.
86. Garzon, D., C. Anselmi, P. J. Bond, and J. D. Faraldo-Gomez. 2013. Dynamics of the Antigen-binding grooves in CD1 proteins: reversible hydrophobic collapse in the lipid-free state. J Biol Chem 288:19528-19536.
87. Fainboim, L., and C. Salamone Mdel. 2002. CD1: a family of glycolypid-presenting molecules or also immunoregulatory proteins? J Biol Regul Homeost Agents 16:125-135.
88. Small, T. N., R. W. Knowles, C. Keever, N. A. Kernan, N. Collins, R. J. O'Reilly, B. Dupont, and N. Flomenberg. 1987. M241 (CD1) expression on B lymphocytes. J Immunol 138:2864-2868.
89. Delia, D., G. Cattoretti, N. Polli, E. Fontanella, A. Aiello, R. Giardini, F. Rilke, and G. Della Porta. 1988. CD1c but neither CD1a nor CD1b molecules are expressed on normal, activated, and malignant human B cells: identification of a new B-cell subset. Blood 72:241-247.

90. Pena-Cruz, V., S. Ito, C. C. Dascher, M. B. Brenner, and M. Sugita. 2003. Epidermal Langerhans cells efficiently mediate CD1a-dependent presentation of microbial lipid antigens to T cells. J Invest Dermatol 121:517-521.
91. Elder, J. T., N. J. Reynolds, K. D. Cooper, C. E. Griffiths, B. D. Hardas, and P. A. Bleicher. 1993. CD1 gene expression in human skin. J Dermatol Sci 6:206-213.
92. Dougan, S. K., A. Kaser, and R. S. Blumberg. 2007. CD1 expression on antigen-presenting cells. Curr Top Microbiol Immunol 314:113-141.
93. Exley, M., J. Garcia, S. B. Wilson, F. Spada, D. Gerdes, S. M. Tahir, K. T. Patton, R. S. Blumberg, S. Porcelli, A. Chott, and S. P. Balk. 2000. CD1d structure and regulation on human thymocytes, peripheral blood T cells, B cells and monocytes. Immunology 100:37-47.
94. Spada, F. M., F. Borriello, M. Sugita, G. F. Watts, Y. Koezuka, and S. A. Porcelli. 2000. Low expression level but potent antigen presenting function of CD1d on monocyte lineage cells. Eur J Immunol 30:3468-3477.
95. Blumberg, R. S., C. Terhorst, P. Bleicher, F. V. McDermott, C. H. Allan, S. B. Landau, J. S. Trier, and S. P. Balk. 1991. Expression of a nonpolymorphic MHC class I-like molecule, CD1D, by human intestinal epithelial cells. J Immunol 147:2518-2524.
96. Bonish, B., D. Jullien, Y. Dutronc, B. B. Huang, R. Modlin, F. M. Spada, S. A. Porcelli, and B. J. Nickoloff. 2000. Overexpression of CD1d by keratinocytes in psoriasis and CD1d-dependent IFN-γ production by NK-T cells. J Immunol 165:4076-4085.
97. Durante-Mangoni, E., R. Wang, A. Shaulov, Q. He, I. Nasser, N. Afdhal, M. J. Koziel, and M. A. Exley. 2004. Hepatic CD1d expression in hepatitis C virus infection and recognition by resident proinflammatory CD1d-reactive T cells. J Immunol 173:2159-2166.
98. Tsuneyama, K., M. Yasoshima, K. Harada, K. Hiramatsu, M. E. Gershwin, and Y. Nakanuma. 1998. Increased CD1d expression on small bile duct epithelium and epithelioid granuloma in livers in primary biliary cirrhosis. Hepatology 28:620-623.
99. Leslie, D. S., C. C. Dascher, K. Cembrola, M. A. Townes, D. L. Hava, L. C. Hugendubler, E. Mueller, L. Fox, C. Roura-Mir, D. B. Moody, M. S. Vincent, J. E. Gumperz, P. A. Illarionov, G. S. Besra, C. G. Reynolds, and M. B. Brenner. 2008. Serum lipids regulate dendritic cell CD1 expression and function. Immunology 125:289-301.
100. Smed-Sorensen, A., M. Moll, T. Y. Cheng, K. Lore, A. C. Norlin, L. Perbeck, D. B. Moody, A. L. Spetz, and J. K. Sandberg. 2008. IgG regulates the CD1 expression profile and lipid antigen-presenting function in human dendritic cells via FcgammaRIIa. Blood 111:5037-5046.
101. Sugita, M., D. C. Barral, and M. B. Brenner. 2007. Pathways of CD1 and lipid antigen delivery, trafficking, processing, loading, and presentation. Curr Top Microbiol Immunol 314:143-164.
102. Kang, S. J., and P. Cresswell. 2002. Calnexin, calreticulin, and ERp57 cooperate in disulfide bond formation in human CD1d heavy chain. J Biol Chem 277:44838-44844.
103. Huttinger, R., G. Staffler, O. Majdic, and H. Stockinger. 1999. Analysis of the early biogenesis of CD1b: involvement of the chaperones calnexin and calreticulin, the proteasome and beta(2)-microglobulin. Int Immunol 11:1615-1623.
104. Balk, S. P., S. Burke, J. E. Polischuk, M. E. Frantz, L. Yang, S. Porcelli, S. P. Colgan, and R. S. Blumberg. 1994. Beta 2-microglobulin-independent MHC class Ib molecule expressed by human intestinal epithelium. Science 265:259-262.
105. Joyce, S., A. S. Woods, J. W. Yewdell, J. R. Bennink, A. D. De Silva, A. Boesteanu, S. P. Balk, R. J. Cotter, and R. R. Brutkiewicz. 1998. Natural ligand of mouse CD1d1: cellular glycosylphosphatidylinositol. Science 279:1541-1544.
106. De Silva, A. D., J. J. Park, N. Matsuki, A. K. Stanic, R. R. Brutkiewicz, M. E. Medof, and S. Joyce. 2002. Lipid protein interactions: the assembly of CD1d1 with cellular phospholipids occurs in the endoplasmic reticulum. J Immunol 168:723-733.
107. Shamshiev, A., H. J. Gober, A. Donda, Z. Mazorra, L. Mori, and G. De Libero. 2002. Presentation of the same glycolipid by different CD1 molecules. J Exp Med 195:1013-1021.

108. Sugita, M., X. Cao, G. F. Watts, R. A. Rogers, J. S. Bonifacino, and M. B. Brenner. 2002. Failure of trafficking and antigen presentation by CD1 in AP-3-deficient cells. Immunity 16:697-706.
109. Angenieux, C., V. Fraisier, B. Maitre, V. Racine, N. van der Wel, D. Fricker, F. Proamer, M. Sachse, J. P. Cazenave, P. Peters, B. Goud, D. Hanau, J. B. Sibarita, J. Salamero, and H. de la Salle. 2005. The cellular pathway of CD1e in immature and maturing dendritic cells. Traffic 6:286-302.
110. Maitre, B., C. Angenieux, J. Salamero, D. Hanau, D. Fricker, F. Signorino, F. Proamer, J. P. Cazenave, B. Goud, S. Tourne, and H. de la Salle. 2008. Control of the intracellular pathway of CD1e. Traffic 9:431-445.
111. Jayawardena-Wolf, J., K. Benlagha, Y. H. Chiu, R. Mehr, and A. Bendelac. 2001. CD1d endosomal trafficking is independently regulated by an intrinsic CD1d-encoded tyrosine motif and by the invariant chain. Immunity 15:897-908.
112. Kang, S. J., and P. Cresswell. 2002. Regulation of intracellular trafficking of human CD1d by association with MHC class II molecules. EMBO J 21:1650-1660.
113. Gelin, C., I. Sloma, D. Charron, and N. Mooney. 2009. Regulation of MHC II and CD1 antigen presentation: from ubiquity to security. J Leukoc Biol 85:215-224.
114. De Libero, G., and L. Mori. 2012. Novel insights into lipid antigen presentation. Trends Immunol 33:103-111.
115. Freigang, S., E. Landais, V. Zadorozhny, L. Kain, K. Yoshida, Y. Liu, S. Deng, W. Palinski, P. B. Savage, A. Bendelac, and L. Teyton. 2012. Scavenger receptors target glycolipids for natural killer T cell activation. J Clin Invest 122:3943-3954.
116. Allan, L. L., K. Hoefl, D. J. Zheng, B. K. Chung, F. K. Kozak, R. Tan, and P. van den Elzen. 2009. Apolipoprotein-mediated lipid antigen presentation in B cells provides a pathway for innate help by NKT cells. Blood 114:2411-2416.
117. Prigozy, T. I., P. A. Sieling, D. Clemens, P. L. Stewart, S. M. Behar, S. A. Porcelli, M. B. Brenner, R. L. Modlin, and M. Kronenberg. 1997. The mannose receptor delivers lipoglycan antigens to endosomes for presentation to T cells by CD1b molecules. Immunity 6:187-197.
118. Hunger, R. E., P. A. Sieling, M. T. Ochoa, M. Sugaya, A. E. Burdick, T. H. Rea, P. J. Brennan, J. T. Belisle, A. Blauvelt, S. A. Porcelli, and R. L. Modlin. 2004. Langerhans cells utilize CD1a and langerin to efficiently present nonpeptide antigens to T cells. J Clin Invest 113:701-708.
119. Beckman, E. M., S. A. Porcelli, C. T. Morita, S. M. Behar, S. T. Furlong, and M. B. Brenner. 1994. Recognition of a lipid antigen by CD1-restricted $\alpha\beta^+$ T cells. Nature 372:691-694.
120. De Libero, G., A. Collmann, and L. Mori. 2009. The cellular and biochemical rules of lipid antigen presentation. Eur J Immunol 39:2648-2656.
121. Kawano, T., J. Cui, Y. Koezuka, I. Toura, Y. Kaneko, K. Motoki, H. Ueno, R. Nakagawa, H. Sato, E. Kondo, H. Koseki, and M. Taniguchi. 1997. CD1d-restricted and TCR-mediated activation of vα14 NKT cells by glycosylceramides. Science 278:1626-1629.
122. van Meer, G. 2005. Cellular lipidomics. EMBO J 24:3159-3165.
123. Garcia-Saez, A. J., and P. Schwille. 2010. Surface analysis of membrane dynamics. Biochim Biophys Acta 1798:766-776.
124. Sloma, I., M. T. Zilber, T. Vasselon, N. Setterblad, M. Cavallari, L. Mori, G. De Libero, D. Charron, N. Mooney, and C. Gelin. 2008. Regulation of CD1a surface expression and antigen presentation by invariant chain and lipid rafts. J Immunol 180:980-987.
125. Amiot, M., H. Dastot, L. Degos, J. Dausset, A. Bernard, and L. Boumsell. 1988. HLA class I molecules are associated with CD1a heavy chains on normal human thymus cells. Proc Natl Acad Sci U S A 85:4451-4454.
126. Campbell, N. A., H. S. Kim, R. S. Blumberg, and L. Mayer. 1999. The nonclassical class I molecule CD1d associates with the novel CD8 ligand gp180 on intestinal epithelial cells. J Biol Chem 274:26259-26265.
127. Li, D., L. Wang, L. Yu, E. C. Freundt, B. Jin, G. R. Screaton, and X. N. Xu. 2009. Ig-like transcript 4 inhibits lipid antigen presentation through direct CD1d interaction. J Immunol 182:1033-1040.

128. Li, D., A. Hong, Q. Lu, G. F. Gao, B. Jin, G. R. Screaton, and X. N. Xu. 2012. A novel role of CD1c in regulating CD1d-mediated NKT cell recognition by competitive binding to Ig-like transcript 4. Int Immunol 24:729-737.
129. Karmakar, S., J. Paul, and T. De. 2011. Leishmania donovani glycosphingolipid facilitates antigen presentation by inducing relocation of CD1d into lipid rafts in infected macrophages. Eur J Immunol 41:1376-1387.
130. Lang, G. A., S. D. Maltsev, G. S. Besra, and M. L. Lang. 2004. Presentation of alpha-galactosylceramide by murine CD1d to natural killer T cells is facilitated by plasma membrane glycolipid rafts. Immunology 112:386-396.
131. Peng, W., C. Martaresche, N. Escande-Beillard, O. Cedile, A. Reynier-Vigouroux, and J. Boucraut. 2007. Influence of lipid rafts on CD1d presentation by dendritic cells. Mol Membr Biol 24:475-484.
132. Park, Y. K., J. W. Lee, Y. G. Ko, S. Hong, and S. H. Park. 2005. Lipid rafts are required for efficient signal transduction by CD1d. Biochem Biophys Res Commun 327:1143-1154.
133. Im, J. S., P. Arora, G. Bricard, A. Molano, M. M. Venkataswamy, I. Baine, E. S. Jerud, M. F. Goldberg, A. Baena, K. O. Yu, R. M. Ndonye, A. R. Howell, W. Yuan, P. Cresswell, Y. T. Chang, P. A. Illarionov, G. S. Besra, and S. A. Porcelli. 2009. Kinetics and cellular site of glycolipid loading control the outcome of natural killer T cell activation. Immunity 30:888-898.
134. Bonetti, P. O., L. O. Lerman, C. Napoli, and A. Lerman. 2003. Statin effects beyond lipid lowering--are they clinically relevant? Eur Heart J 24:225-248.
135. Ghittoni, R., G. Napolitani, D. Benati, C. Ulivieri, L. Patrussi, F. Laghi Pasini, A. Lanzavecchia, and C. T. Baldari. 2006. Simvastatin inhibits the MHC class II pathway of antigen presentation by impairing Ras superfamily GTPases. Eur J Immunol 36:2885-2893.
136. Khan, M. A., R. M. Gallo, G. J. Renukaradhya, W. Du, J. Gervay-Hague, and R. R. Brutkiewicz. 2009. Statins impair CD1d-mediated antigen presentation through the inhibition of prenylation. J Immunol 182:4744-4750.
137. Shimabukuro-Vornhagen, A., T. Liebig, and M. von Bergwelt-Baildon. 2008. Statins inhibit human APC function: implications for the treatment of GVHD. Blood 112:1544-1545.
138. Kuipers, H. F., P. J. Biesta, T. A. Groothuis, J. J. Neefjes, A. M. Mommaas, and P. J. van den Elsen. 2005. Statins affect cell-surface expression of major histocompatibility complex class II molecules by disrupting cholesterol-containing microdomains. Hum Immunol 66:653-665.
139. Zhuang, L., J. Kim, R. M. Adam, K. R. Solomon, and M. R. Freeman. 2005. Cholesterol targeting alters lipid raft composition and cell survival in prostate cancer cells and xenografts. J Clin Invest 115:959-968.
140. Ponce, J., N. P. de la Ossa, O. Hurtado, M. Millan, J. F. Arenillas, A. Davalos, and T. Gasull. 2008. Simvastatin reduces the association of NMDA receptors to lipid rafts: a cholesterol-mediated effect in neuroprotection. Stroke 39:1269-1275.
141. Sahoo, H. 2011. Forster resonance energy transfer - A spectroscopic nanoruler: Principle and applications. Journal of Photochemistry and Photobiology C-Photochemistry Reviews 12:20-30.
142. Roszik, J., G. Toth, J. Szollosi, and G. Vereb. 2013. Validating pharmacological disruption of protein-protein interactions by acceptor photobleaching FRET imaging. Methods Mol Biol 986:165-178.
143. Vereb, G., P. Nagy, and J. Szollosi. 2011. Flow cytometric FRET analysis of protein interaction. Methods Mol Biol 699:371-392.
144. Barnstable, C. J., W. F. Bodmer, G. Brown, G. Galfre, C. Milstein, A. F. Williams, and A. Ziegler. 1978. Production of monoclonal antibodies to group A erythrocytes, HLA and other human cell surface antigens-new tools for genetic analysis. Cell 14:9-20.
145. Gauster, M., A. Blaschitz, and G. Dohr. 2007. Monoclonal antibody HC10 does not bind HLA-G. Rheumatology (Oxford) 46:892-893; author reply 893-894.
146. Perosa, F., G. Luccarelli, M. Prete, E. Favoino, S. Ferrone, and F. Dammacco. 2003. Beta 2-microglobulin-free HLA class I heavy chain epitope mimicry by monoclonal antibody HC-10-specific peptide. J Immunol 171:1918-1926.

147. Stam, N. J., H. Spits, and H. L. Ploegh. 1986. Monoclonal antibodies raised against denatured HLA-B locus heavy chains permit biochemical characterization of certain HLA-C locus products. J Immunol 137:2299-2306.
148. Stam, N. J., T. M. Vroom, P. J. Peters, E. B. Pastoors, and H. L. Ploegh. 1990. HLA-A- and HLA-B-specific monoclonal antibodies reactive with free heavy chains in western blots, in formalin-fixed, paraffin-embedded tissue sections and in cryo-immuno-electron microscopy. Int Immunol 2:113-125.
149. Lampson, L. A., C. A. Fisher, and J. P. Whelan. 1983. Striking paucity of HLA-A, B, C and beta 2-microglobulin on human neuroblastoma cell lines. J Immunol 130:2471-2478.
150. Robbins, P. A., E. L. Evans, A. H. Ding, N. L. Warner, and F. M. Brodsky. 1987. Monoclonal antibodies that distinguish between class II antigens (HLA-DP, DQ, and DR) in 14 haplotypes. Hum Immunol 18:301-313.
151. Yang, S., J. Graham, J. W. Kahn, E. A. Schwartz, and M. E. Gerritsen. 1999. Functional roles for PECAM-1 (CD31) and VE-cadherin (CD144) in tube assembly and lumen formation in three-dimensional collagen gels. Am J Pathol 155:887-895.
152. Schneider, C., R. Sutherland, R. Newman, and M. Greaves. 1982. Structural features of the cell surface receptor for transferrin that is recognized by the monoclonal antibody OKT9. J Biol Chem 257:8516-8522.
153. Horejsi, V., P. Angelisova, V. Bazil, H. Kristofova, S. Stoyanov, I. Stefanova, P. Hausner, M. Vosecky, and I. Hilgert. 1988. Monoclonal antibodies against human leucocyte antigens. II. Antibodies against CD45 (T200), CD3 (T3), CD43, CD10 (CALLA), transferrin receptor (T9), a novel broadly expressed 18-kDa antigen (MEM-43) and a novel antigen of restricted expression (MEM-74). Folia Biol (Praha) 34:23-34.
154. Zemmour, J., A. M. Little, D. J. Schendel, and P. Parham. 1992. The HLA-A,B "negative" mutant cell line C1R expresses a novel HLA-B35 allele, which also has a point mutation in the translation initiation codon. J Immunol 148:1941-1948.
155. Exley, M., J. Garcia, S. P. Balk, and S. Porcelli. 1997. Requirements for CD1d recognition by human invariant Vaα24^{+} CD4^{-}CD8^{-} T cells. J Exp Med 186:109-120.
156. Thomas, M., J. M. Boname, S. Field, S. Nejentsev, M. Salio, V. Cerundolo, M. Wills, and P. J. Lehner. 2008. Down-regulation of NKG2D and NKp80 ligands by Kaposi's sarcoma-associated herpesvirus K5 protects against NK cell cytotoxicity. Proc Natl Acad Sci U S A 105:1656-1661.
157. Szentesi, G., G. Horvath, I. Bori, G. Vamosi, J. Szollosi, R. Gaspar, S. Damjanovich, A. Jenei, and L. Matyus. 2004. Computer program for determining fluorescence resonance energy transfer efficiency from flow cytometric data on a cell-by-cell basis. Comput Methods Programs Biomed 75:201-211.
158. Liu, H., G. Gaza-Bulseco, C. Chumsae, and A. Newby-Kew. 2007. Characterization of lower molecular weight artifact bands of recombinant monoclonal IgG1 antibodies on non-reducing SDS-PAGE. Biotechnol Lett 29:1611-1622.
159. Vereb, G., J. Matko, G. Vamosi, S. M. Ibrahim, E. Magyar, S. Varga, J. Szollosi, A. Jenei, R. Gaspar, Jr., T. A. Waldmann, and S. Damjanovich. 2000. Cholesterol-dependent clustering of IL-2Rα and its colocalization with HLA and CD48 on T lymphoma cells suggest their functional association with lipid rafts. Proc Natl Acad Sci U S A 97:6013-6018.
160. Vereb, G., J. Szöllősi, S. Damjanovich, and J. Matkó. 2004. Exploring membrane microdomains and functional protein clustering in live cells with flow and image cytometric methods. Kluwer Academic / Plenum Publishers, New York.
161. Gombos, I., Z. Bacso, C. Detre, H. Nagy, K. Goda, M. Andrasfalvy, G. Szabo, and J. Matko. 2004. Cholesterol sensitivity of detergent resistance: a rapid flow cytometric test for detecting constitutive or induced raft association of membrane proteins. Cytometry A 61:117-126.
162. Vira, S., E. Mekhedov, G. Humphrey, and P. S. Blank. 2010. Fluorescent-labeled antibodies: Balancing functionality and degree of labeling. Anal Biochem 402:146-150.
163. Pearson, J. E., J. W. Kane, I. Petraki-Kallioti, A. Gill, and P. Vadgama. 1998. Surface plasmon resonance: a study of the effect of biotinylation on the selection of antibodies for use in immunoassays. J Immunol Methods 221:87-94.

164. Humphreys, D. P., S. P. Heywood, A. Henry, L. Ait-Lhadj, P. Antoniw, R. Palframan, K. J. Greenslade, B. Carrington, D. G. Reeks, L. C. Bowering, S. West, and H. A. Brand. 2007. Alternative antibody Fab' fragment PEGylation strategies: combination of strong reducing agents, disruption of the interchain disulphide bond and disulphide engineering. Protein Eng Des Sel 20:227-234.
165. Pereira, M., and E. P. Lai. 2008. Capillary electrophoresis for the characterization of quantum dots after non-selective or selective bioconjugation with antibodies for immunoassay. J Nanobiotechnology 6:10.
166. Liskova, M., I. Voracova, K. Kleparnik, V. Hezinova, J. Prikryl, and F. Foret. 2011. Conjugation reactions in the preparations of quantum dot-based immunoluminescent probes for analysis of proteins by capillary electrophoresis. Anal Bioanal Chem 400:369-379.
167. Mahmoud, W., G. Rousserie, B. Reveil, T. Tabary, J. M. Millot, M. Artemyev, V. A. Oleinikov, J. H. Cohen, I. Nabiev, and A. Sukhanova. 2011. Advanced procedures for labeling of antibodies with quantum dots. Anal Biochem 416:180-185.
168. del Rosario, R. B., and R. L. Wahl. 1990. Disulfide bond-targeted radiolabeling: tumor specificity of a streptavidin-biotinylated monoclonal antibody complex. Cancer Res 50:804s-808s.
169. Hu, C. M., S. Kaushal, H. S. Tran Cao, S. Aryal, M. Sartor, S. Esener, M. Bouvet, and L. Zhang. 2010. Half-antibody functionalized lipid-polymer hybrid nanoparticles for targeted drug delivery to carcinoembryonic antigen presenting pancreatic cancer cells. Mol Pharm 7:914-920.
170. Raju, T. S. 2008. Terminal sugars of Fc glycans influence antibody effector functions of IgGs. Curr Opin Immunol 20:471-478.
171. O'Shannessy, D. J., and R. H. Quarles. 1985. Specific conjugation reactions of the oligosaccharide moieties of immunoglobulins. J Appl Biochem 7:347-355.
172. Jeffery, A. M., D. A. Zopf, and V. Ginsburg. 1975. Affinity chromatography of carbohydrate-specific immunoglobulins: coupling of oligosaccharides to sepharose. Biochem Biophys Res Commun 62:608-613.
173. Jeanson, A., J. M. Cloes, M. Bouchet, and B. Rentier. 1988. Comparison of conjugation procedures for the preparation of monoclonal antibody-enzyme conjugates. J Immunol Methods 111:261-270.
174. Tijssen, P., and E. Kurstak. 1984. Highly efficient and simple methods for the preparation of peroxidase and active peroxidase-antibody conjugates for enzyme immunoassays. Anal Biochem 136:451-457.
175. Husain, M., and C. Bieniarz. 1994. Fc site-specific labeling of immunoglobulins with calf intestinal alkaline phosphatase. Bioconjug Chem 5:482-490.
176. Nakane, P. K., and A. Kawaoi. 1974. Peroxidase-labeled antibody. A new method of conjugation. J Histochem Cytochem 22:1084-1091.
177. Kondejewski, L. H., J. A. Kralovec, A. H. Blair, and T. Ghose. 1994. Synthesis and characterization of carbohydrate-linked murine monoclonal antibody K20-human serum albumin conjugates. Bioconjug Chem 5:602-611.
178. Jenei, A., S. Varga, L. Bene, L. Matyus, A. Bodnar, Z. Bacso, C. Pieri, R. Gaspar, Jr., T. Farkas, and S. Damjanovich. 1997. HLA class I and II antigens are partially co-clustered in the plasma membrane of human lymphoblastoid cells. Proc Natl Acad Sci U S A 94:7269-7274.
179. Bodnar, A., Z. Bacso, A. Jenei, T. M. Jovin, M. Edidin, S. Damjanovich, and J. Matko. 2003. Class I HLA oligomerization at the surface of B cells is controlled by exogenous beta(2)-microglobulin: implications in activation of cytotoxic T lymphocytes. Int Immunol 15:331-339.
180. Szollosi, J., S. Damjanovich, M. Balazs, P. Nagy, L. Tron, M. J. Fulwyler, and F. M. Brodsky. 1989. Physical association between MHC class I and class II molecules detected on the cell surface by flow cytometric energy transfer. J Immunol 143:208-213.
181. Bene, L., A. Bodnar, S. Damjanovich, G. Vamosi, Z. Bacso, J. Aradi, A. Berta, and J. Damjanovich. 2004. Membrane topography of HLA I, HLA II, and ICAM-1 is affected by IFN-γ in lipid rafts of uveal melanomas. Biochem Biophys Res Commun 322:678-683.
182. Damjanovich, L., J. Volko, A. Forgacs, W. Hohenberger, and L. Bene. 2012. Crohn's disease alters MHC-rafts in $CD4^+$ T-cells. Cytometry A 81:149-164.

183. Bacso, Z., L. Bene, L. Damjanovich, and S. Damjanovich. 2002. INF-γ rearranges membrane topography of MHC-I and ICAM-1 in colon carcinoma cells. Biochem Biophys Res Commun 290:635-640.
184. Knorr, R., C. Karacsonyi, and R. Lindner. 2009. Endocytosis of MHC molecules by distinct membrane rafts. J Cell Sci 122:1584-1594.
185. Anderson, H. A., E. M. Hiltbold, and P. A. Roche. 2000. Concentration of MHC class II molecules in lipid rafts facilitates antigen presentation. Nat Immunol 1:156-162.
186. Bouillon, M., Y. El Fakhry, J. Girouard, H. Khalil, J. Thibodeau, and W. Mourad. 2003. Lipid raft-dependent and -independent signaling through HLA-DR molecules. J Biol Chem 278:7099-7107.
187. Kropshofer, H., S. Spindeldreher, T. A. Rohn, N. Platania, C. Grygar, N. Daniel, A. Wolpl, H. Langen, V. Horejsi, and A. B. Vogt. 2002. Tetraspan microdomains distinct from lipid rafts enrich select peptide-MHC class II complexes. Nat Immunol 3:61-68.
188. Khandelwal, S., and P. A. Roche. 2010. Distinct MHC class II molecules are associated on the dendritic cell surface in cholesterol-dependent membrane microdomains. J Biol Chem 285:35303-35310.
189. Zidovetzki, R., and I. Levitan. 2007. Use of cyclodextrins to manipulate plasma membrane cholesterol content: evidence, misconceptions and control strategies. Biochim Biophys Acta 1768:1311-1324.
190. Istvan, E. S., and J. Deisenhofer. 2001. Structural mechanism for statin inhibition of HMG-CoA reductase. Science 292:1160-1164.
191. Strome, S. E., E. A. Sausville, and D. Mann. 2007. A mechanistic perspective of monoclonal antibodies in cancer therapy beyond target-related effects. Oncologist 12:1084-1095.
192. Torres, M., and A. Casadevall. 2008. The immunoglobulin constant region contributes to affinity and specificity. Trends Immunol 29:91-97.
193. Luchowski, R., E. G. Matveeva, I. Gryczynski, E. A. Terpetschnig, L. Patsenker, G. Laczko, J. Borejdo, and Z. Gryczynski. 2008. Single molecule studies of multiple-fluorophore labeled antibodies. Effect of homo-FRET on the number of photons available before photobleaching. Curr Pharm Biotechnol 9:411-420.
194. San Paulo, A., and R. Garcia. 2000. High-resolution imaging of antibodies by tapping-mode atomic force microscopy: attractive and repulsive tip-sample interaction regimes. Biophys J 78:1599-1605.
195. Makky, A., Berthelot, T., Feraudet-Tarisse, C., Volland, H., Viel,P., Polesel-Maris,J. 2012. Substructures high resolution imaging of individual IgG and IgM antibodies with piezoelectric tuning fork atomic force microscopy. Sens. Actuators, B: Chem. 162:269-277.
196. Chen, H., S. S. Ahsan, M. B. Santiago-Berrios, H. D. Abruna, and W. W. Webb. 2010. Mechanisms of quenching of Alexa fluorophores by natural amino acids. J Am Chem Soc 132:7244-7245.
197. Vaiana, A. C., H. Neuweiler, A. Schulz, J. Wolfrum, M. Sauer, and J. C. Smith. 2003. Fluorescence quenching of dyes by tryptophan: interactions at atomic detail from combination of experiment and computer simulation. J Am Chem Soc 125:14564-14572.
198. Sun, Q., R. Lu, and A. Yu. 2012. Structural heterogeneity in the collision complex between organic dyes and tryptophan in aqueous solution. J Phys Chem B 116:660-666.
199. Dave, R., D. S. Terry, J. B. Munro, and S. C. Blanchard. 2009. Mitigating unwanted photophysical processes for improved single-molecule fluorescence imaging. Biophys J 96:2371-2381.
200. Bene, L., M. Balazs, J. Matko, J. Most, M. P. Dierich, J. Szollosi, and S. Damjanovich. 1994. Lateral organization of the ICAM-1 molecule at the surface of human lymphoblasts: a possible model for its co-distribution with the IL-2 receptor, class I and class II HLA molecules. Eur J Immunol 24:2115-2123.
201. Wypych, J., M. Li, A. Guo, Z. Zhang, T. Martinez, M. J. Allen, S. Fodor, D. N. Kelner, G. C. Flynn, Y. D. Liu, P. V. Bondarenko, M. S. Ricci, T. M. Dillon, and A. Balland. 2008. Human IgG2 antibodies display disulfide-mediated structural isoforms. J Biol Chem 283:16194-16205.
202. Sun, M. M., K. S. Beam, C. G. Cerveny, K. J. Hamblett, R. S. Blackmore, M. Y. Torgov, F. G. Handley, N. C. Ihle, P. D. Senter, and S. C. Alley. 2005. Reduction-alkylation strategies for the modification of specific monoclonal antibody disulfides. Bioconjug Chem 16:1282-1290.
203. Dirksen, A., and P. E. Dawson. 2008. Rapid oxime and hydrazone ligations with aromatic aldehydes for biomolecular labeling. Bioconjug Chem 19:2543-2548.

204. Thygesen, M. B., H. Munch, J. Sauer, E. Clo, M. R. Jorgensen, O. Hindsgaul, and K. J. Jensen. 2010. Nucleophilic catalysis of carbohydrate oxime formation by anilines. J Org Chem 75:1752-1755.
205. Rashidian, M., M. M. Mahmoodi, R. Shah, J. K. Dozier, C. R. Wagner, and M. D. Distefano. 2013. A highly efficient catalyst for oxime ligation and hydrazone-oxime exchange suitable for bioconjugation. Bioconjug Chem 24:333-342.
206. Crisalli, P., and E. T. Kool. 2013. Importance of ortho Proton Donors in Catalysis of Hydrazone Formation. Org Lett 15:1646-1649.
207. Zeng, Y., T. N. Ramya, A. Dirksen, P. E. Dawson, and J. C. Paulson. 2009. High-efficiency labeling of sialylated glycoproteins on living cells. Nat Methods 6:207-209.
208. Wolfe, C. A., and D. S. Hage. 1995. Studies on the rate and control of antibody oxidation by periodate. Anal Biochem 231:123-130.
209. Amiot, M., H. Dastot, M. Fabbi, L. Degos, A. Bernard, and L. Boumsell. 1988. Intermolecular Complexes between 3 Human Cd1 Molecules on Normal Thymus-Cells. Immunogenetics 27:187-195.
210. Amiot, M., H. Dastot, M. Schmid, A. Bernard, and L. Boumsell. 1987. Analysis of CD1 molecules on thymus cells and leukemic T lymphoblasts identifies discrete phenotypes and reveals that CD1 intermolecular complexes are observed only on normal cells. Blood 70:676-685.
211. Tysoe-Calnon, V. A., J. E. Grundy, and S. J. Perkins. 1991. Molecular comparisons of the beta 2-microglobulin-binding site in class I major-histocompatibility-complex α-chains and proteins of related sequences. Biochem J 277 (Pt 2):359-369.
212. Otten, G. R., E. Bikoff, R. K. Ribaudo, S. Kozlowski, D. H. Margulies, and R. N. Germain. 1992. Peptide and beta 2-microglobulin regulation of cell surface MHC class I conformation and expression. J Immunol 148:3723-3732.
213. Viville, S., J. Neefjes, V. Lotteau, A. Dierich, M. Lemeur, H. Ploegh, C. Benoist, and D. Mathis. 1993. Mice lacking the MHC class II-associated invariant chain. Cell 72:635-648.
214. Amano, M., N. Baumgarth, M. D. Dick, L. Brossay, M. Kronenberg, L. A. Herzenberg, and S. Strober. 1998. CD1 expression defines subsets of follicular and marginal zone B cells in the spleen: beta 2-microglobulin-dependent and independent forms. J Immunol 161:1710-1717.
215. Duman, M., M. Pfleger, R. Zhu, C. Rankl, L. A. Chtcheglova, I. Neundlinger, B. L. Bozna, B. Mayer, M. Salio, D. Shepherd, P. Polzella, M. Moertelmaier, G. Kada, A. Ebner, M. Dieudonne, G. J. Schutz, V. Cerundolo, F. Kienberger, and P. Hinterdorfer. 2010. Improved localization of cellular membrane receptors using combined fluorescence microscopy and simultaneous topography and recognition imaging. Nanotechnology 21:115504.
216. Lebedeva, T., N. Anikeeva, S. A. Kalams, B. D. Walker, I. Gaidarov, J. H. Keen, and Y. Sykulev. 2004. Major histocompatibility complex class I-intercellular adhesion molecule-1 association on the surface of target cells: implications for antigen presentation to cytotoxic T lymphocytes. Immunology 113:460-471.
217. Ghittoni, R., L. Patrussi, K. Pirozzi, M. Pellegrini, P. E. Lazzerini, P. L. Capecchi, F. L. Pasini, and C. T. Baldari. 2005. Simvastatin inhibits T-cell activation by selectively impairing the function of Ras superfamily GTPases. FASEB J 19:605-607.
218. Maher, B. M., T. N. Dhonnchu, J. P. Burke, A. Soo, A. E. Wood, and R. W. Watson. 2009. Statins alter neutrophil migration by modulating cellular Rho activity-a potential mechanism for statins-mediated pleotropic effects? J Leukoc Biol 85:186-193.
219. Martin, G., H. Duez, C. Blanquart, V. Berezowski, P. Poulain, J. C. Fruchart, J. Najib-Fruchart, C. Glineur, and B. Staels. 2001. Statin-induced inhibition of the Rho-signaling pathway activates PPARα and induces HDL apoA-I. J Clin Invest 107:1423-1432.
220. Copaja, M., D. Venegas, P. Aranguiz, J. Canales, R. Vivar, Y. Avalos, L. Garcia, M. Chiong, I. Olmedo, M. Catalan, L. Leyton, S. Lavandero, and G. Diaz-Araya. 2012. Simvastatin disrupts cytoskeleton and decreases cardiac fibroblast adhesion, migration and viability. Toxicology 294:42-49.
221. Pozo, M., R. de Nicolas, J. Egido, and J. Gonzalez-Cabrero. 2006. Simvastatin inhibits the migration and adhesion of monocytic cells and disorganizes the cytoskeleton of activated endothelial cells. Eur J Pharmacol 548:53-63.

222. Gallo, R. M., M. A. Khan, J. Shi, R. Kapur, L. Wei, J. C. Bailey, J. Liu, and R. R. Brutkiewicz. 2012. Regulation of the actin cytoskeleton by Rho kinase controls antigen presentation by CD1d. J Immunol 189:1689-1698.
223. Vamosi, G., A. Bodnar, G. Vereb, A. Jenei, C. K. Goldman, J. Langowski, K. Toth, L. Matyus, J. Szollosi, T. A. Waldmann, and S. Damjanovich. 2004. IL-2 and IL-15 receptor α-subunits are coexpressed in a supramolecular receptor cluster in lipid rafts of T cells. Proc Natl Acad Sci U S A 101:11082-11087.
224. Locke, D., J. Liu, and A. L. Harris. 2005. Lipid rafts prepared by different methods contain different connexin channels, but gap junctions are not lipid rafts. Biochemistry 44:13027-13042.
225. Roper, K., D. Corbeil, and W. B. Huttner. 2000. Retention of prominin in microvilli reveals distinct cholesterol-based lipid micro-domains in the apical plasma membrane. Nat Cell Biol 2:582-592.
226. Hofman, E. G., M. O. Ruonala, A. N. Bader, D. van den Heuvel, J. Voortman, R. C. Roovers, A. J. Verkleij, H. C. Gerritsen, and P. M. van Bergen En Henegouwen. 2008. EGF induces coalescence of different lipid rafts. J Cell Sci 121:2519-2528.
227. Frisz, J. F., H. A. Klitzing, K. Lou, I. D. Hutcheon, P. K. Weber, J. Zimmerberg, and M. L. Kraft. 2013. Sphingolipid domains in the plasma membranes of fibroblasts are not enriched with cholesterol. J Biol Chem 288:16855-16861.
228. Unternaehrer, J. J., A. Chow, M. Pypaert, K. Inaba, and I. Mellman. 2007. The tetraspanin CD9 mediates lateral association of MHC class II molecules on the dendritic cell surface. Proc Natl Acad Sci U S A 104:234-239.
229. Szollosi, J., V. Horejsi, L. Bene, P. Angelisova, and S. Damjanovich. 1996. Supramolecular complexes of MHC class I, MHC class II, CD20, and tetraspan molecules (CD53, CD81, and CD82) at the surface of a B cell line JY. J Immunol 157:2939-2946.
230. Rubinstein, E., F. Le Naour, C. Lagaudriere-Gesbert, M. Billard, H. Conjeaud, and C. Boucheix. 1996. CD9, CD63, CD81, and CD82 are components of a surface tetraspan network connected to HLA-DR and VLA integrins. Eur J Immunol 26:2657-2665.
231. Gourapura, R. J., M. A. Khan, R. M. Gallo, D. Shaji, J. Liu, and R. R. Brutkiewicz. 2013. Forming a complex with MHC class I molecules interferes with mouse CD1d functional expression. PLoS One 8:e72867.
232. Chen, X., X. Wang, J. M. Keaton, F. Reddington, P. A. Illarionov, G. S. Besra, and J. E. Gumperz. 2007. Distinct endosomal trafficking requirements for presentation of autoantigens and exogenous lipids by human CD1d molecules. J Immunol 178:6181-6190.
233. Solomon, B., R. Koppel, F. Schwartz, and G. Fleminger. 1990. Enzymic oxidation of monoclonal antibodies by soluble and immobilized bifunctional enzyme complexes. J Chromatogr 510:321-329.
234. Bilkova, Z., M. Slovakova, D. Horak, J. Lenfeld, and J. Churacek. 2002. Enzymes immobilized on magnetic carriers: efficient and selective system for protein modification. J Chromatogr B Analyt Technol Biomed Life Sci 770:177-181.
235. Eggeling, C., K. I. Willig, and F. J. Barrantes. 2013. STED microscopy of living cells - new frontiers in membrane and neurobiology. J Neurochem.
236. Agrawal, U., D. T. Reilly, and C. M. Schroeder. 2013. Zooming in on biological processes with fluorescence nanoscopy. Curr Opin Biotechnol.
237. Huckabay, H. A., K. P. Armendariz, W. H. Newhart, S. M. Wildgen, and R. C. Dunn. 2013. Near-field scanning optical microscopy for high-resolution membrane studies. Methods Mol Biol 950:373-394.

11. LIST OF PUBLICATIONS

UNIVERSITY AND NATIONAL LIBRARY UNIVERSITY OF DEBRECEN
KENÉZY LIFE SCIENCES LIBRARY

Register Number: DEENKÉTK/354/2013.
Item Number:
Subject: Ph.D. List of Publications

Candidate: Dilip Shrestha

Neptun ID: SO9IX0

Doctoral School: Doctoral School of Molecular Medicine

List of publications related to the dissertation

1. **Shrestha, D.**, Exley, M.A., Vereb, G., Szöllősi, J., Jenei, A.: CD1d favors MHC neighborhood, GM1 ganglioside proximity and low detergent sensitive membrane regions on the surface of B lymphocytes.
Biochim. Biophys. Acta Gen. Subj. "accepted by publisher", 2013.
DOI: http://dx.doi.org/10.1016/j.bbagen.2013.10.030
IF:3.848 (2012)

2. **Shrestha, D.**, Bagosi, A., Szöllősi, J., Jenei, A.: Comparative study of the three different fluorophore antibody conjugation strategies.
Anal. Bioanal. Chem. 404 (5), 1449-1463, 2012.
DOI: http://dx.doi.org/10.1007/s00216-012-6232-z
IF:3.659

H-4032 Debrecen, Egyetem tér 1. e-mail: publikaciok@lib.unideb.hu

DEENK www.lib.unideb.hu
UNIVERSITY AND NATIONAL LIBRARY UNIVERSITY OF DEBRECEN
KENÉZY LIFE SCIENCES LIBRARY

List of other publications

3. **Shrestha, D.**, Szöllősi, J., Jenei, A.: Bare lymphocyte syndrome: An opportunity to discover our immune system.
Immunol. Lett. 141 (2), 147-157, 2012.
DOI: http://dx.doi.org/10.1016/j.imlet.2011.10.007
IF:2.337

4. Saha, D., Acharya, D., Roy, D., **Shrestha, D.**, Dhar, T.K.: Simultaneous enzyme immunoassay for the screening of aflatoxin B1 and ochratoxin A in chili samples.
Anal. Chim. Acta. 584 (2), 343-349, 2007.
DOI: http://dx.doi.org/10.1016/j.aca.2006.11.042
IF:3.186

The Candidate's publication data submitted to the Publication Database of the University of Debrecen have been validated by Kenezy Life Sciences Library on the basis of Web of Science, Scopus and Journal Citation Report (Impact Factor) databases.

Total IF: 13.03

Total IF (publications related to the dissertation): 7.507

11 November, 2013

H-4032 Debrecen, Egyetem tér 1. e-mail: publikaciok@lib.unideb.hu

12. KEYWORDS

DYE-ANTIBODY CONJUGATION

Amine targeted

Sulfhydryl targeted

Carbohydrate targeted

Mercaptoethylamine

Sodium periodate

APPLICATIONS OF DYE-ANTIBODY CONJUGATES

CD1d

MHC

Rafts

FRET

Methyl-β-cyclodextrin

Simvastatin

13. ACKNOWLEDGEMENTS

It feels like I have spent half of my life in Hungary. Never ever I had thought -not even in my wildest dreams- that I would land up in Hungary, and the time spent here would define me as a person and my career as a researcher. Gradually, I fell in love with this country. Somebody had said, **"What's Meant To Be Will Always Find A Way,"** probably it is true. All these years have been exhausting but exhilarating, frustrating but educative, monotonous but reflective. Everything I have learned being a Ph.D. student would remain with me forever and would help me grow as a person.

Firstly, I would like to thank my supervisors Prof. János Szöllősi and Dr. Attila Jenei for providing me the opportunity to pursue my Ph.D. studies at the Department of Biophysics and Cell Biology, University of Debrecen. They showed more faith in me than I had in myself. They had been generous and friendly and allowed me to explore with my scientific thoughts. I am also thankful to Dr. Jenei for making my life easier in Debrecen with every possible help he could offer. I would also like to appreciate the painstaking effort endured by Prof. Szöllősi while proof reading the series of drafts of my manuscripts and thesis. I have especially enjoyed the numerous long discussions we had at his office. Thanks for teaching me the nuances of manuscript processing.

I also owe thanks to Prof. György Vereb and Dr. Peter Nagy for being accessible every time. I am grateful to those stop-by discussions and suggestions, which took place almost in every place imaginable present at different locations of the department.

I am also grateful to Nikolett Szabó-Szentesi and Éva Pálfi for dealing with my administrative stuffs related to my travel, tax papers and extended stay.

I would also like to express my gratitudes to the present and the past members of the Receptor Tyrosine Kinase group. Among my colleagues Attila Forgács, Árpád Szöőr, Ádám Bartók, Agnès Szabó and Zsuzsanna Gutayné Tóth deserve special mention here with whom I shared the joys and pains of doing PhD.

I would also like to thank Adrienn Bagosi for being an excellent co-worker and for her willingness to contribute in my scientific research.

I am also thankful for the financial support from the European Commission Marie Curie research grant MCRTN-CT-2006-036946-2 (IMMUNANOMAP), the TAMOP-4.2.2/B-10/1-2010-0024 Predoctoral fellowship and the Baross Gábor Program (REG-EA-09-1-2009-0010).

Last but not least, I would like to thank my parents for their unconditional support, sacrifices and unflagging faith in me. I am blessed to be your son. I promise I would never let you down.